Molecular mechanisms of myelin dysfunctions in the nervous system

by

Jihyun Kim

A Dissertation submitted to the

Graduate School-Newark

Rutgers, The State University of New Jersey

In partial fulfillment of the requirements

for the degree of Doctor of Philosophy

Graduate Program in Biological Sciences

written under the direction of

Dr. Haesun Kim

and approved by

_____

_____

_____

_____

_____

_____

Newark, New Jersey

October 2017

Copyright page:

ABSTRACT OF THE DISSERTATION

Molecular mechanisms of myelin dysfunctions in the nervous system

By Jihyun Kim

Dissertation Advisor: Dr. Haesun Kim

Co-advisor: Dr. Radek Dobrowolski

Myelin is generated by Schwann cells (SCs) in the peripheral nervous system (PNS) and by oligodendrocytes (OLs) in the central nervous system (CNS). Myelin not only provides physical and structural support to the axon, it also provides trophic and metabolic supports. In addition, myelin is important for rapid nerve conduction, which is essential for proper communication within a neuronal circuit. Therefore, damage to myelin or myelin loss disrupts axonal integrity and impairs neuronal functions. Elucidating molecular mechanisms underlying myelin defects under pathological conditions will be important in gaining insights into developing a strategy for preventing myelin loss and improving myelin repair. In this study, we investigated molecular mechanisms of aberrant myelination and myelin loss associated with Charcot Marie Tooth disease (CMT) in the PNS and traumatic brain injury (TBI) in the CNS.

In Chapter 1, we investigated the impact of CMT4B1-associated MTMR2 loss in SCs. CMT4B1 is a genetically inherited disorder of the PNS that is caused by loss of MTMR2 gene function. In CMT4B1 patients, myelin outfolding and demyelination are observed resulting in decreased nerve conduction, muscle

weakness, atrophy, and sensory deficits. Previously, it has been shown that SC-specific deletion of MTMR2 in mice results in reduced nerve conduction and myelin abnormalities similar to defects observed in CMT4B1patients. However, the mechanism(s) by which loss of MTMR2 function leads to the myelin abnormalities are not fully understood. To elucidate the underlying mechanisms, we generated MTMR2 knockdown SCs and analyzed the effect of MTMR2 loss on intracellular signaling pathways that are essential for SC myelination. Since MTMR2 is a phosphoinositide 3-phosphatase that regulates the $PI(3,5)P_2$ metabolism, it is possible that abnormal regulation of the $PI(3,5)P_2$ level in MTMR2 KD SCs may be associated with the aberrant SC functions. Recently, $PI(3,5)P_2$ has been shown to serve as a platform for mTORC1 signaling on lysosomal membrane. Since mTORC1 has an important role in SC myelination, we monitored whether MTMR2 loss affects the mTORC1 signaling pathway in SCs. Here, we report an aberrant increase in mTORC1 activity in MTMR2 KD SCs. The mTORC1 activation is also associated with inhibition of autophagy and transcription activity of TFEB, a regulator of lysosomal biogenesis and function.

Myelin repair or promoting remyelination in the PNS is important for improving neuronal function in patients with peripheral myelin dysfunctions. In Chapter 2, we elucidated the promyelination function of recombinant TIMP-3 in SCs. TIMP-3 is a member of the tissue inhibitor of metalloproteinase family proteins and one of the targets includes ADAM17. Endogenous ADAM17 in the PNS negatively regulate axonal Nrg1 type III signaling that is essential for SC myelination. Here, we report that recombinant TIMP-3 enhances myelin

formation by SCs. The TIMP-3 function is associated with an increase in axonal Nrg1 signaling and laminin deposition during the early stages of myelin formation.

In Chapter 3, we investigated molecular mechanisms underlying myelin dysfunction in the CNS associated with TBI. Myelin loss following TBI contributes to axonal degeneration, neuronal death and in long-term, neuronal dysfunction in the patients. Recent studies provide evidence that primary myelin loss contributes to the myelinated axon pathology following TBI. The myelin loss appears to occur without OL death, indicating that demyelination results from a mechanism that actively destroys myelin in viable OLs. Therefore, understanding the mechanisms of OL response to injury may provide insights into preventing demyelination and/or to protecting proper axon- myelin units following TBI. To this end, we investigated the direct impact of mechanical injury on OLs. We developed an OL monoculture system established on a deformable silicone membrane that can be rapidly stretched by a computer-controlled air pulse, which mimics diffused mechanical injury in the brain following TBI. Our data show that stretch injury induces activation of the Erk1/2 pathway in OLs, which leads to myelin protein loss. Furthermore, the Erk1/2 activation was induced by intracellular calcium increase. Inhibition of Erk1/2 or chelating intracellular calcium prevents myelin protein loss after stretch injury. Furthermore, TBI *in vivo* results in rapid Erk1/2 activation in white matter OLs accompanied by losing the mature OL phenotype.

By studying the molecular mechanisms responsible for myelin malformation or myelin loss in demyelinating diseases, we provide evidences of

signaling pathways or signaling molecules that could be potential therapeutic targets for preventing myelin dysfunctions.

Acknowledgements

I would like first to thank Dr. Haesun Kim for giving me opportunity to join the program and for her support on developing my intellectual insights to be a scientist during my Ph.D. I also appreciate for her prodigious help and patience during my thesis preparation.

I thank Dr. Radek Dobrowolski and Dr. Patrice Maurel for their support on conducting my study and encouragement. I am thankful to my thesis committee members, Dr. Nan Gao, Dr. Wilma Friedman, Dr. Teresa Wood, and Dr. Qian Cai, for providing great advise and encouragement.

I would like to thank to Dr. Jeongsil Kim-Ha and Young-Joon Kim for their support and giving me many opportunities on scientific experiences.

I am thankful to my friends, Esther Rho, Edward Martinez, Juan Zanin, Cecilia Blengini, Laura Montroull, Kavya Reddy, Soyoung Choi, and Hyosung Kim for their great support and all wishes for my success during my long journey for Ph.D.

Lastly, I would like to dedicate this work to my family, Jong-Kook Kim, Kyeong-Sook Lee, Jihye Kim, and Kiyeon Kim. I really appreciate them for never letting me give up on my dreams and showing me infinite support, love and encouragement.

Table of Contents

3. Introduction

Myelin is a multi-layered myelin structure that is formed by specialized glial cells, Schwann cell (SC) in the peripheral nervous system (PNS) and oligodendrocyte (OL) in the central nervous system (CNS), wrapping the axons with the extended plasma membrane of a myelinating cell. Although the myelination by SCs and OLs take a role of the wiring nervous system in the PNS and CNS, behaviors of these cells during myelination are different. SCs are restricted to make single axonal myelin segments, while a single OL myelinates multiple axons at the same time forming several myelin segments (Nave, 2010). This myelin is not only important for the rapid propagation of action potentials in the nervous system, but it is important for axon integrity by providing structural, trophic, and metabolic support for axons (Hirrlinger and Nave, 2014; Nave and Ehrenreich, 2014).

Myelin loss has been observed in many human diseases that result in neuronal dysfunctions, such as cognitive, motor, or sensory deficits. These demyelinating diseases are divided into two categories, which are primary demyelination and secondary demyelination (Ryan et al., 2014). Primary demyelination indicates removal of normal myelin structure around intact axons. Primary disorder of myelin is subdivided into two categories, which are dysmyelinating and demyelinating diseases. Dysmyelination refers to malformation or defective myelin formation caused by the genetic mutation shown in Pelizaeus-Merzbacher disease and Charcot Marie Tooth disease (CMT) in the CNS and PNS, respectively. Demyelinating disease indicates the

destruction of myelin caused by extrinsic factors, such as immune responses, viral infection, or toxins such as observed in multiple sclerosis (MS), Devic's disease, and leukodystrophy in the CNS, and Guillain–Barré syndrome and Anti-MAG peripheral neuropathy in the PNS. Secondary demyelination implies the breakdown and/or removal of myelin from the trauma injury and Wallerian degeneration (Ludwin, 1995).

Although a various group of diseases has been shown to result in malfunction of SCs or OLs, molecular mechanisms behind these diseases are still not clear. The present studies focus on investigating molecular mechanisms underlying myelin dysfunction in CMT in the PNS and traumatic brain injury (TBI) in the CNS.

3.1 Introduction to PNS myelination and CMT

3.1.1 SC development and myelination in the PNS

Schwann cells are derived from the neural crest cells and become SC precursors. These committed SC precursors migrate along the axons in developing peripheral nerves and proliferate while they migrate. Once SC precursors develop into immature SCs, membrane processes of immature SCs interact with axons and start sorting large or small diameter axons. According to the size of the axons that SCs interact, immature SCs differentiate into either promyelinating SCs or non-myelinating SCs. A promyelinating SC turns on the myelin gene machinery and expands its membrane to generate myelin to wrap around large diameter axons. However, a non-myelinating SC forms Remak

bundles by ensheathing multiple small diameter axons (Salzer, 2008; Pereira et al., 2012).

Neuregulin 1 type III (Nrg1 type III) is an axonal instructive signaling molecule that regulates Schwann cell proliferation, differentiation, and myelination. The expression level of Nrg1 type III on axonal membrane determines whether axons are ensheathed or myelinated. Mice that are heterozygote for Nrg1 type III showed aberrant axonal sorting and ensheathment of large diameter axons in Remak bundles. In addition, hypomyelination was observed in the mutant mice due to the decreased amount of the Nrg1-III expression on the axons (Taveggia et al., 2005). Nrg1 type III signaling pathway will be discussed further in the following section.

During myelination, spiral ensheathment of axons with multiple layers of SC membrane is followed by formation of distinct subdomains and myelin compaction (Arroyo and Scherer, 2000). Myelin is a polarized structure that can be divided into two domains, compact and non-compact myelin. Compact myelin regions include internodal and juxtaparanodal regions. Non-compact myelin is found in paranodes and Schmidt-Lanterman incisures, which are the lateral cytoplasmic borders and funnel-shaped interruption that runs along the compact myelin sheath, respectively. The nodal region of myelin is tipped with microvilli that contact the nodal axolemma and it rectifies sodium channels that are important for saltatory conduction (Arroyo and Scherer, 2000).

These different structures in myelin show unique protein and lipid compositions and distributions. To establish functional myelin, myelinating cells

require precise membrane sorting and trafficking machineries that allow temporal and spatial distribution of the myelin components. Targeted spatial localization of myelin proteins and adhesion molecules is also important for myelin structure stabilization. For example, myelin protein zero (MPZ), one of the most abundant myelin proteins in myelin in the PNS, has been shown to be sorted into specific endosomal vesicles and targeted to the SC plasma membrane of compact myelin (Trapp et al., 1995, Voshol et al., 1996). A study showed that MPZ is stored in late endosomes and lysosomes, and the secretory lysosome is important for delivering the MPZ to the myelin membranes (Chen et al., 2012). This suggests that acute trafficking of myelin proteins by the endo-lysosomal trafficking is important in SC myelination.

Myelin is a lipid-rich structure, which is mainly composed of cholesterol, phospholipids, and glycospingolipids. These lipids are important for myelination and maintenance of long-term myelin stability (Schmitt et al., 2015). Specifically, cholesterol is essential for myelin formation: levels of myelination are limited to the availability of cholesterol in the Schwann cells. Analysis of mutant mice lacking cholesterol synthesis in SCs showed severe hypomyelination and uncompacted myelin (Verheijen et al., 2009). In addition, it has been shown that myelin protein, MPZ, trafficking and myelin compaction are dependent on cholesterol (Saher et al., 2009).These studies suggest that cholesterol is required for myelin protein trafficking during myelin growth and compaction.

Taken together, endosomal trafficking is important to distribute newly synthesized proteins and lipids during myelination. At the same time, autophagy-

mediated lysosomal degradative machinery is important for homeostatic control of appropriate myelin production and turnover (Jang et al., 2015). Dysregulations in the endo-lysosomal trafficking in SCs have been implicated in the development of demyelinating disease in the PNS, such as CMT.

3.1.2 Charcot Marie Tooth disease

Charcot Marie Tooth (CMT) disease is a genetically inherited disorder of the PNS caused by progressive demyelination and axonal atrophy. Symptoms of CMT include the contractures and bone deformities such as high feet arches, curled toes and claw fingers. In addition, CMT patients have decreased sensation or loss of feeling in the legs and feet. Charcot Marie Tooth disease is caused by mutations in different genes that are associated with myelin formation or maintenance, mitochondrial metabolisms, and axonal transport (Pareyson and Marchesi, 2009). According to its pathophysiological features, CMT diseases are mainly divided into CMT1, CMT2 and CMT4. CMT2, an axonal form, results from the abnormalities in the axon of the peripheral nerve cells rather than the myelin sheath. This CMT2 axonal neuropathy is associated with a blockage of axonal transport and axon degeneration by gene mutations. CMT1 and CMT4, a demyelinating form, are caused by abnormalities in the myelin sheath that shows demyelination and myelin malformation resulting in slow nerve conduction (Nave et al., 2007; Pareyson and Marchesi, 2009; Isfort et al., 2015).

CMT1 and CMT4 are caused by Schwann cell dysfunction due to genetic mutations. CMT1 is an autosomal dominant disease and is divided into two

subtypes, CMT1A and CMT1B, which are caused by mutations in peripheral myelin protein 22 (PMP22) and protein zero (P0), respectively. Aberrant accumulation of the mutant proteins in CMT1 induces production of excessive misfolding proteins resulting in cellular toxic effects in the SCs. On the other hand, CMT4s are autosomal recessive demyelinating motor and sensory neuropathies that are caused by loss of function mutations in various genes.

There are several genes that have been identified, which mutations contribute to CMT4. These include differentiation-associated protein1 (GFAP1, CMT4A), myotubularin-related protein2 or 13 (MTMR2 or 13, CMT4B1 or CMT4B2, respectively), SH3 domain and tetratricopeptide repeats-containing protein 2 (SH3TC2, CMT4BC), early-growth factor2 (ERG2, CMT4E), Periaxin (CMT4F), or Fig4 (CMT4J) (Dubourg et al., 2006; Nave et al., 2007). Regular functions of these CMT4-associated gene products involve regulation of Schwann cell differentiation (ERG2), cytoskeletal organization (GFAP, Periaxin), or intracellular trafficking (MTMR2 and 13, SH3TC2, Fig4).

3.1.3 CMT4B1 and MTMR2

CMT4B1 is caused by loss of function mutations in MTMR2 gene (Bolino et al., 2000). MTMR-null mice develop PNS abnormalities that recapitulate those seen in CMT4B1 patients. These include decreased nerve conduction, dysmyelination and myelin outfolding (Bolino et al., 2004). Later, it was shown that these phenotypes of CMT4B1 occurred only when MTMR2 was deleted in SCs, but not in motor neurons, indicating the myelin dysfunction resulted from

the effects of MTMR2 loss in SCs (Bolis et al., 2005). MTMR2 is a phosphatidylinositol (PI) 3-phosphatase that dephosphorylates 3-phosphate of phosphatidylinositol 3-phosphate [PI3P] and phosphatidylinositol 3,5-bisphosphate [$PI(3,5)P_2$] phosphoinositides. In the absence of MTMR2, $PI(3,5)P_2$, but not PI3P, accumulates within the cells. As a signaling lipid, $PI(3,5)P_2$ is enriched in late endosomes and lysosomes and is thought to provide platforms for intracellular signaling proteins that are necessary for endo-lysosomal trafficking (Robinson and Dixon, 2006). Therefore, it is possible that aberrant accumulation of $PI(3,5)P_2$ in the absence of MTMR2 may result in defects in the endo-lysosomal pathway.

A possible role of $PI(3,5)P_2$ in the regulation of endo-lysosomal function is also suggested from studies investigating Fig4 function in SCs. Fig4 plays an opposite role to MTMR2 in $PI(3,5)P_2$ biosynthesis: it promotes the production of $PI(3,5)P_2$ from PI3P (Duex et al., 2006; Mccartney et al., 2014). Loss of function mutations in Fig4 causes CMT4J, which phenotypes include amyelination or hypomyelination. Loss of Fig4 decreases an intracellular level of $PI(3,5)P_2$, accordingly, crossing Fig4-heterozygote mice to MTMR2 mutant mice rescues the myelin defects in the MTMR2 mutant, presumably by restoring the $PI(3,5)P_2$ levels to normal (Vaccari et al., 2011). Fig4-deficient Schwann cells exhibit defects in lysosomal function, including enlarged lysosome and accumulation of lysosomal Ca++, supporting the notion that aberrant regulation of $PI(3,5)P_2$ biogenesis affects the endo-lysosomal pathway (Zou et al., 2015). It is interesting, however, that studies on MTMR2 deficient mice showed that unlike in

Fig4-deficient mice, lysosome morphology and lysosomal protein expression appear normal in the absence of MTMR2 (Ng et al., 2013). However, effects of MTMR2 loss on lysosomal function or endo-lysosome-associated signaling, which is necessary for myelination, has not been elucidated. For example, our previous study observed that Nrg1-ErbB receptor signaling, which is a key regulator of myelination is modulated by endosomal signaling that spatially regulates the downstream of PI3-kinase (PI3K) and Erk1/2 pathway activation in SCs (unpublished data). mTOR activation, which is essential for SC myelination and myelin-associated lipid synthesis, requires the mTORC1 association to the lysosomal membrane (Norrmén et al., 2014). Therefore, it is possible that aberrant regulation of the PI(3,5)P_2 homeostasis within the endo-lysosomal system may affect key intracellular signaling pathways in SCs that are necessary for myelin formation. In the following section, I will describe the functions of Nrg1 and mTOR signaling on SC myelination.

3.1.4 Functions of Nrg1 and mTOR signaling in SC myelination

3.1.4.1 Neuregulin 1-ErbB2/3 signaling pathway

Neuregulin1 (Nrg1) is an axonal signaling molecule that regulates SC proliferation, migration, and myelination by interacting with the ErbB receptor (Newbern and Birchmeier, 2010). The mammalian Nrg1 gene has 33 different isoforms that are classified under six different topologies (type1-6) (Luo et al., 2011). The continuous bidirectional dialog between axons and the glial cells orchestrated through Nrg1-ErbB signaling is fundamental for myelin formation

and maintenance (Nave and Salzer, 2006; Newbern and Birchmeier, 2010). Nrg1 type III has been shown as a key molecule required for myelination by offering its signal to the SCs (Taveggia et al., 2005).

The regulation of Nrg1 type III activity involves post-translational processing via two proteinases, ADAM17, also known as TACE, or β-secretase BACE1 (Newbern and Birchmeier, 2010; Fleck et al., 2013). A recent study has shown that Nrg1 type III activity is positively regulated by BACE1, which cleaves outside the EGF domain of Nrg1 resulting in activation of Nrg1-ErbB signaling (Luo et al., 2011). BACE1 knockout animals show hypomyelination of peripheral nerves and aberrant SC-mediated segregation of small diameter axons (Willem et al., 2006). These BACE1 knockout phenotypes are similar to those evidenced in mice with mutations in Nrg1 type III or deletion of ErbB2 in SCs (Garratt et al., 2000; Michailov et al., 2004; Willem et al., 2006). It has also been demonstrated that Nrg1 type III activity is negatively regulated by ADAM17, which inactivates Nrg1 through cleaving it within the EGF domain. This finding is supported by evidence showing that knockdown of ADAM17 in neurons accelerates the onset of SC myelination (La Marca et al., 2011).

While Nrg1 type III is expressed on the axonal membrane, it can bind and activate heterodimeric ErbB2/3 receptor complexes on SCs. Initiation of the Nrg1-ErbB signaling triggers a cascade of intracellular signaling events that involves activation of the PI3-kinase and Ras/Raf/Erk pathways (Maurel and Salzer, 2000; Ogata et al., 2004; Newbern and Birchmeier, 2010; Newbern et al., 2011). Axonal Nrg1 type III is the main activator of the PI3-kinase pathway *in vivo*

(Taveggia et al., 2005). The PI3-kinase pathway activation promotes SC survival, proliferation, differentiation, and myelination (Maurel and Salzer, 2000). On the key PI3-kinase downstream signaling events that promote myelination is activation of the mTOR complex (See section 3.1.4.2). In contrast to the myelin-promoting function of the PI3-kinase pathway, the Ras/Raf/Erk activity inhibits myelination and triggers SC migration, de-differentiation, and demyelination (Harrisingh et al., 2004; Ogata et al., 2004).

3.1.4.2 AKT/mTOR signaling pathway

The main signaling effector directly related with PI3K/ AKT pathways is the mechanistic target of rapamycin (mTOR) signaling (Norrmén and Suter, 2013). mTOR is known as a core kinase that controls metabolic homeostasis by regulating cellular processes, such as energy metabolism, cell growth, and cell proliferation (Bar-Peled and Sabatini, 2012; Betz and Hall, 2013; Nnah et al., 2015). mTOR forms two different complexes with several adaptor proteins, mTOR complex1 (mTORC1) and mTOR complex 2 (mTORC2). These two complexes are structurally and functionally different. mTORC1 is composed of mTOR, Raptor, and mLST8 and regulates protein synthesis, lipid biogenesis, lysosome biogenesis, and autophagy while mTORC2 is composed of mTOR, Rictor, mLST8, and SIN1 and regulates cytoskeleton arrangement cell growth, survival, and cytoskeleton organization (Betz and Hall, 2013). Compared to the roles of mTORC1 in regulating cellular metabolisms, mTORC2 has been considered to have a relatively smaller role in regulating cellular metabolisms.

mTORC1 is a kinase that controls cellular metabolic balances in responses to extracellular and intracellular stimuli to the cell by regulating anabolic and catabolic processes such as protein synthesis, lipid synthesis, lysosome biogenesis, and autophagy (Bar-Peled and Sabatini, 2012; Betz and Hall, 2013; Nnah et al., 2015). mTORC1 activity is regulated at the lysosomal membrane by heterodimeric Rag GTPases (RagA, B, C, and D) and Ras homolog enriched in brain (Rheb) GTPase. The Rag GTPases are stimulated by amino acids, especially leucine and glutamate, and recruit the mTORC1 complex to lysosomal membranes. Rheb activates mTORC1 on the lysosomal membrane and the activity is regulated by growth factors signaling pathways. These two events are necessary for mTORC1 activation (Nnah et al., 2015).

Activated mTORC1 turns on downstream signaling by phosphorylating its substrates. Based on mTORC1 activity, the downstream signaling pathways control the balance between anabolic and catabolic states in a cell (Laplante and Sabatini, 2013). Most studied targets of mTORC1 are ribosomal S6 kinase 1 (S6K1) and eukaryotic translation initiation factor 4E (elF4E)-binding protein 1 (4E-BP1), which are known to regulate protein synthesis. mTORC1 also regulates lipid synthesis through sterol regulatory element binding protein 1/2 (SREBP1/2) involved in cholesterol synthesis (Laplante and Sabatini, 2013; Norrmén and Suter, 2013). In addition to its role in regulating anabolic pathways, mTORC1 controls catabolic processes, such as autophagy and lysosome biogenesis.

Autophagy, one of the lysosomal pathways degrading cytoplasmic proteins and organelles, is regulated by activities of unc-51-like kinase 1 (ULK1) and autophagy-related gene 13 (Atg13). These two proteins are required for initiating autophagy and mTORC1 inhibits their activities by phosphorylation. Another mTORC1 target transcription factor EB (TFEB) activates and promotes the catabolic state of the cells by inducing autophagic and lysosomal gene expressions. Activated mTORC1 negatively regulates the transcription activity of TFEB by preventing translocalization of TFEB to the nucleus, resulting in inhibition of lysosome biogenesis (Laplante and Sabatini, 2013; Puertollano, 2014; Nnah et al., 2015). Therefore, mTORC1 has a role in both promoting and inhibiting downstream signaling pathways that are involved in keeping balances between anabolic and catabolic processes.

Recent studies have elucidated the importance of mTOR signaling pathway in regulating myelination in the nervous system (Sherman et al., 2012; Wahl et al., 2014). In the PNS, conditional deletion of mTORC1 in SCs results in hypomyelination and shorter myelin internode formation resulting in the arrest of myelination (Sherman et al., 2012). In another study, rapamycin treatment, which inhibits the mTOR pathway, induced defects in lipogenic gene expression, resulting in failure of SC differentiation (Preitschopf et al., 2014). Furthermore, disruption of mTORC1 activity by deleting raptor in SCs has been shown to affect lipid biogenesis through the SREBP resulting in hypomyelination (Norrmén et al., 2014). Results from the studies suggest the importance of mTORC1 signaling in regulating SC myelin formation and maintenance of the myelin. Therefore,

aberrant regulation of mTORC1 signaling in SCs is likely to disrupt PNS myelination.

In the present study, we investigated the effect of MTMR2 loss on mTORC1 signal regulation in SCs. As mentioned above, MTMR2 loss results in accumulation of lysosome-associated phosphoinositide $P(3,5)P_2$. In other cell types, $PI(3,5)P_2$ has been shown to provide a platform for the mTORC1-S6K association on the lysosomal membrane (Jin et al., 2014). Lysosomal $PI(3,5)P_2$ is also involved in TFEB activation (Medina et al., 2015; Wang et al., 2015; Li et al., 2016). Therefore, we hypothesized that the myelin dysfunction observed in the absence of MTMR2 results from dysregulation of the lysosome associated mTORC1 activity and/or the downstream effector function. The study described in Chapter one tested this hypothesis.

In chapter two, we described a study that investigates the role of TIMP-3, tissue inhibitor of metalloproteinase-3, on SC myelination. Members of TIMP protein family are endogenous inhibitors of ADAMs and matrix metalloproteinases (MMPs) of extracellular proteinases (Bourboulia and Stetler-Stevenson, 2010). Among the TIMPs, TIMP-3 has been shown to specifically target ADAM17 that functions as a negative regulator of the Nrg1 signaling and SC myelination (Amour et al., 1998) (see Section 3.1.4.1). In an effort to identify therapeutic strategies for improving myelin repair and promote PNS myelination, we tested the hypothesis that ectopic TIMP-3 treatment promotes SC myelination by relieving the inhibitory effect of ADAM17 on the Nrg1 signaling.

3.2 Introduction to CNS myelination and TBI

3.2.1 OL development and myelination in the CNS

Oligodendrocytes arise from oligodendrocyte precursor cells (OPCs) derived from neuroepithelial cells of the ventricular zone (VZ) (Baumann and Pham-dinh, 2001; Rowitch and Kriegstein, 2010). The OPCs migrate through the CNS during development and reach the gray matter before they differentiate into myelinating OLs. After migration, OPCs sit along the fiber tracts that will become future white matter and become pre-oligodendrocytes (pre-OLs) that have multiple processes. Pre-OLs transform into immature oligodendrocytes (immature OLs) and start differentiating into mature oligodendrocytes (mature OLs) by turning on expression of myelin genes. Upon interaction with neighboring axons, mature OLs start forming myelin on multiple axons (Rowitch and Kriegstein, 2010.; Nave, 2010; Bergles and Richardson, 2017). The number of myelin segments formed by a OL varies among axonal tracts and it is determined by the size of the axons (Fanarraga et al., 1998). CNS myelination has a distinctive structure from PNS myelination. Contrary to SC myelination, myelin formed by OLs does not have microvilli or incisures (Peters et al., 1991). Molecular components of OL myelin overlap with SC myelin components. Both contain high amounts of lipids, such as cholesterol and phospholipids. In addition, compact myelin contains myelin basic protein (MBP) and myelin-associated glycoprotein (MAG), which are expressed on the adaxonal membrane (Trapp et al., 1989). However, OLs express two unique myelin proteins that are not expressed by SCs, which are myelin-oligodendrocyte glycoprotein (MOG)

expressed on OLs' outer cell membrane and myelin-oligodendrocyte basic protein (MOBP) in the compact myelin (Johns and Bernard, 1999).

The role of the interaction of axon-OL and its preservation is not only crucial for myelin formation but also in demyelinating disease. Impaired myelin function has been suggested to lead to axonal degeneration, as observed in myelin protein deficient animal models and myelin-related disorders, such as MS and CNS injury.

3.2.2 Traumatic brain injury

Traumatic brain injury (TBI) is caused by either rapid head movement or a direct/ indirect force to the head. It is the leading cause of long-term disability that generates a greater risk of developing other neurodegenerative diseases, such as Alzheimer's disease. Neurobehavioral problems, such as cognition deficits are also associated with TBI (Jellinger, 2004; McAllister, 2008). There are two types of forces that cause brain injury: contact forces and inertial forces. Contact-mediated injury occurs from a direct external force to the head resulting in damages to the skull and the brain surface. On the other hand, inertial injury results from a rapid rotation or movement of the brain that produces shearing and compression force that cause brain tissue deformation or tears. This results in widely spread axonal injury termed diffused axonal injury (DAI) or traumatic axonal injury (TAI) (McAllister, 2011).

Long axons in white matter tracts are most vulnerable to TAI following TBI and as a consequence white mater damage is frequently observed in TBI

patients. Long-term degeneration of myelinated axons in white matters has been observed in human patients as well as in animal models following experimental TBI. Myelin loss and OL death have also been observed in human brains after TBI (Ng et al. 1994; Shaw et al. 2001). In rodents, moderate TBI results in extensive myelin loss and OL death accompanied by axonal degeneration (Lotocki et al., 2011; Flygt et al., 2013). Ultra-structural analysis on the corpus callosum following mild TBI in mice showed myelin loss on intact axons indicating primary myelin loss. More importantly, myelin loss was observed in the absence of OL death, indicating the myelin loss occurred on viable OLs (Mierzwa et al., 2015). Similarly, following TAI on optic nerves, damage to the myelin was observed as early as 24 hours post-injury with little or no change in the underlying axons (Bramlett and Dietrich, 2002; Maxwell et al., 2003; Flygt et al., 2013). While axonal degeneration or neuronal loss results in myelin loss in cases of moderate to severe TBI, it is becoming clear that primary myelin loss on intact axons also contributes to the myelin dysfunction, especially following mild TBI. Furthermore, the myelin loss appears without OL death, indicating an active mechanism of myelin breakdown in OLs in a response to injury. Because myelin is crucial for neuronal function and survival, myelin loss on intact axons results in neuronal dysfunction and in long-term, neuronal degeneration. Myelin loss also leaves underlying axons more vulnerable to subsequent injury in the case of repeated TBI (Reeves et al., 2005). Therefore, a therapeutic strategy to prevent demyelination or to promote myelin repair on intact axons after TBI may be

effective in improving neuronal function or preventing secondary injury in TBI patients.

The molecular mechanisms underlying primary demyelination after TBI has not been elucidated. Loss of myelin in viable OLs following TBI indicates an active mechanism of myelin breakdown in the OLs in response to the injury-induced signals. Direct mechanical stimuli, such as stretch injury or mechanical deformation could induce changes in cell behavior through mechanisms of mechanotransduction. Neurotransmitters and cytokines that are known to accumulate in the brain lesions are also capable of activating receptors on neighboring cells to initiate cellular responses. It is not known how mature OLs in adult brains respond to the injury-associated signals. More importantly, it is unknown whether the extracellular signals trigger intracellular events in OLs to initiate myelin breakdown.

Previous studies have shown that TBI induces neuronal hyperexcitability in the brain. An increase in release of neurotransmitters (NTs), including glutamate, has also been reported (Katayama et al., 1990; Magou et al., 2015). The increased glutamatergic signal activates neighboring neurons through the NMDA receptors on the cell membrane and induces an intracellular calcium increase (Shahlaie et al., 2010). The effect of neuronal hyperexcitability and glutamate release on OLs in TBI-brains is not well understood. During development of the CNS, changes in neuronal activity and glutamate release has been shown to modulate OPC proliferation, differentiation, and myelination (Gautier et al., 2015; Hines et al., 2015; Spitzer et al., 2016). A recent study has

shown that myelinating OLs express functional glutamate receptors. Upon glutamate stimulation, the AMPA and NMDA receptors induce intracellular calcium increase in OL cell body and distal myelin, respectively (Micu et al., 2016). Furthermore, NMDA receptor function in adult OLs has been implicated in myelin damage after CNS insults (Micu et al., 2005). Therefore, it is possible that the increased glutamate release from neurons following TBI may induce glutamatergic signaling within OLs that may affect myelin homeostasis in the OLs, leading to myelin dysfunction.

Growth factors and cytokines produced in the brain lesions are also likely to influence the OL response to injury. During OL development, growth factors, such as FGF-2 and insulin-like growth factor 1 (IGF-1) are known to regulate OPC proliferation, differentiation, and myelination. On the other hand, FGF-2 treatment on mature OLs initiates myelin protein loss through activation of the MAPK pathways and leads OLs to re-enter the cell cycle (Fressinaud et al., 1993; Bansal et al., 2003). In our previous study, we observed that platelet-derived growth factor (PDGF) and Nrg1 also trigger myelin breakdown in myelinating OLs through activation of MAPK pathways (unpublished data). Increased level of cytokines, including interleukins (ILs) and interferon-γ (IFN-γ), have been detected in the CSF of TBI patients (Hutchinson et al., 2007). IFN-γ production has been associated with demyelinating pathologies in the CNS. Overexpression of IFN-γ ablates myelin in the white matter of the brain (Corbin et al., 1996). Therefore, it is possible that increased cytokine and/or growth factor production in brain lesions following TBI may affect myelin stability in the OLs.

3.2.3 MAPK pathways and myelin homeostasis in the CNS

During development of the CNS, various growth factors play important roles in regulating proliferation, differentiation, and maturation of the OLs (McMorris and McKinnon, 1996; Cheng et al., 1999; Fredrick et al., 2007). However, when growth factor-derived signaling is activated in adult, the signaling disrupts myelin stability in the OLs. Among the downstream signaling pathways, MAPK-mediated signaling appears to play dual roles in promoting myelination and destabilizing myelin. For example, p38 MAPK plays an important role during differentiation of OPCs into mature OLs (Chew et al., 2010). Inhibition of p38 MAPK activity either by pharmacological inhibitor or siRNA mediated protein knockdown, induces down-regulation of myelin protein expressions *in vitro* (Fragoso et al., 2003, 2007; Chew et al., 2010). On the other hand, our previous study showed that ectopic activation of p38 in mature OLs induced myelin degeneration (unpublished data).

A role of JNK signaling pathway during CNS myelination has also been described. Activation of JNK pathway is necessary for OPC proliferation in the CNS (Zhang et al., 2014). However, during differentiation, JNK pathway inhibits myelin gene transcription by inhibiting c-Jun activity, a target of JNK, thus inhibiting OL differentiation and myelination (Chew et al., 2010).

Lastly, Erk1/2 MAPK has also been shown to play dual roles in OLs. *In vivo*, elevating Erk1/2 activity in OLs during the early stage of myelination results in thicker myelin formation by the OLs (Xiao et al., 2012; Ishii et al., 2013). Erk1/2 activity is also required for OPC proliferation and differentiation into mature OLs

(Ishii et al., 2013, 2014). Accordingly, during development of the CNS, Erk1/2 activity in the OL lineage cells stays high during active myelination and decreases when the myelination is completed in the adult (Ishii et al., 2013). A study has shown that ectopic activation of Erk1/2 in adult OLs results in myelin breakdown (Ishii et al., 2016). In cultures, activation of Erk1/2, either by growth factor stimulation or expression of constitutive active MEK, induces myelin degeneration in OLs (unpublished data).

The p38, JNK, and Erk1/2 MAPKs have an evolutionally conserved function in transducing external stress to the internal molecular signal cascades that initiate cellular response. MAPKs are also key regulators of mechanotransduction in mammalian cells. Accordingly, MAPK activation has been observed in white matter regions following TBI (Otani et al., 2002; Raghupathi et al., 2003). Although functions of JNK and Erk1/2 MAPKs pathways were largely studied following neuronal injury, the role of these MAPK pathways associated with myelin damage are not fully understood. In the PNS, both p38 and Erk1/2 MAPKs transduce injury signals in SCs, initiating myelin breakdown. More importantly, inhibition of the injury-induced MAPK activation provide myelin protection in injured nerves (Guertin et al., 2005; Tapinos et al., 2006; Jolivalt et al., 2011; Yang et al., 2012). These findings present a possibility that Erk1/2 may play a similar role in mediating the injury signals that lead to OL demyelination. Therefore, understanding the mechanisms of MAPK pathways that are associated with injury responses in OLs will be important to identify a molecular target to prevent myelin loss for developing therapeutic strategies.

In chapter 3, we investigated the role of Erk1/2 pathways underlying myelin degeneration following TBI. As mentioned above, Erk1/2 activity has been shown to be required for OPC proliferation, differentiation, and myelination during development. However, our previous study has shown that activation of Erk1/2 induces myelin degeneration in OLs, suggesting an opposite role of Erk1/2 in mature OLs. Previous studies have shown the myelin degeneration in white matter of the TBI-brains. TBI-induced Erk1/2 activation in OL lineage cells in white matter tracts has also been observed. However, it is not known whether TBI-induced Erk1/2 activation in mature OLs is associated with myelin loss.

Here, we tested the hypothesis that Erk1/2 activation in OLs following TBI induces myelin degeneration. The study described in Chapter 3 tests OL injury responses to mechanical injury that are associated with Erk1/2 pathways.

4. Chapter one: MTMR2 knockdown alters mTORC1 signaling resulting in Schwann cell differentiation and autophagy defects

4.1. Abstract

Myotubularin-related protein 2 (MTMR2) is a phosphoinositide 3-phosphatase that dephosphorylates PI(3,5)P_2 and PI(3)P to generate PI(5)P and PI, respectively. Mutations in the MTMR2 gene can cause Charcot-Marie-Tooth 4B1 (CMT4B1), a form of inherited peripheral neuropathy that affects myelin in the peripheral nervous system (PNS). Genetic conditional knockout mice for MTMR2 in Schwann cells (SCs) recapitulate several aspects of CMT4B1, including reduced nerve conduction, loss of myelinated axons and myelin outfolding. A previous study has shown that MTMR2 loss results in accumulation of PI(3,5)P_2 in fibroblasts, suggesting that the MTMR2-associated myelin abnormalities may be due to dysregulation of the biological function related to PI(3,5)P_2. PI(3,5)P_2 is found within the endo-lysosomal membranes, specifically within membranes of late endosomes and lysosomes. Therefore, it is possible that aberrant regulation of PI(3,5)P_2 levels in MTMR2 mutant may contribute to dysregulation of the endo-lysosome signaling and/or function.

To investigate the effects of MTMR2 loss in SCs, we generated MTMR2 knockdown (KD) SCs using lentivirus-mediated shRNA transduction. In the KD cells, we observed increased mTORC1 activity accompanied by inhibition of ULK1 and TFEB, which regulate initiation of autophagy and lysosome biogenesis, respectively. The effect of MTMR2 KD in SCs on mTORC1 was

reversed with a PIKfyve inhibitor, which decreases level of $PI(3,5)P_2$. This inhibitor also reversed the decreased activities of TFEB and ULK1. Altogether, our data suggest that loss of MTMR2 in SCs induces increased levels of $PI(3,5)P_2$ that activate mTORC1 signaling pathways, resulting in inhibition of autophagy and lysosome biosynthesis.

In addition, we observed that loss of MTMR2 in differentiated SCs showed more elongated cell morphology. Loss of MTMR2 decreased Krox-20 expression, a promyelinating transcription factor, suggesting a defect in cell differentiation. However, overall expression levels of myelin proteins were not significantly changed in MTMR2 KD SCs compared to the control. Although overall Krox-20 expression level was decreased in MTMR2 KD SC cultures, we did not observe any differences in numbers of myelin segments or length of individual myelin internodes between control and MTMR2 KD SCs in co-cultures.

4.2. Introduction

4.2.1 Loss of MTMR2 results in human Charcot-Marie-Tooth type 4B1 demyelinating disease

Charcot-Marie-Tooth (CMT) disease type 4B1 (CMT4B1) is an autosomal recessive demyelinating human disease that is caused by mutations in the MTMR2 gene (Previtali et al., 2007). Loss of MTMR2 function in CMT4B1 results in dysmyelination and myelin outfolding generated by overproduction of myelin membranes along with abnormal myelin formation that slows down the nerve conduction velocity (Bolis et al., 2005). Recently, two independent groups have established MTMR2 global knockout mouse models that show CMT4B1-like pathological phenotypes (Bolis et al., 2005; Ng et al., 2013). These mouse models recapitulate the myelin outfolding that was seen in CMT4B1 patients (Bolis et al., 2005, 2009; Ng et al., 2013). Interestingly, while the myelin outfolding demonstrated in MTMR2 global knockout was observed in MTMR2 conditional knockdown mice using P0-Cre (Schwann cell specific Cre), this outfolding was not observed in MTMR2 conditional knockdown mice using HB9-Cre (neuron specific Cre) (Bolis et al., 2005). This shows that loss of MTMR2 function in SCs, not in neurons, contributes to the myelin defects. This suggests that MTMR2 plays an important role in regulating myelination and/or maintaining myelin homeostasis in SCs.

4.2.2 Role of PI(3,5)P_2 in endo-lysosomal pathways

MTMR2 is a phosphoinositide-3 phosphatase that dephosphorylates phosphatidylinositol 3-phosphate [PI3P] and phosphatidylinositol 3,5-bisphosphate [PI(3,5)P_2] phosphoinositides (Robinson and Dixon, 2006). Previous research has shown that loss of MTMR2 results in accumulation of PI(3,5)P_2, without affecting the level of PI3P in fibroblasts (Vaccari et al., 2011). PI(3,5)P_2 is a signaling lipid that is mainly localized in the membranes of late endosomes or lysosomes and serves as a docking site for effector proteins (Mayinger, 2012). The synthesis of PI(3,5)P_2 is controlled by lipid kinases and phosphatases including MTMR2 (Robinson and Dixon, 2006; Mccartney et al., 2014). Mutations in these kinases or phosphatases have been shown to cause neurological diseases such as CMTs or amyotrophic lateral sclerosis (ALS).

PIKfyve is a phosphoinositide-5 kinase that phosphorylates PI3P to PI(3,5)P_2, while MTMR2 catalyzes PI(3,5)P_2 to PI5P. In addition, Fig4 is a phosphoinositide-5 phosphatase that dephosphorylates PI(3,5)P_2 to PI3P. However, Fig4 also serves as an activator for PIKfyve predominantly, resulting in promotion of PI(3,5)P_2 synthesis rather than dephosphorylating it. Therefore, mutations in Fig4 results in reduction of PI(3,5)P_2 levels in cells (Vaccari et al., 2011; Mironova et al., 2016), suggesting that Fig4 has an opposite role to MTMR2 in controlling PI(3,5)P_2 homeostasis. To support this, a study has shown that knockdown of PIKfyve in MTMR2 KO or giving the heterozygosity of Fig4 in MTMR2 KO mice (MTMR2-/-Fig4+/-) rescues the myelin outfolding phenotype in MTMR2 KO SCs (Vaccari et al., 2011).

In Fig4 deficient cells, enlarged lysosomes were observed, resulting in abnormal lysosome functions due to the decreased level of $PI(3,5)P_2$. Since $PI(3,5)P_2$ has been shown as a ligand for the lysosomal calcium channel, TRPML, decreased $PI(3,5)P_2$ level suppresses calcium efflux through the TRPML, resulting in lysosome fission failure in Fig4 deficient fibroblast, DRG neurons and SCs (Zou et al., 2015). Currently, a study has suggested that $PI(3,5)P_2$ has a role in myelin protein trafficking through the late endosomes and lysosomes in OLs. The study showed that loss of Fig4 impaired myelin associated glycoprotein (MAG) trafficking to the myelin membranes in differentiating OLs, resulting in hypomyelination (Mironova et al., 2016). This research supports the role of $PI(3,5)P_2$ in regulating endo-lysosomal trafficking that may associate with myelin formation. Therefore, a possibility exists that abnormal accumulation of $PI(3,5)P_2$ in MTMR2 deficient SC endo-lysosomal membranes may affect endo-lysosomal function and signaling, resulting in myelin abnormalities. However, the signaling mechanisms that may regulate endo-lysosomal pathways are still not clear.

4.2.3 The function of mTORC1 signaling in the PNS myelination

Previous studies have shown that $PI(3,5)P_2$ has roles in providing a platform for mTORC1 complex 1 (mTORC1) signaling by recruiting its substrates, such as S6K, in yeast (Jin et al., 2014). Therefore, $PI(3,5)P_2$ accumulation in MTMR2 KO cells may affect mTORC1 association to lysosomes and/or activation of the downstream targets of mTORC1 on the lysosomes.

The mechanistic target of rapamycin (mTOR) forms a complex with several adaptor proteins and is recruited to the lysosomal membrane. Through mTORC1 at the lysosomal surface, cells moderate metabolic balance via continuously monitoring available energy and nutrients (Menon et al., 2014; Puertollano, 2014). Active mTORC1 modulates activation of transcription factors involved in protein and lipid synthesis, lysosome biogenesis, and autophagy (Bar-Peled and Sabatini, 2012; Puertollano, 2014; Nnah et al., 2015).

In the PNS, mTOR associated signaling plays a key role in regulating SC myelination. mTORC1 activation through AKT acts as a positive regulator of Schwann cell myelination (Norrmén and Suter, 2013). Conditional inactivation of mTORC1 in SCs results in hypomyelination and shorter myelin internode formation resulting in the arrest of myelination (Sherman et al., 2012). A recent study has shown that disruption of phosphatase and tensin homolog (PTEN), one of the phosphoinositide phosphatases, results in increased mTORC1 activity through AKT activation and leads to hypermyelination and myelin outfolding in sciatic nerve tissue (Goebbels et al., 2012).

During the SC myelination, SCs expand cell membranes, which requires high amount of cholesterol and lipid biosynthesis. The sterol regulatory element-binding proteins (SREBPs), one of the direct targets of mTORC1, are transcription factors that regulate expression of the enzymes that are necessary for fatty acid and cholesterol synthesis (Shao and Espenshade, 2012). A current study shows that SC specific-deletion of raptor, a component of mTORC1,

induces defective SREBP signaling, resulting in hypomyelination (Norrmén et al., 2014).

ULK1 is one of the downstream molecules of mTORC1 signaling. ULK1 is a kinase that regulates initiation of autophagy. Autophagy is one of the lysosomal pathways that degrade cytoplasmic proteins and organelles (Eskelinen and Saftig, 2009). A recent study has demonstrated that loss of autophagy-related gene 12 (Atg12) in SCs, a molecule required for control of autophagosome formation, results in the increase of myelin proteins (Rangaraju et al., 2010). In addition, activation of autophagy by using an inhibitor of mTORC1 promotes SC myelination (Rangaraju et al., 2010). In other studies, it has been shown that abnormal accumulation of myelin protein, peripheral myelin protein 22 (PMP22), was observed in lysosomes within a CMT neuropathy mouse model and this phenotype can be attenuated by activating autophagy (Notterpek et al., 1997; Fortun et al., 2003). These studies suggest that mTORC1-dependent autophagic and lysosomal pathways are involved in regulating myelination.

In this study, we investigated the function of MTMR2 in SCs. To investigate mechanisms underlying CMT4B1, we generated MTMR2 KD SCs and analyzed the effect of MTMR2 loss in SCs. Here, we show that MTMR2 loss induces an aberrant increase in mTORC1 activity. The increased mTORC1 activity is also associated with inhibition of autophagy and down-regulated TFEB activity, which regulates lysosomal biogenesis and functions.

4.3 Materials and Methods

Culture media

D10 media [Dulbecco's Modified Eagle's medium (DMEM) supplemented with 10% FBS, 1% glutamine, 0.1 mg/ml penicillin/streptomycin]; NB media [neurobasal medium with B-27 supplement, 0.08% glucose, 1% glutamine, 0.1 mg/ml penicillin/streptomycin and 50 ng/ml nerve growth factor (NGF) (#BT-5017, Harlan Bioproducts for Science Inc.)]; C10 media [Minimal Essential Medium (MEM) containing 10% FBS, 0.08% glucose, and 50ng/ml NGF]; D1 media [Dulbecco's Modified Eagle's medium (DMEM) supplemented with 1% FBS, 1% glutamine, 0.1 mg/ml penicillin/streptomycin], 293FT cell standard media [DMEM medium supplemented with 10% FBS, 1% glutamine, 1x non-essential amino acids (#11140076, Gibco), 1mM sodium pyruvate (#11360070, Gibco) and 0.05% geneticin (#11811031, Invitrogen); 293 FT cell advanced media [advanced DMEM supplemented with 1% FBS, 1% glutamine, 1% (v/v) chemically defined lipid concentrate (#11905031, Gibco) and 0.03mM cholesterol (#C4951, Sigma)].

Antibodies

The following primary antibodies were used for immunostaining or Western blot analysis: rabbit anti-mTORC1 (#2983, Cell signaling), mouse anti-Lamp1 (#sc-65236, Santa Cruz), chicken anti-GFP (#GFP-1020, Aves), mouse anti-MTMR2 (#H00008898-M03, Abnova), rabbit anti-pS6K (#9234, Cell signaling), mouse anti-pAkt (Ser473) (#4051, Cell signaling), rabbit anti-pAkt

(Thr308) (#2965, Cell signaling), mouse anti-pErk1/2 (#5726, Cell signaling), guinea pig- anti-p62 (#GP62-C, Progen), rabbit anti-LC3I/II (#4108, Cell signaling), rabbit anti-p4EBP1 (#2855, cell signaling), rabbit-anti-pULK1 (#14202, Cell signaling), rabbit anti-RagA (#4357, Cell signaling), rabbit anti-RagD (#4470, Cell signaling), rabbit anti-Rheb (#13879, Cell signaling), rabbit anti-Raptor (#2280, Cell signaling), rabbit anti-Krox20 (#PRB-236P, Covance), mouse anti-MBP(#SMI-94R, Covance), mouse anti-MAG (MAB1567, Millipore) and mouse anti-actin (#A5441, Sigma).

Schwann cell isolation and cultures

SCs were isolated from postnatal day 2 (P2) rat sciatic nerves. Dissected sciatic nerves were treated with trypsin-collagenase (L15 media supplemented with 0.3125% trypsin and 0.125% of collagenase) at 37 °C. Thirty minutes later, cells were pelleted at 50x g for 5 minutes and dissociated by pipetting in NB media. All dissociated cells were plated in PLL-coated 60mm dish. Next day, cells were treated with D10 media supplemented with 10μM cytosine-ß-arabino furanoside hydrochloride (AraC) (# C6645, Sigma) to avoid fibroblast contamination. Two-three days after, cultures were washed with 1X HBSS and replaced with D10 media supplemented with 10ng/ml EGF-domain of neuregulin (#396-HB-050, R&D systems) and 2.5μM forskolin (#F6886, Sigma).

Once cells were confluent, cells were harvested by 0.25% Trypsin-EDTA and spun at 200x g for 5 minutes at room temperature. Harvested cells were treated with 60μl of Thy1.1 (#MCA04G, AbD Serotec) antibody in 3ml of D10 media and

incubated for 30 minutes at 37 °C. Cells were spun down at 200x g for 5 minutes at room temperature and treated with 1ml of rabbit complement (#S7764, Sigma), and incubated for 30 minutes at 37 °C. After spinning cells down, cells were plated in a PLL-coated 100mm dish and expanded in D10 media supplemented with 10ng/ml EGF-domain of neuregulin and 2.5μM forskolin.

Generation of MTMR2 knockdown SCs

Small hairpin RNA (shRNA) constructs to MTMR2 (5'-TGGTGATAAGTAGAGTAGAATTCAAGAGATTCTACTCTATTATCACCTTTTTTC-3') and luciferase were designed. PLL3.7 expressing vector (#11795, Addgene) was digested with XhoI and HpaI restriction DNA enzymes and eluted by DNA purification kit (#A9281, Promega). 100 ng of digested PLL3.7 vector and 2.5 ng each of shRNA constructs were incubated with T4 ligases (#M0202, NEB). Ligated constructs were confirmed by sequencing. Lentivirus, which carries shRNA to either MTMR2 or luciferase, was produced by transfecting 293FT cells (#R70007, Invitrogen). 293 FT cells were plated at the density of 5x 10^6 in 8ml of 293TF cell standard media in a 100mm plate and cultured at 37°C overnight. One hour before transfection, culture media was switched to 6ml of 293 FT cell advanced media. The mixture of DNA, 11μg of enveloping plasmid pMD2.G, 22μg of packing plasmid psPAX2, 33μg of shRNA plasmid were mixed with 75μl of 2M CaCl2 in total volume of 600μl. Additional 600μl of 2 X HBS that was offered by transfection kit (#K278001, Invitrogen) was added to the culture. Five hours after transfection, media was changed to 7ml of fresh 293FT

advanced media. Forty-eight hours after transfection, 6ml of viral supernatant was collected and purified using a Lenti-X concentrator (#631232, Clontech).

SCs were plated in 3ml of D10 media supplemented with 10ng/ml EGF-domain of neuregulin and 2.5μM forskolin at the density of 3.5x 10^5 in 60mm dish on the previous day and infected by the virus resuspended in 3ml of D10 media supplemented with 10ng/ml EGF-domain of neuregulin, 2.5μM of forskolin, and 10μg/ml protamine (#3369, Sigma). Thirty-six hours after infection, the virus was removed, and SCs were expanded in D10 medium supplemented with 10ng/ml of EGF-domain of neuregulin and 2.5μM of forskolin.

Induction of Schwann cell differentiation

To induce SC differentiation in the absence of axons, we plated undifferentiated SCs onto PLL-coated 12mm coverslips at the density of 5x10^4 in D10 media supplemented with 10ng/ml EGF-domain of heregulin and 2.5μM of forskolin. On the next day, the media was switched to D1 media for a day. Then, cells were treated with 0.75mM N6,2'-O-Dibutyryladenosine 3',5'-cyclic monophosphate (db-cAMP) (#D0627, Sigma) for 5 days in D1 media at 37°C.

Measurement of Schwann morphology

Cell cultures were fixed and visualized by immunostaining for GFP. Images were taken from 20 fields each coverslip with the epifluorescence microscope (Nikon E800) using a 20x objective. Two-three coverslips per experiments from three independent experiments were used. Cell length was

measured using Image J software (NIH). Change of cell length was normalized by the value of length from the control cells.

For measurements of aspect ratio (AR), cell length vs. cell width, and cell area in differentiated SCs, cells were traced using Image J software (NIH). Based on the tracing of the cells, the mean value of the cell area and AR were analyzed by the software. Cell area was normalized by the value of area from the control cells.

SDS-PAGE and Western blot analysis

To harvest the cell lysates, Schwann cell cultures or DRG neuron-Schwann cell co-cultures were washed twice with PBS, then cells were collected in lysis buffer (25mM Tris (pH7.4), 1% SDS, 1mM EDTA (pH 8.0), 95mM NaCl, 20μM leupeptin, 10μg/ml aprotinin, 1mM PMSF, 1mM sodium orthovanadate, and 10mM sodium fluoride). Same amount of total protein was loaded and separated by size in SDS-PAGE and then transferred to a polyvinylidene fluoride (PVDF) membrane. After blocking in 2% skim milk (#1706404, Bio Rad) in TBS (10mM Tris and 150mM NaCl, pH8.0) for an hour at room temperature, the membranes were incubated with the appropriate primary antibodies in TBS containing 5% BSA overnight at 4°C. After incubating with fluorescence-dye conjugated secondary antibodies in 2% skim milk containing 0.001% SDS for an hour at room temperature, the protein bands were detected and quantified by the LiCor Odyssey imaging system.

Immunostaining

Cultures were fixed in 4% paraformaldehyde for 20 minutes at room temperature. After washing with PBS, samples were permeabilized in cold-methanol for 20 minutes at -20°C and then washed with PBS. Samples were incubated with blocking solution (10% normal donkey serum in PBS supplemented with 0.3% Triton X-100) for an hour at room temperature and then incubated with primary antibody in blocking solution overnight at 4°C. After washing with PBS, samples were incubated with secondary antibody for an hour at room temperature. Cell nuclei were stained with DAPI.

Autophagy flux test

SCs were plated in D10 media at the density of 5x 10^5 in 6-well plates. Twenty-four hours later, cells were treated with lysosomal inhibitors, 20mM of ammonium chloride (NH_4Cl) and 200μM of leupeptin, for two or four hours in D10 media at 37°C. Cells were lysed and centrifuged at 1000g for 5 minutes at 4°C. Cleared cell lysates were used for western blot for p62, LC3I/II and actin.

CLEAR assay

To transfect Schwann cells with 4x CLEAR-Luciferase plasmid and SV40 Renilla-Luciferase plasmid, two hundred thousand SCs in 500μl of D1 medium per well were plated in PLL-coated wells of a 24-well plate. Mixture of 0.72 μg of 4x CLEAR-Luciferase plasmid, 0.08 μg of SV40 Renilla-Luciferase plasmid DNA and 2.5μl of lipofectamine (#L3000008, Thermo Fisher Scientific) in 500μl of

advanced DMEM media was added to a well and incubated for 24 hours at 37°C. The media was switched to 400µl of D10 media per well in the absence or in the presence of either 100nM of YM2013636 or 20µM of MLSA-1 for 24 hours at 37°C. On the next day, cells were lysed with 1x Passive Lysis buffer from the Dual-Luciferase reporter assay kit (#E1910, Promega) and the luciferase assay was processed according to the manufacturer's protocol. A value of Renilla-Luciferase activity was used for normalization of the transfection efficiency between samples.

Dorsal root ganglion (DRG) neuron isolation and DRG -Schwann cell myelinating co-cultures

Dorsal root ganglion (DRG) neurons were dissected from E15 rat embryos and incubated with 0.25% trypsin for 30 minutes at 37°C. Cells were spun down at 50x g for 10 minutes at room temperature and resuspended in NB media. Cells were plated onto matrigel (BD)-coated glass coverslips at the density of 1.5 DRGs/coverslip in NB media. After 24 hours, Cells were treated with NB media with 15µM 5-fluorodeoxyuridine (FUdR) (#0503, Sigma) for 3 days to remove proliferating non-neuronal cells and then changed to NB medium without FUdR. Cells were maintained until DRG neurons reached the periphery of the coverslip fully. SCs were plated onto DRG neurons at the density of $7.5x10^4$cells/coverslip in C10 media. After 5 days, cells were changed to myelinating medium by adding 50µg/ml ascorbic acid (VitC) in C10 media.

For nonmyelinating SC morphology experiments, cultures were fixed before inducing myelination with VitC and immunostained for GFP.

Quantification of number of myelin segments and length of internodes

Myelin segments were visualized by immunostaining for MBP and examined by the epifluorescence microscope (Nikon E800) with a 20x objective. The MBP-positive myelin segments were counted by using ImageJ software (NIH) from 20 fields selected across each coverslip with three coverslips per condition per experiment. The number of myelin segments (myelin index) was determined as described previously (Syed et al., 2010). From the same images, length of individual myelin segments was measured using Image J software (NIH). An average of myelin length per condition was obtained and normalized by the length of control cells.

4.4. Results

4.4.1 MTMR2 knockdown increases mTORC1 activation independent of AKT and ERK1/2 MAPK activation

To determine the cell autonomous effect of MTMR2 loss in SCs, MTMR2 KD SCs were generated using lentivirus induced shRNA transduction. We tested four different shRNA sequences against MTMR2 in rat SCs. While all of the MTMR2 shRNA constructs down-regulated MTMR2 protein expression, the construct 3 gave the most efficient KD with a 76% decreased of MTMR2 expression (Figure 4.1A). For all experiments, we generated MTMR2 KD SCs using construct 3 and 70-80% knockdown efficiency was confirmed each time of MTMR2 KD SC were generated (Figure 4.1B).

Phosphoinositides, such as $PI(3,5)P_2$ have been shown to modulate lysosomal mTORC1 activation by recruiting downstream effectors (Jin et al., 2014). Since loss of MTMR2 leads to accumulation of $PI(3,5)P_2$ (Vaccari et al., 2011; Ng et al., 2013), it is possible that it may affect activation of mTORC1 targets in SCs. First, we compared the levels of phospho-S6K, a direct target of mTORC1, in control and MTMR2 KD SCs. As shown in Figure 4.2A, loss of MTMR2 resulted in a significant increase of phospho-S6K levels, indicating elevated mTORC1 activity in MTMR2 KD SCs.

PI3-kinase-AKT and Erk1/2 pathways mediate growth factor-induced mTORC1 activation (Mendoza et al., 2011). To test whether increased mTORC1 activity in MTMR2 KD SCs is through the activated AKT and Erk1/2 signaling pathways, we performed Western blot analysis to detect phospho-AKT and

phospho-Erk1/2. We did not observe significant differences in levels of phospho-AKT (T308), phospho-AKT (S473) and phospho-Erk1/2 MAPK between control and MTMR2 KD cells (Figure 4.2B). These results suggest that loss of MTMR2 affects mTORC1 activation at the downstream levels of AKT or ERK1/2 activation.

Next, we monitored mTORC1 activity during cell differentiation. SCs were induced to differentiate using dibutyryl-cyclic- AMP (db-cAMP), an analog of cAMP, as previously described (Morgan et al., 1991). Increased mTORC1 activity in MTMR2 SCs appears in the early stages of SC differentiation, while no difference was observed in mTORC1 activities between control and MTMR2 KD cells when cells were differentiated (Figure 4.3A). mTORC1 activity was also monitored during myelination. SCs were plated onto DRG neuron cultures and allowed to proliferate, and then align along the axons for five days. Myelination was induced by addition of ascorbic acid (VitC), and mTORC1 activity was monitored during the myelination. Similar to the differentiated SCs, increased mTORC1 activity was also observed at early stages of myelination in SC-DRG myelinating co-cultures *in vitro* (Figure 4.3B).

4.4.2. mTORC1-lysosome association is increased in MTMR2 KD SCs.

mTORC1 is composed of regulatory proteins, such as mTOR, Raptor, and mLST8. Its activity is regulated by small GTPases, such as Rheb and Rags, that are anchored on the lysosomal membranes as shown in Figure 4.4A. mTORC1 is recruited to the lysosome membrane by the function of Rag GTPases and

subsequently activated by lysosome-tethered Rheb GTPases. First, we determined whether the increased mTORC1 activity is associated with changes in expression level of the mTORC1 regulators. There were no significant changes in the overall expression levels of Raptor, Rheb, RagA and RagD in MTMR2 KD SCs (Figure 4.4B). Therefore, MTMR2 does not affect the expressions of mTOR regulators, suggesting that the increased mTOR activity is not due to the changes in effectors' expressions.

Previous studies have shown that $PI(3,5)P_2$ has roles in providing a platform for mTORC1 signaling by recruiting its substrate, such as S6K in yeast, to the lysosomes (Jin et al., 2014). It is possible that elevated $PI(3,5)P_2$ in MTMR2 KD SCs may enhance mTORC1 recruitment to the lysosomal surface, thus, increasing its activity. To test this, we performed double-immunostaining to determine co-localization between mTOR and LAMP1-positive lysosomes. The Pearson's coefficient analysis showed a significant increase in co-localization between mTOR and LAMP1 in MTMR2 KD SCs (Figure 4.4C). This result indicates an increase in mTORC1 recruitment to the lysosome membranes in the absence of MTMR2.

4.4.3 TFEB and ULK1 activation is decreased in MTMR2 KD SCs

Since mTORC1 activity was increased in MTMR2 KD SCs, we also monitored activities of different targets of mTORC1. In addition to S6K, mTORC1 directly phosphorylates 4EBP1 and ULK1. Phosphorylated 4EBP1 by mTORC1 activates protein synthesis by modulating mRNA translation (Gebauer and

Hentze, 2004). ULK1 is a kinase that initiates autophagy processes and mTORC1-mediated phosphorylation inhibits ULK activity (Gebauer and Hentze, 2004). The phosphorylation level of 4EBP1 was not changed in the absence of MTMR2, whereas the level of phsopho-ULK1 was increased (Figure 4.5A).

mTORC1 also phosphorylates TFEB, which is a critical factor for lysosomal biogenesis by regulating activity of CLEAR (coordinated lysosomal expression and regulation) gene network that encodes autophagic and lysosomal genes (Settembre et al., 2012) as described in Figure 4.5B. To test whether MTMR2 loss affects TFEB activity, we transfected control and MTMR2 KD SCs with 4x repeated CLEAR-luciferase reporter construct for measuring TFEB activity and Renilla-luciferase construct for measurement of transfection efficiency. The level of relative luciferase activity indicating TFEB activity was significantly decreased in MTMR2 KD SCs compared to the control (Figure 4.5C).

TFEB is involved in autophagy by promoting expressions of autophagy and lysosomal genes. Since we observed a decrease in ULK1 and TFEB functions in MTMR2 KD cells, we first tested whether MTMR2 loss affects autophagy-related protein expression. LC3 and p62 are adaptor proteins that regulate autophagosome formation as described in Figure 4.5D. LC3 is required for the biogenesis of autophagosome membranes while p62 is an adaptor protein that links LC3 to ubiquitinated cargo proteins that are marked to be degraded (Lippai and Low, 2014). The immunoblots for LC3I/II and p62 show that there are

decreases in the basal expression level of LC3I and p62 in MTMR2 KD cells compared to the control (Figure 4.5E, in the absence of the lysosome inhibitors).

Since decreased expression level of LC3I and p62 could be due to the changes in autophagy flux in MTMR2 KD SCs, we monitored autophagy flux in control and MTMR2 KD SCs. Cytosolic LC3I is converted to membrane bounded LC3II during autophagosome formation and the LC3II is eventually degraded by autophagy. Therefore, autophagy flux can be monitored by western blot for LC3I/II in presence of lysosomal inhibitors as described in previous research (Mizushima and Yoshimori, 2007). In presence of the lysosome inhibitor, accumulated p62 and LC3-II was observed in both control and MTMR2 KD cells. However, the total amount of accumulated p62 and LC3-II was lower in the MTMR2 KD SCs compared to the control cells (Figure 4.5E). This indicates that decreased basal expression level of LC3I and p62 is not due to the increased autophagy flux.

4.4.4 PIKfyve kinase inhibitor reverses SC phenotypes associated with MTMR2 knockdown

PIKfyve kinase generates $PI(3,5)P_2$ by phosphorylating PI3P. Inhibition of PIKfyve kinase activity has shown decreased level of $PI(3,5)P_2$ accumulation in MTMR2 KO cells (Vaccari et al., 2011) (Figure 4.6A). We tested whether the increased mTORC1 activity in MTMR2 KD SCs is due to increased $PI(3,5)P_2$. Cells were treated with different doses of PIKfyve inhibitor and mTORC1 activity was monitored. The immunoblot for pS6K shows that increased mTORC1 activity

in MTMR2 KD cells was reversed under the PIKfyve inhibitor treatment in a dose-dependent manner (Figure 4.6B). PIKfyve inhibition also reduced ULK1 phosphorylation in MTMR2 KD cells to the level comparable to control. The inhibitor treatment did not have an effect on ULK1 phosphorylation in control cells (Figure 4.6C). Similarly, PIKfyve inhibition restored TFEB activity in MTMR2 KD SCs (Figure 4.6D). This suggest that increased phosphorylation of ULK1 and decreased TFEB activity may be due to the changes in level of $PI(3,5)P_2$ level in MTMR2 KD SCs.

4.4.5 MTMR2 knockdown alters differentiated SC morphology

A morphological change of SCs in CMT4B1 is myelin outfolding, which is caused by excessive expansion of myelin membranes. Therefore, we first tested whether MTMR2 loss affects SC morphology. To visualize cell morphologies, we immunostained undifferentiated SCs for GFP since control and MTMR2 knockdown cells carry GFP in the backbone vector that allows for identification of infected cells. We first measured the length of undifferentiated SCs. We did not observe a significant difference in cell length between GFP labeled control cells and MTMR2 knockdown cells (Figure 4.7A). Next, we induced SC differentiation by treating the cells with db-cAMP. In control cultures, the SCs exhibited flattened morphology with the enlarged membrane; a typical morphology of differentiated cells. In the absence of MTMR2, SCs exhibited a morphology that appeared to have more elongated and narrowed processes compared to the controls (Figure 4.7B).

Aspect ratio (AR) analysis shows the cell morphology, specifically cell elongation by measuring the ratio of cell length versus cell width (Urbanski et al., 2016). The numeric analysis shows that cells with high AR ratio will have more elongated cell morphology. Analysis of the AR showed that the ratio was significantly increased in MTMR2 KD SCs (Figure 4.7C). To understand whether the elongated cell morphology was due to an excessive membrane expansion, we measured overall area of cells. No significant differences in overall area of cells were observed between control and MTMR2 KD SCs (Figure 4.7D).

Axonal contact is important for myelination by offering an instructive cue for SC myelination. To investigate whether a morphological change appears in SCs lacking MTMR2 when in the presence of the axonal contact, we plated MTMR2 KD SCs onto the DRG neuronal cultures and monitored SC morphology. We observed elongated cell morphology in MTMR2 KD SCs upon axon contact (Figure 4.7E). Compared to the cAMP-induced differentiated SCs, morphological changes in MTMR2 KD cells were more prominent in the presence of the axonal contact.

Next, we tested whether the cell morphology changes in differentiated SCs are associated with increased $PI(3,5)P_2$ levels in MTMR2 KD SCs. We treated a PIKfyve inhibitor to the differentiated SC cultures. PIKfyve inhibition reversed cell morphology changes in MTMR2 KD (Figure 4.7F).

4.4.6 MTMR2 loss attenuates Krox-20 expression without affecting myelin formation

For myelination in the PNS, SCs go through many stages of postnatal development including SC differentiation, initiation of myelin formation, extension of myelin sheath, determination of myelin thickness and internode length, and myelin maintenance. During these processes, appropriate expression levels of myelin genes or lipids are important for SC differentiation. mTORC1 pathway has been implicated in promoting the lipid biosynthesis and SC myelination. Recent studies showed that mTORC1 function through sterol regulatory element-binding protein (SREBP), which is one of mTORC1 targets, is important for SC differentiation by regulating lipid biosynthesis, which is required for myelin formation (Norrmén et al., 2014; Preitschopf et al., 2014). mTORC1 function has been indicated to regulate Krox-20, which is a promyelinating transcription factor. A study has shown a slightly increased Krox-20 expression in sciatic nerves from mTORC1 KO mice (Sherman et al., 2012).

We monitored the expression level of Krox-20 in MTMR2 KD SCs. First, we compared the Krox-20 expression in SCs induced to differentiate by db-cAMP treatment. While control SCs show induction of Krox-20 expression during differentiation, MTMR2 knockdown cells showed decreased Krox-20 compared to the control (Figure 4.8A). Interestingly, the expression level of the myelin-associated glycoprotein (MAG), one of the myelin proteins that is expressed in both differentiated and myelinating cells, was not significantly changed between control and the knockdown cells (Figure 4.8A). This indicates that in the absence

of MTMR2, expression of Krox-20 is impaired or attenuated in SCs under differentiating conditions, while the myelin protein expression is unaffected.

We tested whether MTMR2 loss affects Krox-20 expression and myelin formation in co-cultures. SCs were plated onto DRG neuron cultures and allowed to proliferate, and myelination was induced by addition of ascorbic acid (VitC). Levels of Krox-20 and MBP expression were monitored on Day 10 and day 21. On day 10 after initiating myelination, expression of Krox-20 and MBP were detected in co-cultures without a significant difference in the expression levels between control and KD cells. On day 21, control cultures showed further increase in both Krox-20 and MBP expression, whereas in MTMR2 KD culture, no detectable change in Krox-20 expression was observed, while MBP expression increased to a level compared to the control. (Figure 4.8B). Next, we tested whether decreased level of Krox-20 expression is reversed by PIKfyve treatment. To test this, cells were treated withYM201636 in the early stage of differentiation, which showed up-regulated mTORC1 activity and monitored Krox-20 expression level by western blot. In the control condition, decreased Krox-20 expression in MTMR2 KD SCs was observed. Upon the PIKfyve inhibitor treatment, decreased Krox-20 in MTMR2 mutant was not observed compared to the control (Figure 4.8C). This result indicates that MTMR2 loss that is associated with aberrant level of $PI(3,5)P_2$ affects level of Krox-20 expression in SCs.

To assess myelination, cultures were fixed and immunostained for MBP to visualize myelin segments on day 10 and 21 after myelination (Figure 4.9A).

Myelination assay was assessed by counting the number of MBP-positive myelin segments in control and MTMR2 KD cultures. There was no significant difference in numbers of myelin segments between control and MTMR2 knockdown cultures on both day 10 and 21 (Figure 4.9B). We also measured the length of individual myelin internodes, as an indication of myelin elongation and maturation. There was no significant difference in internode length between control and MTMR2 KD cultures (Figure 4.9C). This suggests that deficiency in MTMR2 function does not affect SC myelin formation in SC-DRG co-culture system *in vitro*.

4.5 Discussion

Mutations in MTMR2 gene have been identified to cause the demyelinating disease, CMT4B1 (Bolino et al., 2000). However, a molecular mechanism of how loss of MTMR2 induces dysmyelination and myelin outfolding is not well understood. Previous studies showed that deletion of mTOR function in SCs showed a hypomyelination (Sherman et al., 2012; Norrmén et al., 2014). This indicates that mTOR signaling pathway involves in SC myelination.

$PI(3,5)P_2$ has been shown to regulate lysosomal mTORC1 activation by recruiting downstream effectors (Jin et al., 2014). Loss of MTMR2 leads to accumulation of $PI(3,5)P_2$ (Vaccari et al., 2011; Ng et al., 2013), suggesting that it may affect activation of mTORC1 targets in SCs.

Here, we first showed increased mTORC1 activity and effects on its downstream signaling pathways in MTMR2 deficient SCs. Thus, our following question was how mTORC1 activation is increased in MTMR2 KD SCs and what are the consequences of increased mTORC1 in MTMR2 KD cells.

mTORC1 activity is known to be regulated by growth factor-induced AKT signaling (Norrmén and Suter, 2013). In SCs, the PI3-kinase/ AKT/ mTOR signaling pathway is a main signaling cascade for myelination that is mainly regulated by Nrg1/ErbB signaling (Nave and Salzer, 2006; Nave, 2010). However, we did not observe a significant change in level of phospho-AKT as shown in Figure 4.2B. In addition, MTMR2 KD did not affect the Ras/ Raf/ MAPK signaling pathway, which is also known to regulate mTORC1 activity (Figure

4.2B). This result suggests that increased mTORC1 activation in MTMR2 KD SCs is induced downstream of AKT or Erk1/2.

Activity of mTORC1 on the lysosome is regulated by effectors, such as Rags and Rheb, which are GTPases anchoring on the lysosomal membrane as described in Figure 4.3A (Betz and Hall, 2013; Puertollano, 2014). To understand whether the increased mTORC1 activity in MTMR2 KD SCs is associated with changes in expression level of the mTORC1 regulators, we monitored overall expression levels of the regulators, such as Raptor, Rheb, RagA, and RagD. We did not observe significant changes in overall expression levels of these molecules (Figure 4.4B), suggesting that increased mTORC1 activity in MTMR2 KD SCs was not due to the increased expression levels of the mTOR regulators.

A possible reason for the increase in mTORC1 activity in MTMR2 KD SCs may be an increase in mTORC1 association to lysosomal membrane, where mTORC1 activity is regulated. Recent studies showed that $PI(3,5)P_2$ provides a platform for mTORC1 signaling, promoting recruitment of its substrate S6K to the lysosomal membrane (Bridges et al., 2012; Jin et al., 2014). In addition, Loss of MTMR2 has been shown to result in accumulation of $PI(3,5)P_2$ in fibroblast cells (Vaccari et al., 2011). This suggest a possibility of increased recruitment of mTORC1 to the lysosomal membrane due to the increased level of $PI(3,5)P_2$ in MTMR2 deficient cells.

We monitored mTORC1 localization on the lysosomes. The results showed an increased co-localization of mTORC1 to the lysosomes in MTMR2 KD SCs (Figure 4.4C). Therefore, the increased mTORC1 activity in MTMR2 KD

SC is likely due to an increased recruitment of mTORC1 to the lysosomal membrane where mTORC1 activity is regulated.

The cellular level of $PI(3,5)P_2$ is controlled by phosphatases and kinases, such as MTMR2 and PIKfyve, respectively. A study showed that the myelin outfolding phenotype in MTMR2 KO myelinating cultures was decreased by inhibiting the function of PIKfyve kinase that promotes the production of $PI(3,5)P_2$ (Vaccari et al., 2011). Accordingly, we tested whether the mTORC1 activity in MTMR2 KD SCs can be reversed by PIKfyve inhibition. Treatment with PIKfyve inhibitor decreased mTORC1 activity in MTMR2 KD SCs (Figure 4.6B), suggesting that $PI(3,5)P_2$ contributes to the mTORC1 activation in the MTMR2 KD cells.

Another possible mechanisms by which MTMR2 loss contributes to mTOR activation is through $PI(3,5)P_2$-mediated opening of calcium channels on the lysosomal membrane. $PI(3,5)P_2$ binds and activates TRPML, a lysosome-associated calcium channel, thus increasing intracellular calcium (Dong et al, 2010). A recent study showed that increased lysosomal calcium efflux through TRPML channels activates mTORC1 by promoting its interaction with calmodulin (CaM) (Li et al., 2016). Interestingly, a recent study showed that, in the absence of Fig4, which resulted in $PI(3,5)P_2$ down-regulation, the lysosome TRPML activity was decreased resulting in calcium accumulation in lysosomal compartment. The lysosomal defects in Fig4 deficient cells were reversed by re-activating TRPML channels with an agonist for TRPML (Zou et al., 2015). These results suggest a possibility that increased mTORC1 activity in MTMR2 KD SCs

may be associated with increased calcium efflux from the lysosome resulting from an increased $PI(3,5)P_2$ that activates TRPML. Supporting this, we observed that treatment with a TRPML agonist increases mTORC1 activation in SCs, mimicking the effect of MTMR2 KD (data not shown).

To assess the consequences of increased mTORC1 activity in MTMR2 KD SCs, we monitored activities of mTOR downstream effectors including ULK1 and TFEB. ULK1 is a kinase that promotes autophagy, and phosphorylation by mTORC1 inhibits its functions. We observed an increase in phospho-ULK1 level in MTMR2 KD SCs (Figure 4.5A), suggesting an inhibition of autophagy. Supporting this, ULK phosphorylation was accompanied by a decrease in LC3I and p62 expression, suggesting a defect in autophagy induction.

TFEB is a target protein of mTORC1 that regulates lysosomal biogenesis and function. Our results from the CLEAR assay, which measures the activity of TFEB indirectly, indicate that transcriptional activity of TFEB is decreased in MTMR2 KD SCs (Figure 4.5C). This may lead to aberrant lysosomal biogenesis and /or function. Not only does loss of MTMR2 function result in a defect of autophagy induction, this could also cause an imbalance between the catabolic and anabolic regulations of myelin proteins and lipids, resulting in disruption of myelin homeostasis. The increased phosphorylation of ULK1 and decreased TFEB activity in MTMR2 KD SCs were reversed by PIKfyve inhibition, suggesting that the defects are associated with the increased $PI(3,5)P_2$ levels in the MTMR2 KD SCs.

Myelin outfolding is a common phenotype of CMT4B1 patients, and it was recapitulated in MTMR2 null mice (Bolino et al., 2004; Bolis et al., 2005; Ng et al., 2013). However, we did not observe myelin outfolding in our co-culture system using the MTMR2 KD SCs. It may be due to the insufficient knockdown of MTMR2 since we frequently observed 70-80% knockdown at the protein level following lenti-viral shRNA transduction against MTMR2 transcript. CMT4B1 is an autosomal recessive inherited disease that is caused by complete loss of protein functions (Dubourg et al., 2006). In our system, MTMR2 KD SCs still contain 20-30% functional MTMR2 proteins, which may be sufficient to prevent full indication of myelin defects. Although myelin outfolding was not observed, we did observe an increase in myelin protein expression accompanied with the decreased Krox-20 level in MTMR2 KD SCs (Figure 4.8A), which may indicate an imbalance in transcriptional regulation of myelin protein expression. In a previous study, SC-specific deletion of mTOR, which results in PNS hypomyelination, showed a decrease in myelin protein accompanied with increased Krox-20 in sciatic nerves (Sherman et al., 2012). This suggests the level of Krox-20 expression may be related to regulating myelin protein expressions through mTOR signaling pathway.

Although myelin morphology appeared normal, MTMR2 KD SC exhibited aberrant cell morphology prior to myelin formation. Individual cell length was significantly longer than control SC, especially when the cells were in contact with axons. It is unclear whether the morphological defect contributes to subsequent myelin abnormality in CMT4B1 patients. However, it clearly indicates

aberrant cytoskeletal organization in the absence of MTMR2. mTORC2 has been shown to regulate cytoskeletal dynamic through Rho GTPase activation. In our study, the high mTORC1 activation appears to inhibit mTORC2, shown by a slight decrease in the level of AKT phosphorylation at serine 473. To support this, a study has shown that inhibition of Rho GTPases induced elongated SC morphology (Melendez-Vasquez, 2004).

In conclusion, we investigated the effects of MTMR2 KD on the intracellular signaling function of SCs. We found that MTMR2 KD results in increased mTORC1 activation in a PI(3,5)P2 associated manner. MTMR2 KD also results in increased phosphorylation of S6K, ULK1 and TFEB, but not 4EBP1. The increase in mTORC1 signaling is associated with inhibition of autophagy induction, overproduction of myelin protein, and changes in SC morphology. These events that are associated with increased mTORC1 activity may induce an imbalance of anabolic and catabolic metabolisms in SCs.

4.6 Figures and Figure legends

Figure 4.1.

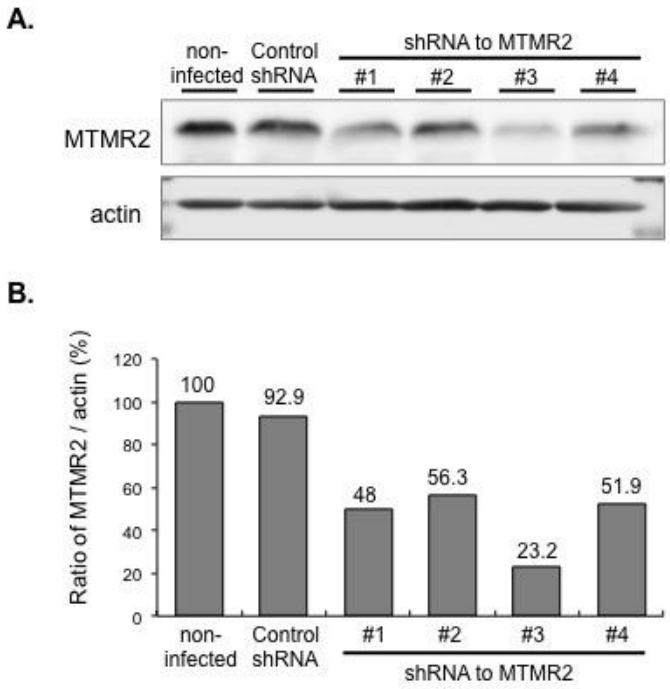

Figure 4.1. Generation of MTMR2 knockdown SCs.

Four different shRNA constructs were designed against the MRMR2 gene. Schwann cells infected with lentivirus encoding each of shRNA sequences against MRMR2 were generated. MTMR2 knockdown efficiency for each construct was assessed by Western blot analysis. (A) Immunoblot for MTMR2 showed different KD efficiencies on MTMR2 by different shRNA constructs to MTMR2. (B) Corresponding quantification of blot. Among four different constructs, construct #3 (red labeled) showed most efficient knockdown with about 76%of MTMR2 compared to the controls, non-infected and shRNA control.

Figure 4.2.

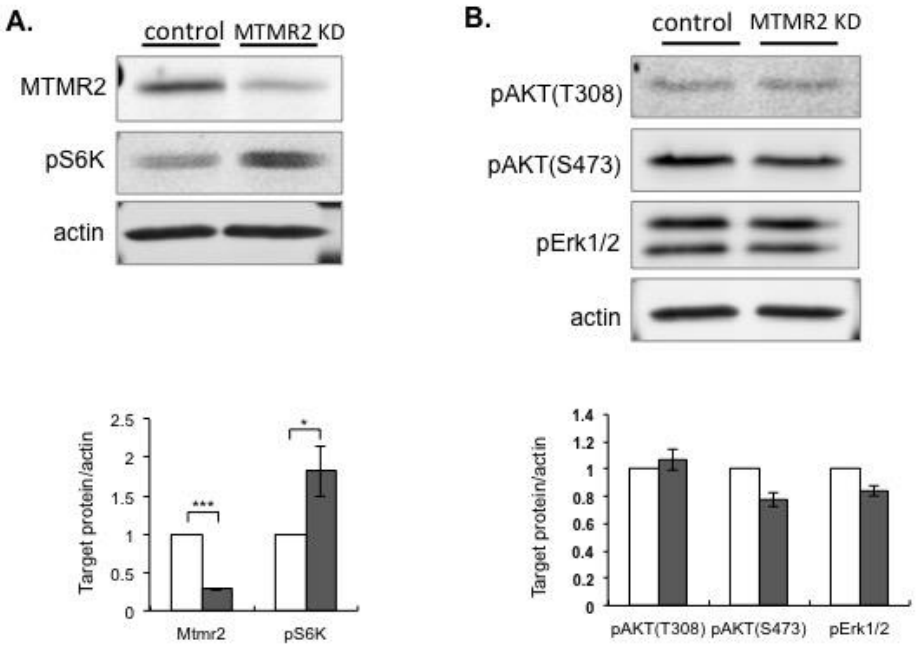
A.
control
MTMR2 KD
MTMR2
pS6K
actin
Target protein/actin
2.5
2
1.5
1
0.5
0
***
*
Mtmr2
pS6K
B.
control
MTMR2 KD
pAKT(T308)
pAKT(S473)
pErk1/2
actin
Target protein/actin
1.4
1.2
1
0.8
0.6
0.4
0.2
0
pAKT(T308)
pAKT(S473)
pErk1/2

Figure 4.2. Increased mTORC1 activity is independent of AKT and Erk1/2 pathways in MTMR2 knockdown SCs.

(A) Immunoblots for phospho-S6K and MTMR2 (top) and its quantification (bottom) showing an increase of mTORC1 activity in MTMR2 knockdown cells. *** $p<0.001$, * $p<0.05$, The means +/- SEM were determined from three independent experiments. (B) Immunoblots for phospho-AKTs (T308 and S473) and phospho-Erk1/2, which are upstream molecules that activate mTORC1 signaling pathway (top) and quantification of immunoblots shown in B (bottom). No changes in activation of either AKTs or Erk1/2 while mTORC1 were significantly increased in MTMR2 KD SCs. The means +/- SEM were determined from three independent experiments.

Figure 4.3.

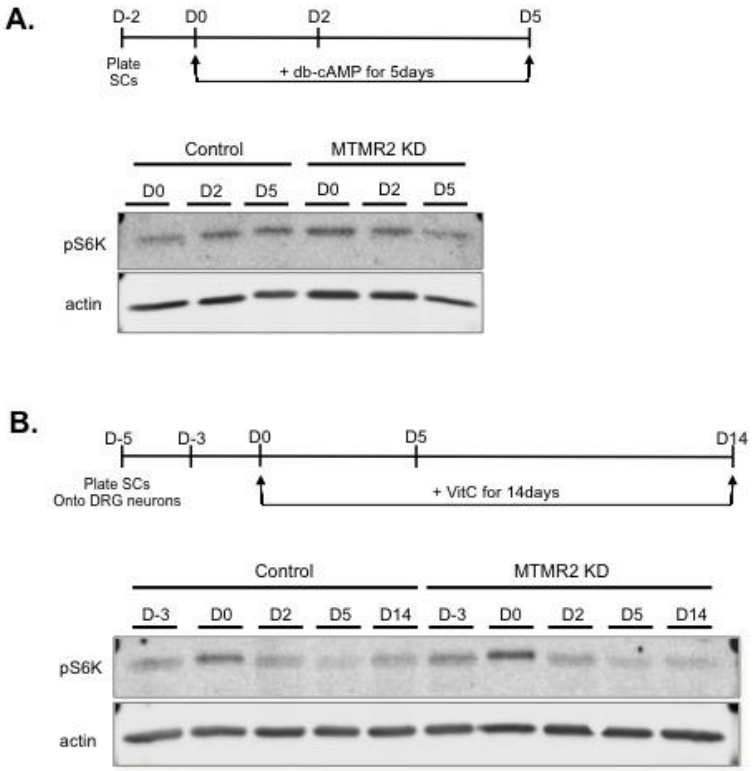
A.
D-2
D0
D2
D5
Plate SCs
+ db-cAMP for 5days
Control
MTMR2 KD
D0
D2
D5
D0
D2
D5
pS6K
actin
B.
D-5
D-3
D0
D5
D14
Plate SCs Onto DRG neurons
+ VitC for 14days
Control
MTMR2 KD
D-3
D0
D2
D5
D14
D-3
D0
D2
D5
D14
pS6K
actin

Figure 4.3. mTORC1 activity is higher in MTMR2 knockdown SCs in early stages of differentiation and myelination.

(A) SCs were treated with db-CAMP for 5 days to induce differentiation. Cell lysates were harvested at the different time points (day 0, 2, and 5 after db-cAMP treatment) during the differentiation as shown in the schematic diagram of the experiment (top). Corresponding western blot analysis (bottom). Blots for phospho-S6K shows that MTMR2 KD shows increased mTORC1 activity at the beginning of differentiation. (B) SCs were plated onto DRG neurons and cultured for 5 days. Myelination was induced with VitC treatment for 14 days and lysates were collected at different time points (3 days before or 0, 2, 5, 14 days after induction of myelination) during the myelination as described (top). Immunoblot for phospho-S6K shows that increased mTORC1 activity in MTMR2 appears in early stage of myelination in co-cultures with MTMR2 KD SCs (bottom).

Figure 4.4.

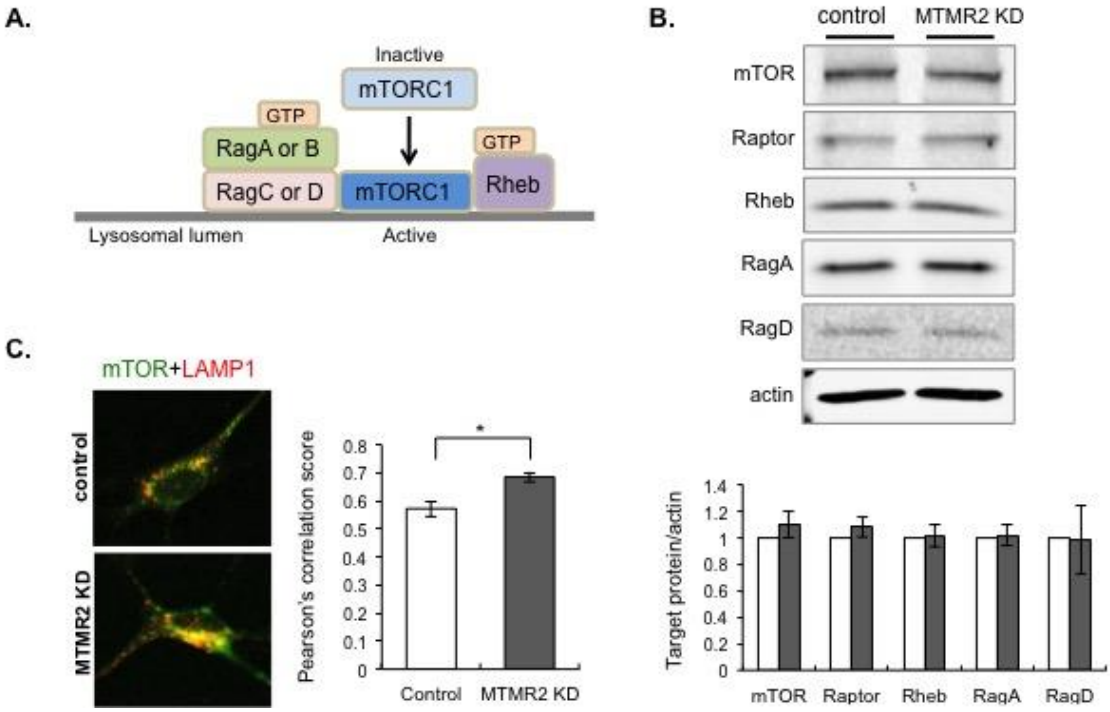
A.
Inactive
mTORC1
GTP
RagA or B
RagC or D
mTORC1
GTP
Rheb
Lysosomal lumen
Active
B.
control
MTMR2 KD
mTOR
Raptor
Rheb
RagA
RagD
actin
Target protein/actin
mTOR
Raptor
Rheb
RagA
RagD
C.
mTOR+LAMP1
control
MTMR2 KD
Pearson's correlation score
Control
MTMR2 KD

Figure 4.4. Loss of MTMR2 increases mTORC1 localization to the lysosomes without affecting expression levels of mTORC1 effectors on the lysosomes.

(A) Schematic of effector proteins on lysosomal membrane that regulate mTORC1 activity. (B) Immunoblots for MTMR2, pS6K and mTORC1 regulators (top). Quantification from the immunoblots (bottom) showing that no changes in overall expression levels of mTORC1 regulators have been observed while mTORC1 is significantly increased in MTMR2 KD SCs. (C) Undifferentiated SCs were immunostained for mTORC1 and LAMP1, a lysosomal marker (left). A Score of Pearson's Correlation shows increased mTORC1 localization to lysosomes in MTMR2 KD SCs compared to control (right). * $p<0.05$, The means +/- SEM were determined from three independent experiments.

Figure 4.5.

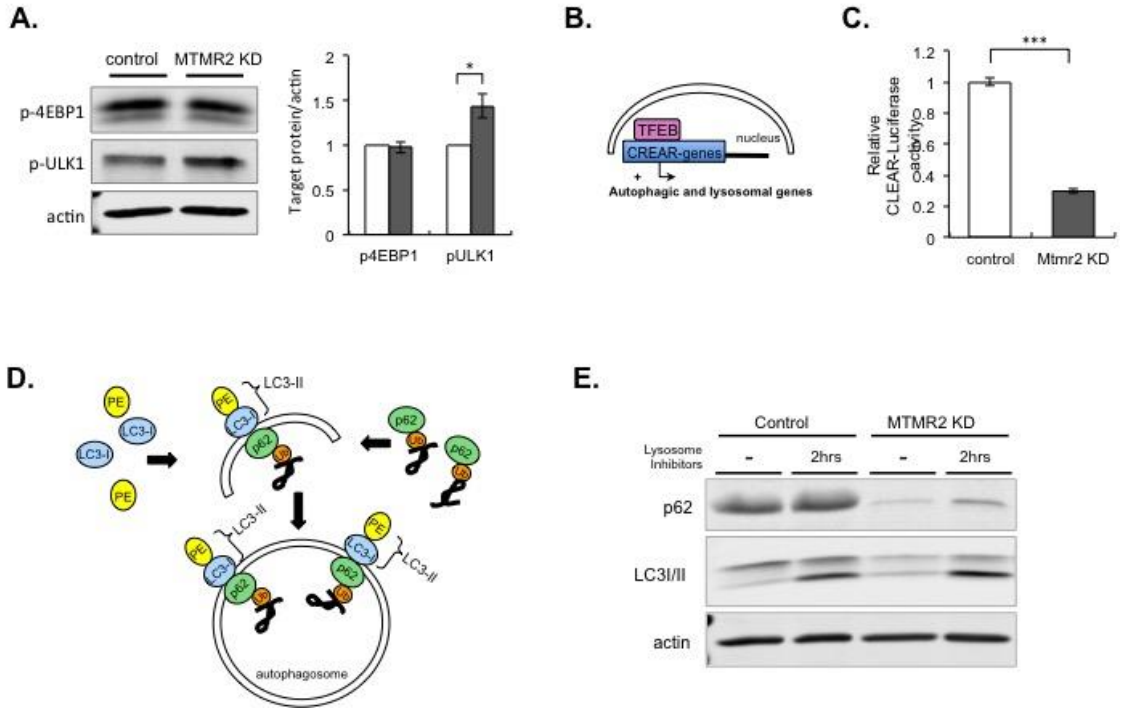
A.
control
MTMR2 KD
p-4EBP1
p-ULK1
actin
Target protein/actin
p4EBP1
pULK1
B.
TFEB
nucleus
CREAR-genes
Autophagic and lysosomal genes
C.
Relative CLEAR-Luciferase activity
control
Mtmr2 KD
D.
PE
LC3-I
LC3-II
p62
autophagosome
E.
Control
MTMR2 KD
Lysosome Inhibitors
2hrs
p62
LC3I/II
actin

Figure 4.5. MTMR2 knockdown reduces the basal level autophagy induction.

(A) Immunoblots for phospho-4EBP1, phospho-ULK1 (left) and quantification (right) showing that level of phospho-ULK1, which inhibits autophagy, was up regulated in MTMR2 knockdown cells while there was no change in the level of phospho-4EBP1. * $p<0.05$, The means +/- SEM were determined from three independent experiments. (B) Schematic of translocalization of TFEB into nucleus, resulting in autophagic and lysosomal gene expressions (left). A graph shows the decreased luciferase activity by CLEAR assay (right) indicating decreased TFEB activity in MTMR2 KD SCs compared to the control.

(C) Schematic of processes in autophagosome formation. *** $p<0.001$, The means +/- SEM were determined from three independent experiments. (D) Schwann cells were treated with lysosome inhibitors for two hours to block its functions, resulting in less degradation of proteins. Immunoblots for p62 and LC3I/II show that basal levels of p62 and LCI/II are decreased in MTMR2 KD SCs in the absence of the inhibitor. In presence of the inhibitor, autophagy flux appeared to happen in both control and MTMR2 KD SCs.

Figure 4.6.

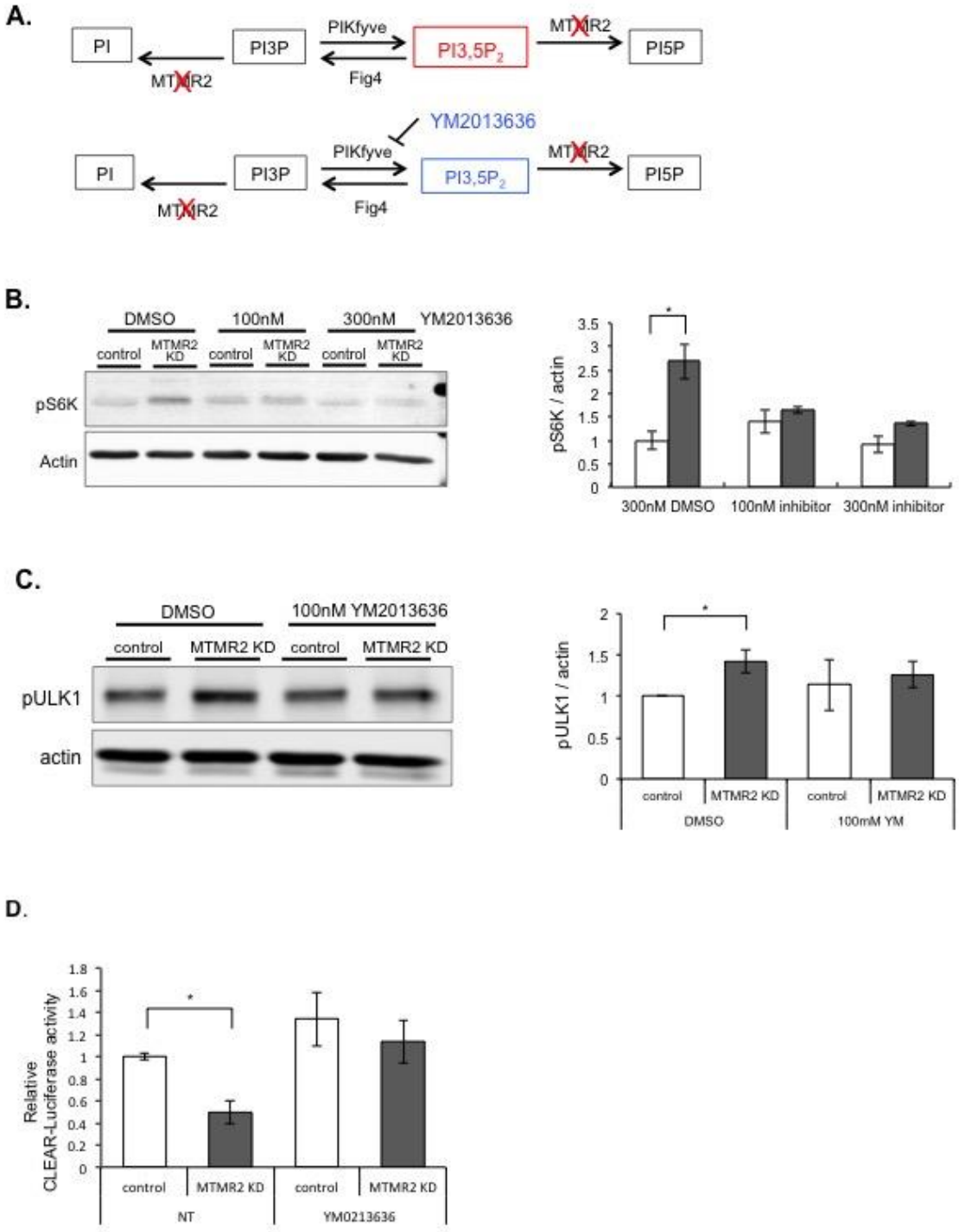
A.
PI
PI3P
PIKfyve
PI3,5P2
MTMR2
PI5P
Fig4
YM2013636
B.
DMSO
100nM
300nM
YM2013636
control
MTMR2 KD
pS6K
Actin
pS6K / actin
300nM DMSO
100nM inhibitor
300nM inhibitor
C.
100nM YM2013636
pULK1
actin
pULK1 / actin
100mM YM
D.
Relative CLEAR-Luciferase activity
NT
YM0213636

Figure 4.6. Increased mTORC1 activity and ULK1 phosphorylation in MTMR2 knockdown SCs are reversed by PIKfyve inhibitor treatment.

(A) Schematic of regulation of phospholipids in MTMR2 deficient SCs (top) and regulation of phospholipids in MTMR2 KD SCs upon the PIKfyve inhibitor, YM2013636, treatment (bottom). (B) Immunoblot for phospho-S6K (left). The quantification shows that treatment with PIKfyve inhibitor reverses increased pS6K in dose-dependent manner (right). * $p<0.05$, The means +/- SEM were determined from three independent experiments. (C) Immunoblot for phospho-ULK1 (left) and its quantification, showing an increase in phospho-ULK1 in MTMR2 knockdown SCs is reversed by 100nM of PIKfyve inhibitor treatment (right). * $p<0.05$, The means +/- SEM were determined from three independent experiments. (D) The CLEAR assay shows that decreased TFEB activity in MTMR2 knockdown cells was restored upon the 100nM PIKfyve inhibitor treatment. * $p<0.05$, The means +/- SEM were determined from three independent experiments.

Figure 4.7.

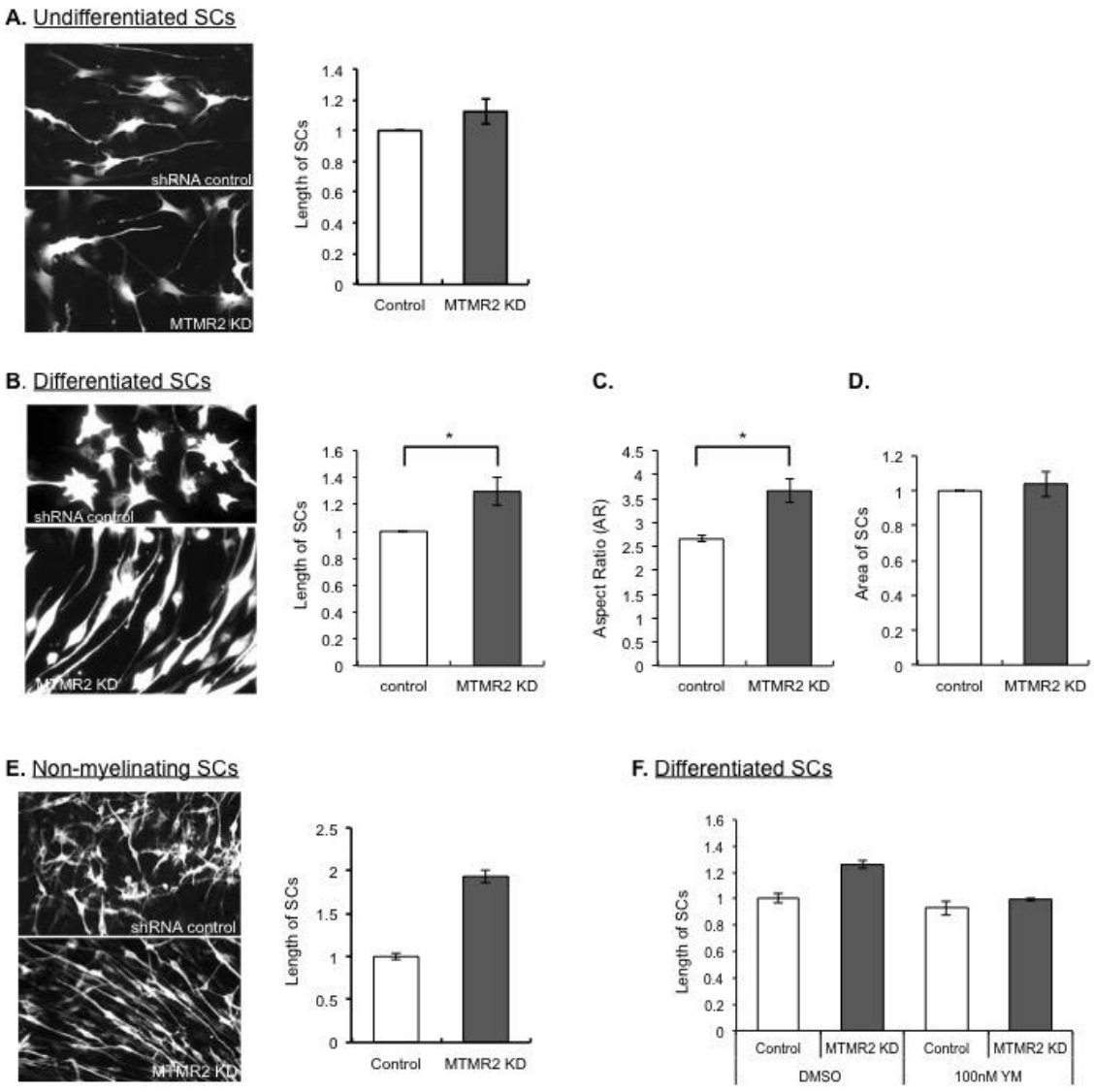
A. Undifferentiated SCs
shRNA control
MTMR2 KD
Length of SCs
Control
MTMR2 KD
B. Differentiated SCs
shRNA control
MTMR2 KD
Length of SCs
control
MTMR2 KD
C.
Aspect Ratio (AR)
control
MTMR2 KD
D.
Area of SCs
control
MTMR2 KD
E. Non-myelinating SCs
shRNA control
MTMR2 KD
Length of SCs
Control
MTMR2 KD
F. Differentiated SCs
Length of SCs
Control
MTMR2 KD
Control
MTMR2 KD
DMSO
100nM YM

Figure 4.7. MTMR2 knockdown alters Schwann cell morphology

(A) Undifferentiated SCs were immunostained for GFP to visualize cell morphology (left). A graph shows that there was no difference in length of cells between control and MTMR2 KD cells (right). The means +/- SEM were determined from three independent experiments. (B) db-cAMP induced differentiated SCs were immunostained for GFP as shown in left. The graph shows increased cell lengths in MTMR2 KD SCs compared to the control (right). * $p<0.05$, The means +/- SEM were determined from three independent experiments. (C) A graph shows the increased average values of aspect ratio (AR), ratio of cell length vs. cell width, indicating elongated cell shapes in differentiated MTMR2 KD SCs. * $p<0.05$, The means +/- SEM were determined from three independent experiments. (D) A graph shows that MTMR2 loss does not affect area of cells in differentiated SCs. The means +/- SEM were determined from three independent experiments. (E) SCs were plated on DRG neurons. Nonmyelinating SCs on the DRG axons were visualized by immunostaining for GFP (left). A graph shows that MTMR2 KD non-myelinating SCs show elongated processes along the axons compared to the control (right). The means +/- SEM were determined from two independent experiments.

(F) SCs were treated with 100nM of YM2013636 for 24 hours before inducing differentiation with 0.75mM of db-cAMP. Five days later, cultures were immunostained for GFP and the length of individual cells were measured. Data was collected from three cultures per condition per experiments. The means +/- SEM were determined from two independent experiments.

Figure 4.8.

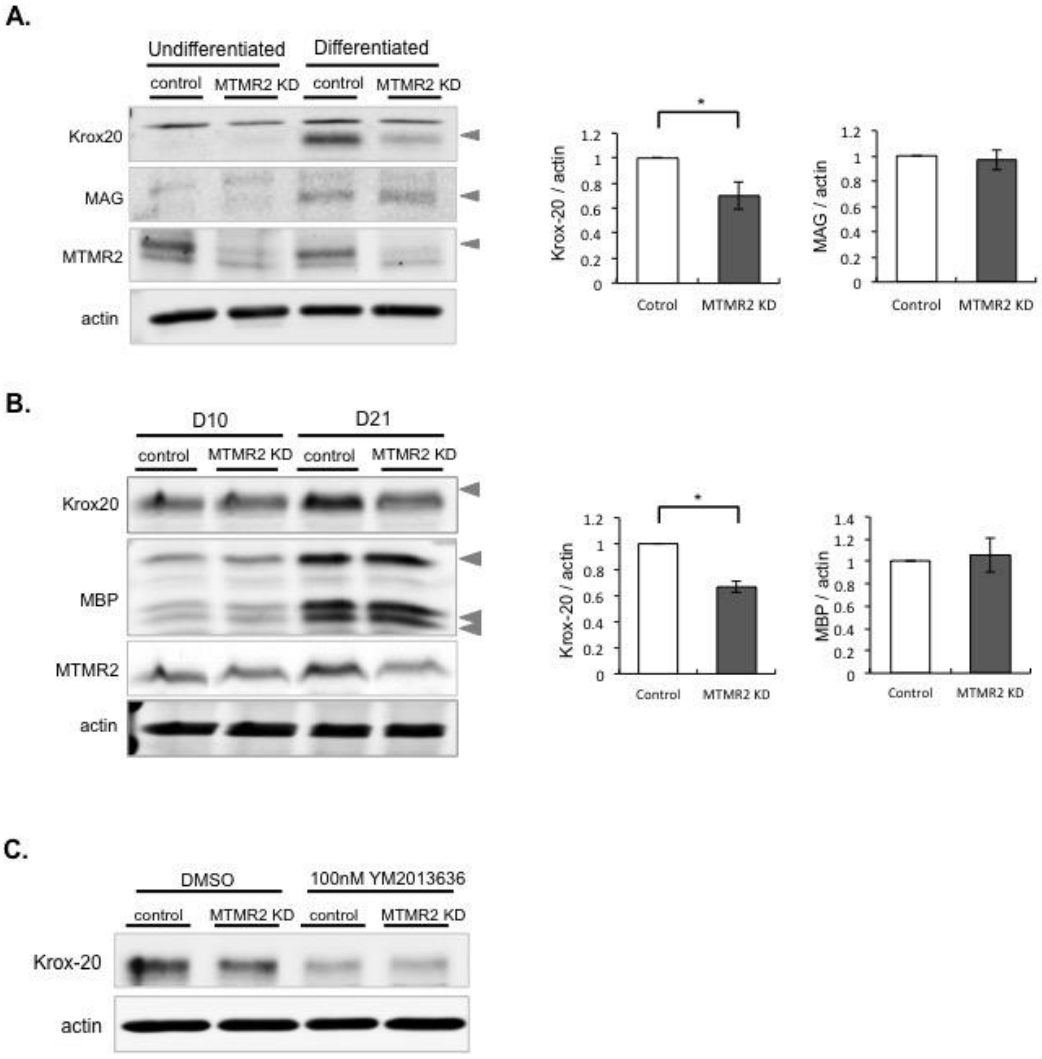
A.
Undifferentiated
Differentiated
control
MTMR2 KD
control
MTMR2 KD
Krox20
MAG
MTMR2
actin
Krox-20 / actin
MAG / actin
Cotrol
MTMR2 KD
Control
MTMR2 KD
B.
D10
D21
control
MTMR2 KD
control
MTMR2 KD
Krox20
MBP
MTMR2
actin
Krox-20 / actin
MBP / actin
Control
MTMR2 KD
Control
MTMR2 KD
C.
DMSO
100nM YM2013636
control
MTMR2 KD
control
MTMR2 KD
Krox-20
actin

Figure 4.8. MTMR2 knockdown attenuates Krox-20 expression.

(A) Schwann cells were treated with 0.75mM of db-cAMP to induce differentiation. Five days later, cells were processed for Western blot analysis. Immunoblots for Krox-20, MAG and MTMR2 (left) and the result of quantifications for level of Krox-20 and MAG from the blots (right), showing decreased Krox-20 expression with no changes in the level of MAG expression in differentiated MTMR2 KD SCs. * $p<0.05$, The means +/- SEM were determined from three independent experiments. (B) Myelinating co-cultures with either control SCs or MTMR2 KD SCs were harvested 10 days or 21 days after myelin induction with VitC treatment. Immunoblots for Krox-20, MBP, and MTMR2 in myelinating co-cultures after induction of myelination for 10 days or 21 days (left) and quantification for day 21 blots (right). No significant changes were observed at day 10 between control and MTMR2 KD cells. The quantification shows decreased Krox-20 expression on day 21 without affecting MBP expression in MTMR2 KD SCs. * $p<0.05$, The means +/- SEM were determined from three independent experiments. (C) Expression level of Krox-20 in differentiated SCs that were treated with 0.75mM db-cAMP. Immunoblots for Krox-20 shows no significant differences between control and MTMR2 KD SCs in the presence of 100nM YM201636 while decreased Krox-20 in MTMR2 KD SCs were observed in the control condition.

Figure 4.9.

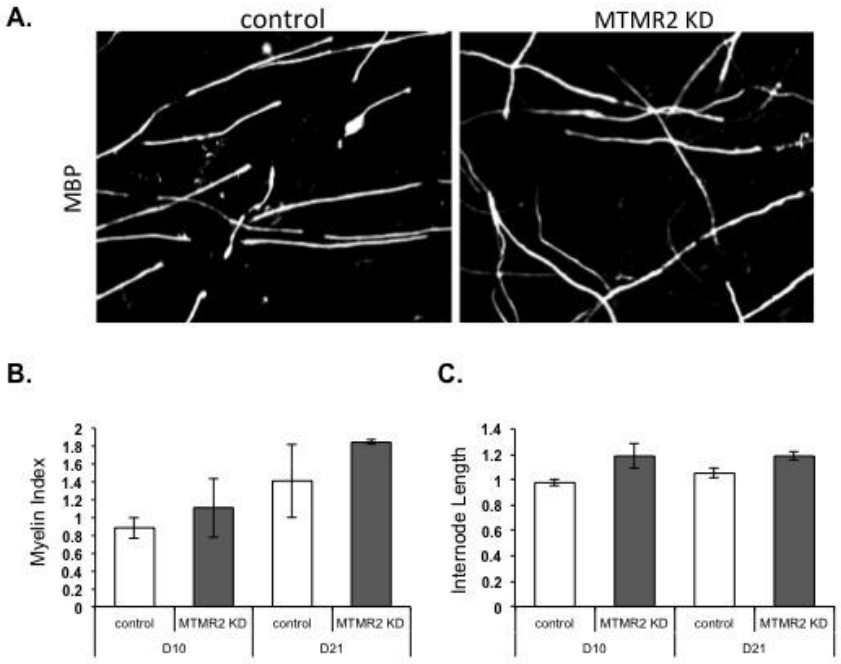
A.
control
MTMR2 KD
MBP
B.
Myelin Index
2
1.8
1.6
1.4
1.2
1
0.8
0.6
0.4
0.2
0
control
MTMR2 KD
control
MTMR2 KD
D10
D21
C.
Internode Length
1.4
1.2
1
0.8
0.6
0.4
0.2
0
control
MTMR2 KD
control
MTMR2 KD
D10
D21

Figure 4.9. MTMR2 loss does not affect myelin formation.

(A) Myelinating cultures with control or MTMR2 KD SCs were immunostained for MBP to visualize myelinated segments. (B) Myelin index shows no significant differences in numbers of myelin segments between control and MTMR2 KD SCs at the time of day 10 and day 21 after myelin induction by VitC treatment. (C) The measurement of myelin internodes' length shows no changes between control and MTMR2 KD SCs at the time of day 10 and day 21 after myelination is induced. The means +/- SEM were determined from two independent experiments.

5. Chapter two: Tissue Inhibitor of Metalloproteinase-3 (TIMP-3) promotes Schwann cell myelination

5.1. Abstract

Tissue inhibitor of metalloproteinase-3 (TIMP-3) inhibits activities of various metalloproteinase including MMPs and ADAM family proteins. In the peripheral nervous system, ADAM17, also known as TACE, cleaves extracellular domain of Nrg1 type III, an axonal growth factor that is essential for Schwann cell myelination. The processing by ADAM17 attenuates Nrg1 signaling and inhibits Schwann cell (SC) myelination. TIMP-3 targets ADAM17, suggesting a possibility that TIMP-3 may elicit a promyelinating function in SCs by relieving ADAM17-induced myelination block. To investigate this, we used myelinating co-culture system to determine the effect of TIMP-3 on SC myelination. Treatment with TIMP-3 enhanced myelin formation in co-cultures, evident by an increase in the number of SC generated myelin segments and up-regulated expression of Krox20 myelin protein expression. Treatment with TIMP-3 also increased Nrg1 type III signaling in co-culture, suggesting its function towards inhibition of ADAM17. Supporting this, the N-terminus fragment of TIMP-3, which exhibits a selective inhibitory function towards ADAM17, elicited a similar myelination promoting effects and increased Nrg1 type III activity. TIMP-3 also increased total laminin contents in co-cultures indicating its role in modulating ECM components during SC myelination.

5.2. Introduction

5.2.1 Regulation of Nrg1-III by metalloproteinases

Myelination in the peripheral nervous system (PNS) is regulated by a close-contact signaling between axon and Schwann cells (SCs). One of the axonal factors that provides key promyelinating signal is neuregulin type III (Nrg1 type III), which activates ErbB2/3 heterodimeric receptor complex on the SC surface (Falls, 2003). Subsequent activation of the downstream PI3-kinase/AKT pathway is regarded as a crucial signaling event that promotes Nrg1 type III-induced SC myelination (Maurel and Salzer, 2000; Taveggia et al., 2005).

Nrg1 type III is a type I membrane protein, which expression is enriched in the PNS neurons (Ho et al., 1995; Meyer et al., 1997). Unlike the other members of the Nrg1 family, type III Nrg1 acquires a two transmembrane structure through the N-terminus cystine-rich domain that anchors itself into the plasma membrane (Falls, 2003). Proteolytic processing at the juxtamembrane region by various proteases generates a membrane anchored N-terminus fragments (NTF) that presents a signaling-capable EGF domain to the luminal space (Falls, 2003). Notably, Nrg1 type III processing by □-secretase (or BACE1) generates an NTF that activates ErbB receptors and promotes SC myelination. Similarly, ADAM10, a member of disintegrin metalloprotenase family also generates Nrg1 NTF that activates ErbB receptor signaling, albeit without an effect on SC myelination (Luo et al., 2011). In comparison, processing of Nrg1 type III by ADAM17 (or TACE) generates an NTF that attenuates ErbB receptor signaling and inhibits AKT activation (La Marca et al., 2011), indicating its role as a negative regulator of the

axonal Nrg1 signaling. Supporting this, knockdown of ADAM17 in the PNS enhances Nrg1 type III-associated AKT activation and increases SC myelination (La Marca et al., 2011). These findings suggest that the myelin-promoting activity of Nrg1 type III is regulated by combined activities of proteases that modulate the signaling effectiveness of the Nrg1 NTF.

5.2.2 Role of TIMP-3 on TACE activity

Tissue inhibitors of metalloproteinases (TIMPs) are endogenous inhibitors of matrix metalloprotenases (MMPs) and ADAM family proteins. Among the TIMPs, TIMP3 has the broadest inhibition spectrum towards ADAM proteins that include ADAM10 and ADAM17 (Nagase and Murphy, 2008). More important, TIMP3 is the only member of the TIMP family able to effectively inhibit ADAM17 (Amour et al., 1998). Considering the role of ADAM 17 as an endogenous inhibitor of axonal Nrg1 signaling and PNS myelination, it is possible that the inhibitory function of TIMP3 towards ADAM 17 may be effective in promoting SC myelination.

In this study, we used DRG neuron-Schwann cell co-cultures to investigate the effects of TIMP3 on SC myelination. We observed that TIMP3 promoted myelin formation by increasing both the numbers and the lengths of individual myelin segments generated by SCs. A similar effect was observed with the N-terminus domain of TIMP3, which exhibits a selective inhibitory function towards ADAM17. TIMP3 also increased axon-contact mediated AKT activation in SCs,

indicating that the promyelinating effect is likely mediated by an increased Nrg1 type III signaling in SCs.

5.3. Materials and Methods

Media

D10 media [Dulbecco's Modified Eagle's medium (DMEM) supplemented with 10% FBS, 1% glutamine, 0.1 mg/ml penicillin/streptomycin]; NB media [neurobasal medium with B-27 supplement, 0.08% glucose, 1% glutamine, 0.1 mg/ml penicillin/streptomycin and 50 ng/ml nerve growth factor (NGF) (#BT-5017, Harlan Laboratories, Inc.)]; C10 media [Minimal Essential Medium (MEM) containing 10% FBS, 0.08% glucose, and 50ng/ml NGF]; N2 media [F12/ DMEM (1:1) medium supplemented with N2 supplement, and 50ng/ml NGF].

Antibodies

The following primary antibodies were used for immunostaining or Western blot analysis: anti-mouse myelin basic protein (MBP) [1:300, #SMI-94R (Covance)], anti-mouse BrdU [1:1000, #B2531 (Sigma)], anti-rabbit phospho-AKT [1:1000, # 4051 (Cell Signaling Technology)], anti-rabbit phospho-Erk1/2 [1:5000, #V8031 (Promega)], anti-rabbit total-AKT [1:1000, #9272 (Cell Signaling Technology)], anti-rabbit total Erk1/2 [1:5000, #V1141 (Promega)], anti-rabbit phospho-ErbB3 were used [1:500, #4791 (Cell signaling)], anti-rabbit laminin [1:1000, #ab11575 (Abcam)], anti-mouse β-actin [1:5000, #A5441 (Sigma)].

Schwann cell preparation and cultures

Schwann cells were isolated from postnatal day 2 (P2) rat sciatic nerves. Dissected sciatic nerves were treated with trypsin-collagenases (L15 media

supplemented with 0.225% trypsin and 0.1% of collagenase) at 37 °C. Thirty minutes later, cells were spun down at 50 g for 5 minutes and dissociated by pipetting in NB media. All dissociated cells were plated in a PLL-coated 60mm dish. Next day, cells were treated with D10 media supplemented with 10μM cytosine-ß-arabino furanoside hydrochloride (AraC) (#C6645, Sigma) to avoid fibroblast contamination. Two-three days after cultures were washed with HBSS and replaced with D10 media supplemented with 10ng/ml EGF-domain of heregulin (#396-HB-050, R&D systems) and 2.5μM forskolin (#F6886, Sigma).

Once cells were confluent, cells were harvested by 0.25% Trypsin-EDTA and spun at 200 g for 5 minutes at room temperature. Harvested cells were treated with 20μl of Thy1.1 (#MCA04G, AbD Serotech) antibody in 1ml of D10 media and incubated at 37 °C. Thirty minutes later, cells were spun down at 200 g for 5 minutes at room temperature and treated with 1ml of rabbit complement (#S7764, Sigma), and incubated for 30 minutes at 37 °C. After spinning cells down, cells were plated in PLL-coated 100mm dish and expanded in D10 media supplemented with 10ng/ml EGF-domain of heregulin and 2.5μM forskolin.

Dorsal root ganglia neuron (DRG) cultures and DRG-Schwann cell co-cultures

Dorsal root ganglion (DRG) neurons were dissected from E15 rat embryos and incubated with 0.25% trypsin for 30 minutes at 37°C. Cells were spun down at 50 g for 10 minutes at room temperature and resuspended in NB media. Cells were plated onto matrigel (BD)-coated glass coverslips at the density of 0.7-0.8

DRGs/coverslip in NB media. After 24 hours, Cells were treated with NB media with 15μM 5-fluorodeoxyuridine (FUdR) (#F0503, Sigma) for 3 days to get rid of proliferating non-neuronal cells, and then changed to NB medium without FUdR. Neuronal cells were maintained in NB medium for 8-10 days. Once DRG neurons reached the periphery of the coverslip fully, Schwann cells were plated onto DRG neurons at the density of 150,000 cells per coverslip in C10 media. After 5-6 days, cells were changed to myelinating medium by adding 50μg/ml ascorbic acid (VitC) in C10 media to initiate myelination in the absence or in the presence of the either 0.3μM of F-TIMP-3 or 0.3μM of N-TIMP-3.

Immunostaining for myelin basic protein

Cultures were fixed in 4% paraformaldehyde for 20 minutes at room temperature. After washing with PBS, samples were permeabilized in cold-methanol for 20 minutes at -20°C and then washed with PBS. Samples were incubated with blocking solution (5% normal goat serum in PBS supplemented with 0.3% Triton X-100) for an hour at room temperature and then incubated with primary antibody for MBP in blocking solution overnight at 4°C. After washing with PBS, cultures were incubated with goat anti-mouse Alexa Fluor 488 secondary antibody (Jackson immunoresearch laboratories) in PBS supplemented with 0.3% Triton X-100 for an hour at room temperature. After washing with PBS, cell nuclei were stained with DAPI for 10 minutes at room temperature. Followed washing with PBS, coverslips were mounted on the slides with Fluoromount-G solution (#0100-01, Southern Biotech).

In vitro myelination assay

Myelin segments were visualized by immunostaining for MBP as described above. Ten images, which were randomly selected across each coverslip, were taken with the epifluorescence microscope (Nikon E800) under a 20x objective. The numbers of MBP-positive myelin segments were counted from the individual image by using Image J software (NIH). The total numbers of segments were obtained from each coverslip with three coverslips used per condition per experiment. The myelin index from four to five separate experiments was analyzed as described previously (Syed et al., 2010).

Lengths of individual myelin segments were measured using Image J software (NIH). A total of 100-600 individual myelin segments were measured from each experiment. An average of length per condition was analyzed from four separate experiments. Student t-test was performed using GraphPad Prism 5.03 software.

BrdU incorporation and immunostaining

Cell proliferation was tested by BrdU (#B5002, Sigma) incorporation. After 48 hours plating Schwann cells onto the DRG neurons, cells were incubated with 10μM 5-bromo-2-deoxyuridine (BrdU). After two hours, cultures were fixed in 4% paraformaldehyde. Washed cultures with PBS were permeabilized in cold methanol for 20 min at -20°C, and then washed 3 times in PBS. The cultures were treated with 2N HCl for 15min at 37°C. Cells were washed with 0.1M borate buffer (pH8.5) for 10 minutes, and then washed 3 times in PBS. After blocking in 5% normal goat serum including 0.3% Triton X-100 for 30 min, cultures were

incubated with antibody in blocking solution for BrdU overnight at 4°C. Next day, cultures were washed with PBS and then incubated with Alexa488-conjugated goat anti-mouse Alexa Fluor 488 secondary antibody (Jackson immunoresearch laboratories) for an hour. After washing with PBS, DAPI was incubated for 10 minutes at room temperature to visualize nuclei. After washing with PBS, cultures were mounted on the slides using Fluoromount-G solution (#0100-01, Southern Biotech). Images were taken with the epifluorescence microscope (Nikon E800) under a 20x objective. Proliferation rate was determined by calculating percentage of the number of BrdU positive nuclei over DAPI positive nuclei.

Neuronal induction of AKT activation in Schwann cells

For TIMP-3 treatment conditions, DRG neurons were pre-treated with either 0.3μM of F-TIMP3 or 0.3μM of N-TIMP3 in N2 media for one hour at 37°C. Ten thousands Schwann cells were plated onto DRG neurons in the absence or in the presence of the either 0.3μM of F-TIMP-3 or 0.3μM of N-TIMP-3 in N2 media. Twenty-four hours later, cells were lysed with the lysis buffer to access Western blot analysis for phospho-AKT, total Atk, phospho-Erk1/2, and total Erk1/2.

Western Blot analysis

To harvest the cell lysates, Schwann cell cultures or DRG neuron-Schwann cell co-cultures were washed twice with PBS, then cells were collected in lysis buffer (20mM Tris, pH7.4, 1% NP-40, 10% glycerol, 2.5mM EGTA, 2.5mM EDTA, 150mM NaCl, 20μM leupeptin, 10μg/ml aprotinin, 1mM PMSF, 1mM sodium

orthovanadate, and 10mM sodium fluoride). Same amount of total protein was loaded and separated by size in SDS-PAGE, transferred to polyvinylidene fluoride (PVDF) membrane. After blocking in 5% skim milk in TBS (10mM Tris and 150mM NaCl, pH8.0) for an hour at room temperature, the membranes were incubated with appropriate primary antibodies in TBS containing 5% BSA overnight at 4°C. After incubating with fluorescence-dye conjugated secondary antibodies (LI-COR) in 5% skim milk in TBS containing 0.001% SDS for an hour at room temperature, the protein bands were detected and quantified by the LI-COR Odyssey imaging system.

5.4. Results

5.4.1 TIMP-3 promotes Schwann cell myelination in co-cultures

Schwann cell myelination can be assessed *in vitro* using a co-culture system established using purified DRG neurons and SCs. When co-cultured together, SCs associate with DRG neurons and proliferate in response to the contact-mediated neuronal signal. Subsequent addition of ascorbic acid (VitC) to the culture initiates myelin formation by promoting SC basal lamina assembly, an event prerequisite for myelination. Seven to ten days after the initiation, myelin segments can be visualized by immunostaining for myelin basic protein (MBP). To determine the effect of TIMP-3 on SC myelination, co-cultures were treated with recombinant full length TIMP-3 (F-TIMP-3, 0.3 μM) at the time of initiating myelin formation and the cultures were maintained in the continuous presence of F-TIMP-3 for nine days, after which the cultures were fixed and immunostained for MBP. Control cultures were maintained in the absence of ascorbic acid or F-TIMP-3. Representative images of the MBP-positive myelin segments in the cultures are shown in Figure 5.1. Under myelinating condition (+ascorbic acid), F-TIMP-3 treatment enhanced myelin formation, shown by an increase in the number of myelin segments generated in the co-cultures. TIMP-3 also increased internodal length of the individual myelin segments (Table 5.1). Full length TIMP-3 had no effect on neuronal contact-mediated Schwann cell proliferation, indicating that the increase in the myelin segment number was not due to an increased SC number (Figure 5.1B). The enhanced myelination was

accompanied by an increase in Krox20 expression, a promyelinating transcription factor that is necessary for SC commitment to myelination (Figure 5.1C).

5.4.2 TIMP-3 increases axonal Nrg1 type III signaling in Schwann cells

Axonal Nrg1 type III signaling is essential for SC myelination. The Nrg1 function is modulated by proteolytic processing of the N-terminus that alters the signaling activity towards the ErbB receptors on Schwann cells (Fleck et al., 2013). Among the Nrg1-processing proteinases, ADAM10 and ADAM17 are inhibited by TIMP-3 (Rapti et al., 2008), suggesting a possibility that the TIMP-3 effect on myelination may be associated with altered Nrg1 type III signaling in the SCs. To investigate this, we monitored changes in Nrg1 type III activity in SC-DRG neuron co-culture upon TIMP-3 treatment. Phosphorylation of AKT was used as a readout for the Nrg1 type III activity, which has been shown previously as a sole activator of the PI3-kinase-AKT pathway in co-cultures (Taveggia et al., 2005). Schwann cells were place on DRG neurons to initiate contact-mediated Nrg1 signaling. Neuron- or SC-only monocultures served as controls. Twenty-four hours after plating SCs, AKT activation was assessed by Western blot analysis. While AKT phosphorylation was minimal in monocultures, placing SCs on DRG neurons increased AKT phosphorylation, which is expected of the Nrg1 type III-mediated PI3-kinase pathway activation in the SCs. Pre-treating DRG with TIMP-3 enhanced the AKT activation in co-culture, indicating an increase in Nrg1 type III signaling (Figure 5.2A, top). Quantification of the Western blot analysis showed that the TIMP-3 effect on AKT activation was significant. Erk1/2

activation, which occurs independent of the Nrg1 type III function in co-culture, was not affected by the TIMP-3 treatment (Figure 5.2A, bottom). Altogether, these results show that the promyelinating effect of TIMP-3 in co-culture is associated with enhanced Nrg1 type III signaling in the SCs.

5.4.3 N-terminus TIMP-3 is sufficient to increase Nrg1 type III activity and Schwann cell myelination in co-cultures

Nrg1 processing by ADAM17 inhibits Nrg1 activity and myelination in SCs whereas cleavage by ADAM10 increases Nrg1 activity (La Marca et al., 2011; Luo et al., 2011). Therefore, the increased Nrg1 type III activity and SC myelination observed above are likely associated with the inhibitory function of TIMP-3 targeting ADAM 17. While full length recombinant TIMP-3 inhibits both ADAM10 and ADAM 17, N-terminus TIMP-3 domain exhibit selective inhibitory effect towards ADAM17 and does not inhibit ADAM10 (Lee et al., 2001; Rapti et al., 2008). Therefore, we tested the effects of N-terminus TIMP-3 on SC myelination and Nrg1 type III signaling. Treatment with N-TIMP-3 had a similar myelination promoting effect in co-cultures as seen with F-TIMP-3 (Figure 5.1A). Both the number of myelin segments and the myelin internodal length increased to the equivalent levels observed with F-TIMP-3 treatment (Table 5.1). N-terminus TIMP-3 also increased Krox 20 and MBP expression as well as AKT phosphorylation in co-cultures (Figure 5.1C). These results indicate that the promyelinating function of TIMP-3 is associated with the activity of the N-terminus fragment, likely that inhibits ADAM17.

5.4.4 TIMP-3 increases laminin contents during Schwann cell myelination

Extracellular matrix produces by SCs plays an important role during myelin formation. One of the components is laminin, which production is essential for SC differentiation and myelin ensheathment. In SC-DRG co-cultures, addition of purified laminin is sufficient to increase SC myelin formation (Eldridge, Binge 1989, A. Baron-Van Evercooren et al., 1986). In addition to ADAM proteins, TIMP-3 inhibits wide range of matrix metalloproteinases (MMPs) that degrade components of ECM including laminin (Apte et al., 1995; Amour et al., 1998). This presents a possibility that the effects of TIMP-3 on myelination may be associated with a decrease in laminin processing, thus an increase in laminin contents during myelination. To this end, we monitored laminin levels in co-cultures maintained under non-myelinating (-ascorbic acid) and myelinating (+ascorbic acid) condition treated with TIMP3. We focused on the first five days after initiating myelination, a period that correspond to early stages of myelination that is impacted by laminin. Antibodies against pan-laminin were used to detect the total laminin contents using Western blot analysis. In control cultures without TIMP-3, laminin levels were higher in cultures undergoing myelination compared to the non-myelinlating cultures (Figure 5.3A). This is in agreement with previous reports that laminin production by SCs increases with initiation of myelination. Treatment with TIMP-3 further increased the total laminin contents in co-cultures, with a more profound effect under myelinating condition (Figure 5.3). This result suggests that TIMP-3 increases overall laminin levels during SC myelination.

5.5. Discussion

Myelination in the PNS is dependent on contact-mediated signaling between SCs and the associated axons. One of the axonal signals that is essential for myelination is Nrg1 type III, which binds and activates the ErbB2/3 receptor complex on the SC surface (Falls, 2003; Taveggia et al., 2005). Subsequent activation of the PI3-kinase pathway in the SCs is then required for initiating myelin formation (Maurel and Salzer, 2000).

The signaling function of Nrg1 type III is regulated by proteolytic processing that modulates the receptor activating EGF domain within the N-terminus (La Marca et al., 2011; Luo et al., 2011; Fleck et al., 2013). A variety of metalloproteinases have been implicated in Nrg1 type III cleavage, including □-secretase and ADAM17. Previous studies have shown that Nrg1 cleavage by these proteases has opposing functional effects on SC myelination. Processing by □-secretase activates Nrg1 and is required for myelination in the PNS (Luo et al., 2011). In contrast, ADAM17 processing attenuates Nrg1 signaling. *In vivo* inhibition of ADAM17 results in increased Nrg1 activity and SC hypermyelination in the PNS (La Marca et al., 2011). Other members of the ADAM family, such as ADAM10 have also been implicated in regulating Nrg1 signaling (Luo et al., 2011). Therefore, PNS myelination is regulated in part by modulation of the proteases activities that alter the signaling function of Nrg1.

In this study, we investigated the effect of TIMP-3 on SC myelination. Proteins of the TIMP family are endogenous inhibitors of matrix metalloproteinases and ADAM proteins. Among the TIMPs, TIMP-3 exhibits a

strong inhibitory activity towards ADAM17, which function has been shown to negatively regulates Nrg1 and SC myelination (Amour et al., 1998; La Marca et al., 2011). TIMP-3 also inhibits ADAM10, which cleavage activates Nrg1, but without a significant consequence on myelin formation (Rapti et al., 2008; Luo et al., 2011). Our data show that TIMP-3 increases neuronal contact-mediated AKT activation in SC-DRG neuron co-cultures, indicating an increase in neuronal Nrg1 type III activity (Figure 5.2). This is a result expected of TIMP-3 targeting negative regulators of Nrg1 signaling, such as ADAM17. Accordingly, TIMP-3 treatment enhances myelin formation by SCs (Figure 5.1A), which is likely to occur if TIMP-3 relieves the myelination block imposed by ADAM17. Altogether, the positive impact of TIMP-3 on Nrg1 signaling and myelination implicates its role in targeting ADAM17. This notion is further corroborated by the observation that N-TIMP-3, which has selective inhibitory activity towards ADAM17 elicits a similar myelination promoting effect on SCs. Future study is required to directly assess ADAM17 activity in co-cultures treated with TIMP-3.

The promyelinating function of TIMP-3 was associated with an increase in Krox20 expression (Figure 5.1C), indicating its role during the very early stages of SC myelination. As a promyelinating transcription factor, Krox20 induction allows SCs in one-on-one contact with individual axons to proceed past the pre-myelinating stage and initiate radial membrane wrapping of the axons (Topilko et al., 1994). TIMP-3 treatment also increased internodal length of individual myelin segments indicating enhanced growth of myelin sheath (Table 5.1). These effects on myelination have also been observed in co-cultures with an ectopic

increase in Nrg1 activity, which corroborate with our observation in the present study that TIMP-3 treatment increases Nrg1 signaling in co-cultures.

In addition targeting ADAM proteins, TIMP-3 inhibits wide range of MMPs that cleave and modify components of ECM (Apte et al., 1995; Amour et al., 1998). This suggests a possibility that the TIMP-3 effect on myelination may be associated with inhibition of functional MMPs that modulate ECM. Laminin is a major component of SC basal lamina that is important for myelin formation (Fernandez-Valle et al., 1993; Fernandez-valle et al., 1994). In PNS, expression laminin is upregulated during the first week of birth in rat, when basal lamina assembly and myelin formation by SC commence (Masaki et al., 2002). In co-cultures, laminin expression increases with the onset of myelination when ascorbic acid is added (Eldridge et al., 1989). Furthermore, addition of purified laminin is sufficient to initiate and increase SC myelination in co-cultures (McKee et al., 2012). Our data show that TIMP-3 treatment increases total laminin content produced during the early stages of myelin formation (Figure 5.3). It is unclear whether the increase in laminin content was due to enhanced production or attenuated degradation of laminin. As an MMP proteases inhibitor, one can speculate that TIMP-3 mediated inhibition of laminin-processing MMPs may be involved in the process. In this regards, SCs and DRG neurons express MMP-2, which degrades ECM components including laminin (Muir, 1995; Ali et al., 2014). Schwann cells also express laminin-processing MMP-9, which function has been implicated in ECM remodeling following PNS injury (La Fleur et al., 1996).

Considering the promyelinating function of laminin in SCs, accumulation of laminin in TIMP-3 treated culture is likely to enhance myelin formation.

In summary, results from the present study illustrate a function of TIMP-3 that enhances myelination by SCs. The promyelinating function is associated with increased neuronal Nrg1 type III signaling and laminin deposition during the early stages of myelin formation.

5.6. Figure Legends

Figure 5.1.

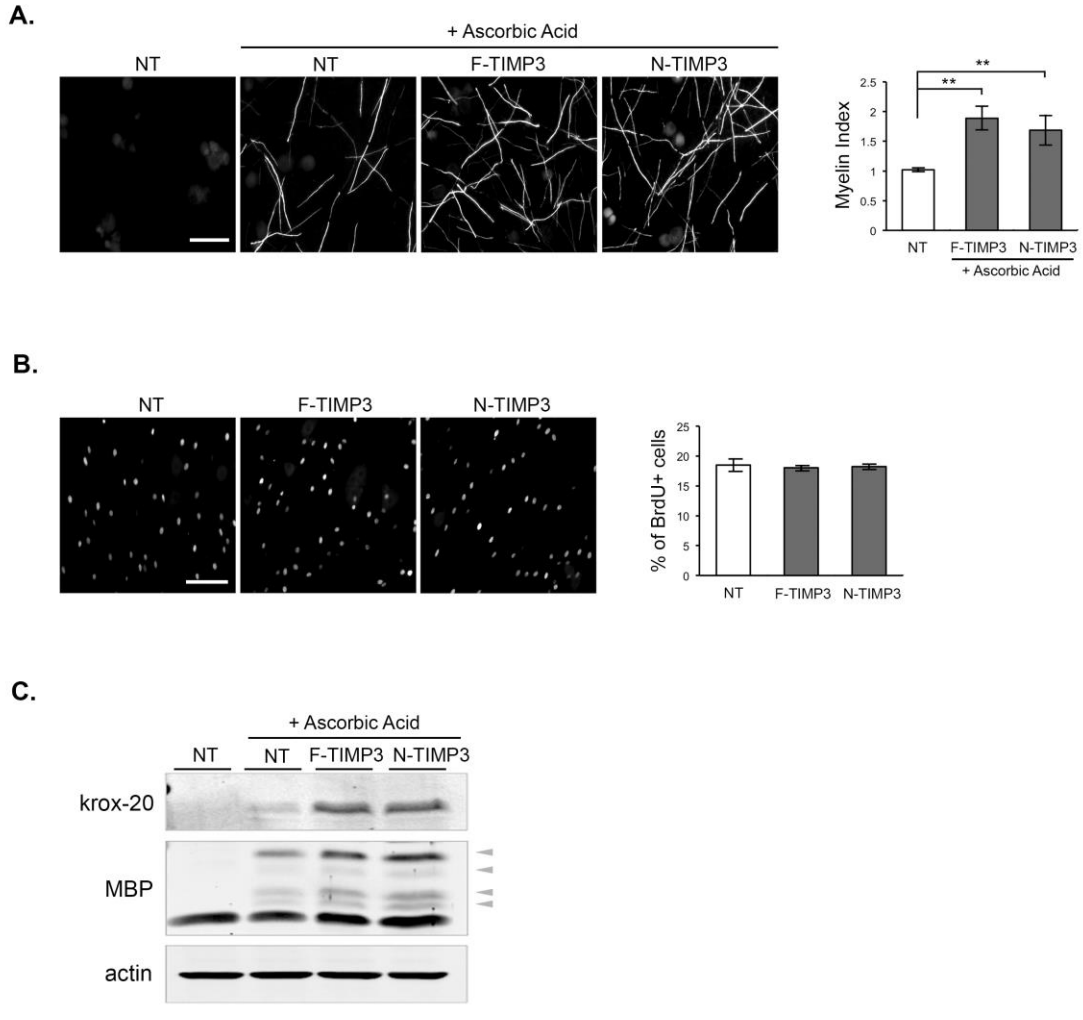

Figure 5.1. TIMP-3 promotes Schwann cell myelination

(A) Representative mages of MBP+ myelin segments generated in myelinating co-cultures treated with F-TIMP-3 (0.3 μM) or N-TIIMP-3 (0.3 μM). The TIMP-3 peptides were added to the SC-DRG neuron co-cultures at the time of initiating myelination and remained for 9 days, at which time, the cultures were fixed and immunostained for MBP. Scale bar: 100 □m. No myelin segment is visible without ascorbic acid. After initiating myelination (+ascorbic acid) addition of F-TIMP-3 or N-TIMP-3 increased the overall number of myelin segments formed in co-cultures. Quantification of myelination is shown on the right. **p<0.01. The means +/- SEM were determined from three coverslips/condition from four to five independent experiments. (B) TIMP-3 does not affect neuronal contact-mediated SC proliferation. Schwann cell proliferation in co-cultures was assessed by BrdU incorporation. The result is presented as percentage BrdU+ cells detected in the cultures. Scale bar: 100 □m. There was no significant difference in Schwann cell proliferation among control (NT), F-TIMP-3 and N-TIMP-3 treated cultures (mean +/- SEM, determined from three coverslips/condition from four independent experiments) (C) TIMP-3 upregulates expression of myelin-associated protein. Krox 20 and MBP expression were assessed in co-cultures maintained under myelinating condition for 9 days in the presence or absence of TIMP-3. Both F-TIMP-3 and N-TIMP-3 increased expression levels of Krox 20 and MBP. The protein expression is absent in cultures kept under non-myelinating condition (-ascorbic acid).

Figure 5.2.

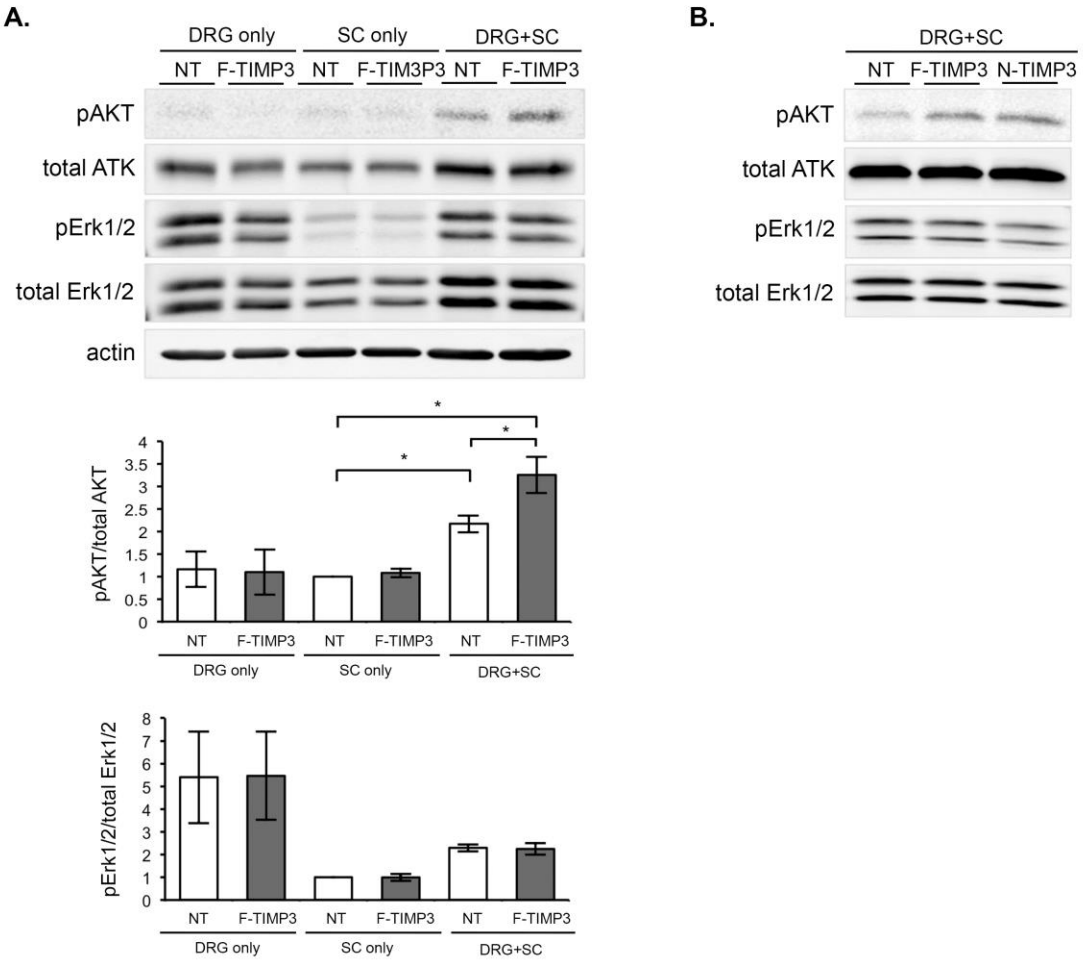
A.
DRG only
SC only
DRG+SC
NT
F-TIMP3
NT
F-TIM3P3
NT
F-TIMP3
pAKT
total ATK
pErk1/2
total Erk1/2
actin
pAKT/total AKT
pErk1/2/total Erk1/2
B.
DRG+SC
NT
F-TIMP3
N-TIMP3
pAKT
total ATK
pErk1/2
total Erk1/2

Figure 5.2. TIMP-3 enhances neuronal contact-mediated Nrg1 signaling in Schwann cells

(A) Sensory neurons were pre-treated with F-TIMP-3 for 2 hours, after which Schwann cells were plated on the neurons to initiate contact mediated Nrg1 signaling. Two hours later, lysates were prepared and levels of phospho-AKT, phospho-Erk as well as total AKT and Erk were assessed by immunoblotting. Control lysates were prepared from neuron-only or Schwann cell-only cultures treated with F-TIMP-3. AKT activation (phospho-AKT) was initiated when Schwann cells were plated on neurons (DRG+SC). Treatment with F-TIMP-3 further increased the neuronal contact (Nrg1 type III)-mediated AKT activation in co-cultures. Erk activation was mostly detected in neurons and was not affected by the TIMP-3 treatment. *$p<0.05$. The means +/- SEM were determined from three independent experiments. (B) AKT activation in co-cultures treated with F-TIMP-3 or N-TIMP-3. Treatment with N-TIMP-3 increased AKT activation as seen in F-TIMP-3 treated cultures.

Figure 5.3.

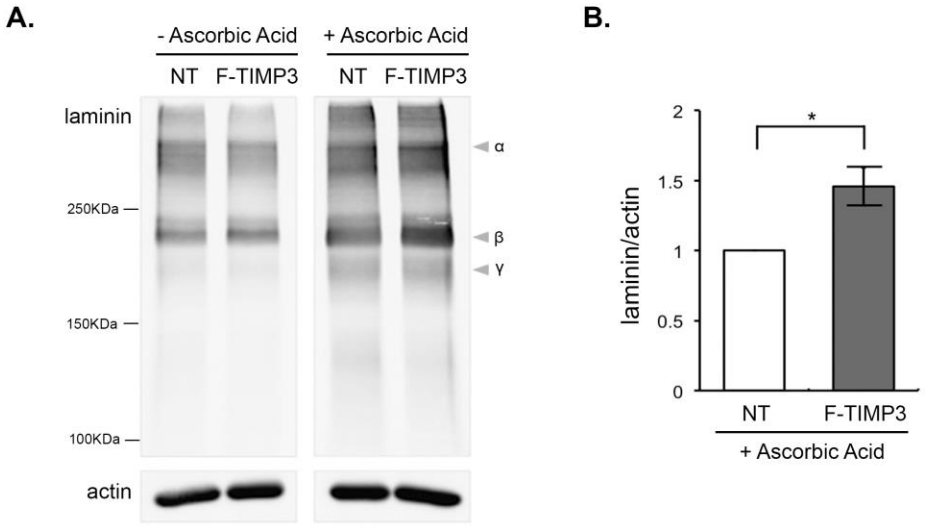
A.
- Ascorbic Acid
+ Ascorbic Acid
NT
F-TIMP3
NT
F-TIMP3
laminin
250KDa
150KDa
100KDa
actin
α
β
γ
B.
laminin/actin
2
1.5
1
0.5
0
*
NT
F-TIMP3
+ Ascorbic Acid

Figure 5.3. TIMP-3 treatment increases laminin contents during Schwann cell myelination

(A) Schwann cell-DRG co-cultures were treated with F-TIMP-3 and placed under non-myelinating (-ascorbic acid) or myelinating condition (+ascorbic acid) in the continuous presence of F-TIMP-3. Control cultures were maintained in the absence of TIMP-3. Five days later lysates were prepared and total laminin content was determined using antibodies against pan-laminin. Overall laminin content increased in cultures under myelinating condition. Treatment with TIMP-3 further increased the levels of laminin. (B) Quantification of the TIMP-3 effects on laminin contents in myelinating cultures. *$p<0.05$. The mean +/- SEM was determined from three independent experiments.

Table 5.1.

	Ascorbic Acid	Ascorbic Acid + 0.3μM F-TIMP-3	Ascorbic Acid + 0.3μM N-TIMP-3
Mean segment length (μm)	158.57	170.51 ***	171.66 **
SEM	3.82	5.02	3.54
Total number of segments	1105	1389	1459
Fold changes	1	1.075	1.082

Table 1. Average length of myelin segments in control and TIMP-3 treated co-cultures

Schwann cell-DRG co-cultures were treated with F-TIMP-3 or N-TIMP-3 at the time of initiating myelination and maintained for nine days, at which time, the cultures were fixed and immunostained for MBP. Length of individual myelin segments was measured from three coverslips/condition from four to five independent experiments. **p<0.01, ***p<0.001

6. Chapter three: Ca^{++}-dependent Erk1/2 MAPK activation following mechanical stretch injury induces myelin loss in oligodendrocytes

6.1. Abstract

Traumatic brain injury (TBI) is caused by mechanical force to the brain, and it is associated with a long-term disability of cognition or neuronal behavior. TBI-associated oligodendrocyte (OL) pathology includes myelin degeneration and cell death. In myelin loss in the absence of OL death frequently occurs especially after mild TBI. Since myelin is crucial for neuronal function and survival, loss of myelin is likely to impair axonal integrity, resulting in axonal degeneration. While axon pathology associated with TBI has been actively studied, the molecular mechanisms understanding the OL response and the consequences on the myelin are not fully understood.

In this study, we investigated the effect of mechanical injury on OL and the intracellular signaling. *In vivo* TBI-induced Erk1/2 in mature OLs within white matter tracts accompanied by loss of myelin protein expression. To elucidate the OL autonomous response to mechanical injury, we have established OL monocultures on deformable silicone membranes, which are later rapidly stretched to initiate OL response *in vitro*.

The stretch injury induced efflux of Ca^{++} in mature OLs. Also, stretch injury-induced Erk1/2 activation and MBP loss in mature OLs without cell death. Inhibition of Erk1/2 activation prevents the MBP loss following injury. Chelating intracellular Ca^{++} during the injury inhibited Erk1/2 activation following injury.

Increasing intracellular Ca^{++} with a Ca^{++} ionophore was sufficient to activate Erk1/2 that results in MBP loss. Altogether, our data show that the mechanical injury in OL initiates activation of intracellular signaling that disrupts the myelin maintenance. The process is mediated by Ca^{++}-dependent Erk1/2 activation.

Results from the study promote insights into signaling pathways that are associated with myelin loss following TBI suggest a therapeutic target that may attenuate myelin loss following the injury.

6.2. Introduction

6.2.1 TBI and myelin damage

Diffuse, or traumatic axonal injury (TAI) is a widely distributed damage to axons in the brain that results from the inertial forces exerted on the white matter tracts in the brain during traumatic incidents such as automobile accidents, falls, and assaults. Such head injuries cause large intracranial shear deformations of the brain resulting in rapid longitudinal or uniaxial stretching of axon fibers (Pfister et al., 2003), which are believed to be the major factor in post-traumatic comma and persistent cognitive deficits (Capruso and Levin, 1992; Goldstein and Levin, 2001; Levin and Hanten, 2005).

White matter atrophy or degeneration of myelinated axon following TBI has been reported in human patients and in animal models using experimental TBI. It is unclear whether the white matter damage results mainly from progressive axonal pathology or is a consequence of myelin disturbance that leads to axon degeneration. Because myelin is vital for neuronal survival and function, demyelination has detrimental effects on the nervous system. Myelin loss is also thought to exacerbate axon damage by providing a mechanism of posttraumatic Ca^{++} influx into the axons (Maxwell et al., 1999, 2003). Furthermore, myelin protects axons against mechanical injury: unmyelinated axons sustain more severe functional and structural damage than myelinated axons following experimental TBI (Reeves et al., 2005). Therefore, identifying a molecular target to prevent myelin loss may be clinically relevant in developing therapeutic strategies for future intervention.

6.2.2. Myelin loss after TBI

The molecular mechanisms associated with demyelination after TBI are not fully understood. Previous studies are limited to immunohistochemical analysis on brains of human patients or experimental animal models. Acute myelin damage and cell death are observed in human brains after TBI (Ng et al., 1994; Shaw et al., 2001). In animal models, myelin loss and OL death are seen within 2 days after injury (Lotocki et al., 2011; Flygt et al., 2013), indicating that OL death following injury contributes to the myelin loss. Axonal degeneration and neuronal death are also considered to be main factors that result in myelin loss in the brain, especially after severe brain injury. However, in the brain affected by mild TBI, myelin loss in the white matter tracts is frequently observed in the absence of axonal and OL loss. Ultra-structural analysis on optic nerves after TAI shows structural damages to the myelin as early as 24 hours post-injury with little or no change in the underlying axons (Bramlett and Dietrich, 2002; Maxwell et al., 2003; Flygt et al., 2013). Myelin loss on intact axons and formation of aberrant myelin figure during remyelination following mild TBI have been reported in rats. Most important, the myelination defects were observed in the absence of obvious OL death indicating that the injury-induced myelin responses occurred in viable OLs. These observations present a possibility that demyelination may be triggered by an OL-autonomous event following the mechanical injury. Supporting this notion, it has been shown that mechanical injury triggers a secondary biochemical change in the OLs that promotes demyelination (Sun et al., 2012). Therefore, demyelination after TBI may be

prevented in part by targeting an intra-cellular component in the OLs that initiates myelin degeneration.

6.2.3. Erk1/2 signaling pathway in response to injury

Traumatic brain injury is likely to activate a complex array of signal transduction machinery in the OLs, leading to demyelination. For example, mechanical stimulus itself can activate various intracellular signaling pathways that trigger cellular response. Cytokines, growth factors and oxidative stress produced in the brain lesions are also likely to influence the OL response to injury. The post-Ca^{++} influx has also been linked to cellular damage after TBI.

The MAPK cascades, which include the Erk1/2, p38 MAPK, and JNK pathways, have an evolutionally conserved function of transducing external stress to the internal molecular machinery that initiates cellular response. MAPKs are also key regulators of mechanotransduction in mammalian cells. Accordingly, MAPK activation has been observed in white matter regions following TBI (Otani et al., 2002; Raghupathi et al., 2003).

In the peripheral nervous system (PNS), Erk1/2 is an important signal transducer that triggers Schwann cell demyelination under various pathological conditions. For example, mechanical injury induces an immediate Erk1/2 activation in the SCs, the myelin forming cells of the PNS (Guertin et al., 2005). Inhibition of the Erk1/2 activation is sufficient to block demyelination after PNS injury. Furthermore, ectopic activation of Erk1/2 in myelinating Schwann cells initiates demyelination (Napoli et al., 2012). Interestingly, Erk1/2 inhibition also

provides myelin protection against other PNS insults (microbial, metabolic) that cause myelin loss (Tapinos et al., 2006; Jolivalt et al., 2011). Therefore, in the PNS, Erk1/2 appears to be a key player that mediates various demyelinating signals in the SCs.

It is unknown whether TBI initiates Erk1/2 activation in white matter OLs and if so, whether it contributes to TBI-associated myelin loss. Data from our previous study indicate that aberrant Erk1/2 activation in mature OLs trigger myelin loss. In myelinating OL cultures, treatment with growth factors initiates myelin degeneration. Inhibition of the Erk1/2 activation blocked the FGF-2 function, whereas inhibition of the other pathways concomitantly activated by FGF-2 (PI3-kinase and JNK) had no effect. Furthermore, our previous study showed that expression of constitutively active MEK1 is sufficient to trigger myelin protein loss and myelin breakdown.

6.2.4. A role of Erk1/2 in OL myelination

Recent studies have shown that Erk1/2 plays an important role in regulating myelin homeostasis in the CNS. During development, Erk1/2 activation in the OL lineage correlates temporally with the period of myelination: the activation level is at the highest during active myelination then declines in the adult CNS (Ishii et al., 2013). *In vivo* studies using OL-specific Erk1/2 knockdown mice showed that while Erk1/2 is dispensable for OL differentiation and the initiation of myelination, it is crucial for the subsequent myelin growth (Ishii et al., 2013). Other studies showed that elevating the Erk1/2 activity during active

myelination results in thicker myelin formation by the OLs (Fyffe-Maricich et al., 2013; Ishii et al., 2013). In adult mice with mature myelin, ectopic Erk1/2 activation in OLs destabilizes the myelin (Ishii et al., 2012). These results indicate that fine balance in the kinase activity is essential for proper OL myelination and myelin maintenance.

In this study, we investigated whether TBI initiates Erk1/2 activation in white matter OLs. We also elucidated the direct effects of mechanical injury on mature OLs. For the study, we combined the OL culture system with an *in vitro* stretch injury device that applies computer controlled mechanical force (stretch injury) to cultured cells. Our data show that *in vivo*, white matter OLs respond to TBI by increasing Erk1/2 activation. Our *in vitro* study shows that mechanical injury plays a direct role in inducing Erk1/2 activation in mature OLs. Furthermore, the Erk1/2 activation is mediated by intracellular Ca^{++} increase in OLs in response to injury. Lastly, we show that the Ca^{++}-dependent Erk1/2 activation contributes to myelin loss in OLs and inhibition of either the Ca^{++} increase or the Erk1/2 activity prevents OL myelin loss following mechanical injury.

6.3 Materials and Methods

Culture media

The following culture media were used: MEM-C media [10% serum, 0.6% glucose, 0.1mg/ml penicillin-streptomycin, 1% glutamate in MEM]; N2B2 [DMEM/F-12 (1:1) with 0.6mg/ml BSA, 10ng/ml d-biotin, 20nM progesterone, 100nM putrescine, 5ng/ml selenium, 50µg/ml apo-transferrin, and 0.1mg/ml penicillin/streptomycin]; N2S media [66% of N2B2, 33.5% of B104-conditioned media, 5ng/ml FGF-2 and 0.5% fetal bovine serum (FBS)]; NB media [Neurobasal medium with B-27 supplement, 0.08% glucose, 1% glutamine, 0.1 mg/ml penicillin/streptomycin and 50 ng/ml nerve growth factor (NGF) (#BT-5017, Harlan Laboratories, Inc.)]; NB-T3 media [97% NB media, 1x B-27 supplement, 30ng/ml 3,3',5-Triiodo-L-thyronine sodium salt (T3) (#6397, Sigma) and 0.1mg/ml penicillin/streptomycin]; C10 media [Minimal Essential Medium (MEM) containing 10% FBS, 0.08% glucose, and 50ng/ml NGF].

Antibodies

The following primary antibodies were used for immunostaining or Western blot analysis: mouse anti-pErk1/2 (#9106, Cell signaling for immunostaining), mouse anti-pErk1/2 (#5726, Cell signaling), rabbit anti-total Erk1/2 (#V114A, Promega), mouse anti-MBP (#SMI-94R, Covance for immunostaining), rabbit anti-MBP (#AB980, Chemicon), rabbit anti-olig2 (from Dr. Alberta at Dana-Farber cancer institute), mouse anti-actin (#A5441, Sigma).

Fluid percussion injury on rat brain

Postnatal day 21- 22 rats were anesthetized with ketamine/ xylazine and subjected to a craniotomy surgery. The Ø 4.8mm of skull above the left cortex at 3mm posterior from and 3.5mm lateral from Bregma was removed to expose the brain; a Luer/Loc syringe hub was implanted on the top of the opening; and an additional cap that surrounds the syringe hub was applied. Dental cement was applied between the syringe hub and the cap to ensure the fluid transmission and support. Next day, rats were anesthetized with 5% isoflurane for 30 seconds to 1 minute until foot pinch resulted in no response. Then, rats were randomly assigned to have a FPI or a sham injury. Four hours or 2 days after injury, rats were anesthetized with ketamine/ xylazine and then perfused with 50ml of 4% paraformaldehyde containing 1mM sodium orthovanadate and 10mM sodium fluoride in PBS. The brain was isolated and placed in 4% paraformaldehyde overnight at 4°C. Fixed brains were rinsed with PBS and then placed in 30% sucrose solution until the brain sunk to the bottom of the container (about 2 days). The brain was embedded in OTC tissue freezing medium and frozen on the dry ice. Frozen brain samples were sectioned at 30μm thickness.

Oligodendrocyte Progenitor Cells isolation and culture

Cerebral cortex from the frontal lobe of the brain was isolated from postnatal day 1-2 rats. Meninges were removed from the surface of the isolated brain tissues before dissociation by pipetting in L15 media. Cells were filtered through a 40μm cell strainer. Harvested cells were centrifuged at 2000rpm at

room temperature and resuspended in MEM-C media. Cells were plated at the density of 1 brain per T75 flask and kept in MEM-C media to obtain mixed glia cultures.

Ten to twelve days later, oligodendrocyte progenitor cells (OPCs) were isolated from the mixed glia culture. Briefly, mixed glia cultures were shaken at 200 rpm for two hours to remove microglial cells and replaced to 37°C with fresh MEM-C media. Cultures were shaken at 250 rpm overnight at 37°C to obtain the OPCs. Next day, the cell suspension was passed through the 20μm pore-sized nylon mesh. Isolated OPCs were centrifuged at 2000rpm for 10 minutes at room temperature and plated on a non-treated 100mm plate for 10 minutes in 10ml of N2B2 media to avoid astrocytes contamination. N2B2 media was harvested from the plate and re-centrifuged at 2000rpm for ten minutes. Harvested OPCs were resuspended in N2S media and plated on PLL-laminin coated silicone membrane injury wells at a density of $0.7x10^5$ cells per well or PDL-laminin coated glass coverslips (#354087, Corning) at a density of $2x\ 10^4$ cells per coverslip. To differentiate OPCs to mature oligodendrocytes, culture media was switched to the NB-T3 media one day after plating OPCs in N2S media and kept for 5 days to induce differentiation.

Assembly of injury wells and stretch injury

An injury well consists of two PEEK rings, an o-ring and a 1.5cm x1.5cm piece of silicone membrane (0.005” gloss/gloss silicone sheeting, Specialty Manufacturing, Inc.). PEEK rings were cleaned by sonication in DI water and

silicone membranes were rinsed with DI water. Between the PEEK rings, the inner PEEK ring has a groove for an o-ring insertion. A piece of silicone membrane was put over the outer PEEK ring, and the inner PEEK ring that has o-ring inserted was placed on the top of the silicone membrane and pressed into the outer one gently as described in Magou et al. (Magou et al., 2011)

Immunostaining for MBP on cultures and sectioned brain tissues

Cultures or tissues were fixed in 4% paraformaldehyde for 20 minutes at room temperature. After washing with PBS, samples were permeabilized in cold-methanol for 20 minutes at -20°C and then washed with PBS. Samples were incubated with blocking solution (10% normal donkey serum in PBS supplemented with 0.3% Triton X-100) for an hour at room temperature and then incubated with primary antibody for MBP in blocking solution overnight at 4°C. After washing with PBS, samples were incubated with secondary antibody in PBS for an hour at room temperature. Cell nuclei were stained with DAPI for 10 minutes at room temperature. Following washes with PBS, coverslips were mounted on the slides with the Fluoromount-G solution (#0100-01, Southern Biotech). The percentage of MBP-positive cells was calculated by the number of MBP and olig2 co-labeled cells over a number of total olig2 positive cells.

Immunostaining for phospho-Erk1/2 on OL monocultures and sectioned brain tissues

Cultures or sectioned tissues were fixed in 4% paraformaldehyde for 20 minutes at room temperature. After washing with TBS, samples were permeabilized in TBST (TBS supplemented with 0.02% Triton X-100) for an hour at room temperature and then washed with TBS. Samples were incubated with blocking solution (10% normal donkey serum in TBS) for one hour and then incubated with primary antibody for phospho-Erk1/2 in blocking solution at 4°C for 48 hours with OL mono-cultures on coverslips or silicone membrane, or for 72 hours with sectioned brain tissues. After washing with TBS, samples were incubated with secondary antibody in TBS overnight at 4°C. After washing with TBS, cell nuclei were stained with DAPI for 10 minutes at room temperature. Following washes with TBS, coverslips were mounted on the slides with the Fluoromount-G solution. The percentage of phospho Erk1/2-positive cells was calculated by the number of phospho Erk1/2 and olig2 co-labeled cells over a number of total olig2 positive cells.

Immunostaining for CC1 on sectioned brain tissues

Tissues were rehydrated with PBS for 10 minutes and then processed for antigen retrieval by boiling for 5 minutes in 10mM citrate buffer (pH 6.0). After washing with PBS, tissues were incubated with the blocking solution (10% normal donkey serum in PBS supplemented with 0.3% Triton X-100) for an hour at room temperature and then incubated with primary antibody for CC1 and phospho-Erk1/2 in blocking solution for three days at 4°C. After washing with PBS, cell nuclei were stained with DAPI for 10 minutes at room temperature.

Following washes with PBS, coverslips were mounted on the slides with the Fluoromount-G solution.

Immunostaining and TUNEL assay

Cultures were fixed in 4% paraformaldehyde for 20 minutes. After washing with PBS, fixed samples were immunostained for olig2. After the staining, samples were post-fixed with 4% paraformaldehyde for 25 minutes at 4°C and washed with PBS. After permeabilization with 0.2% Triton X-100 solution in PBS, apoptotic cells were detected by DeadEnd^{TM} Fluorometric TUNEL system (#G3250, Promega) by following manufacturer's protocol. Briefly, post-fixed and permeabilized cultures were washed twice with PBS for five minutes each at room temperature. After removing the excess PBS by tapping the wells, cultures were incubated with equilibration buffer for 10 minutes. The buffer was switched to the reaction buffer (5µl of nucleotide mix, 1µl of the rTdT enzyme in 50 µl of Equilibration buffer) and incubated at 37°C for an hour. The reaction was stopped by washing the cultures with 2x SSC for 15 minutes at room temperature. Cultures were washed with PBS and stained with DAPI for 10 minutes at room temperature. After PBS washing, cultures were mounted on the slide with Fluoromount-G solution.

Ca^{++} Imaging using Fluo-4AM

Cells cultures were washed with PBS, either Ca^{++}/magnesium containing PBS or Ca^{++}/magnesium free PBS, and loaded with 3.2µM Fluo-4 and an equal

volume of Pluronic-F127 detergent in PBS for 30 minutes at 37°C. After rinsing the Fluo-4 solution with PBS, cultures were placed on the injury device that was placed on the stage of Nikon Eclipse TE- 2000 inverted microscope. One or one and half minutes after starting time-lapse imaging with two seconds interval in NIE software (Nikon), a stretch injury was applied. Time-lapse images were taken every 2 seconds for a total of 5 minutes. The intensity of fluorescence of images was measured by using Image J software (NIH) and each image following injury was normalized by average intensity of fluorescence from the images that were taken before the injury.

Ca^{++}-ionophore experiment

Oligodendrocytes cultures were incubated with 10μM Ca^{++} ionophore, A23187 (Sigma) in the NB-T3 media. To test phospho-Erk1/2 activation by intracellular Ca^{++} increase, cells were incubated for 30 minutes in Ca^{++} ionophore-containing media and then lysed in lysis buffer (25mM Tris (pH7.4), 1% SDS, 1mM EDTA (pH 8.0), 95mM NaCl, 20μM leupeptin, 10μg/ml aprotinin, 1mM PMSF, 1mM sodium orthovanadate, and 10mM sodium fluoride). The lysates were accessed by Western blot for phospho-Erk1/2. To test the effect of Ca^{++} increases in OL on MBP expression, 10μM Ca^{++} ionophore in NB-T3 media was applied for 1hour at 37°C and then media was switched to NB-T3 media without Ca^{++} ionophore and incubated for additional 24 hours at 37°C before lysed. Collected samples were analyzed by Western blot for phospho-Erk1/2 or MBP.

6.4. Results

6.4.1 Erk1/2 is activated in mature OLs following FPI *in vivo*

Previous studies have reported Erk1/2 activation in brain lysate affected by TBI. In our study, we observed that ectopic Erk1/2 activation in mature OLs disrupts myelin homeostasis resulting in the myelin loss. Therefore, we hypothesized that myelin loss following TBI may result from an increased Erk1/2 activation in the OL. To address this, we first monitored whether TBI induces Erk1/2 activation in white matter OLs. Rats were subjected to either FPI or sham injury. Four hours after injury, the TBI-brains were cryosectioned and immunostained for phospho-Erk1/2 and olig2, which is a marker for oligodendrocyte lineage cells. Erk1/2 activation was observed in olig2-positive cells in the white matters of the brains, in external capsules (Figure 6.1A). Since olig2 antibody marks both OPCs and mature OLs, we determined whether Erk1/2 activation occurs specifically in the mature OLs by immunostaining the brain tissue for CC1, a marker for mature OLs, with phospho-Erk1/2. TBI-induced Erk1/2 activation was seen in CC1-positive cells (Figure 6.1B), suggesting TBI induces Erk1/2 activation in mature OLs in the brain.

We also monitored the level of myelin basic protein (MBP) level in white matters 48 hours following FPI. In sham control brains, MBP staining showed dense and organized myelin pattern within the white matter (Figure 6.1C, left). In injured brains, we observed area with MBP loss in white matter tracts, indicating loss of myelin and/or mature OLs (Figure 6.1C). OL death was not observed indicating that the MBP loss occurred in viable OLs.

6.4.2 Mechanical injury activates Erk1/2 in mature OLs

Mechanical injury to cells initiates intracellular signaling events that alter the cellular behavior. One of the common signal transducers of extracellular mechanical force is Erk1/2, which has been shown to induce an injury-dependent cellular response in mammalian cells. Therefore, we hypothesized that the Erk1/2 activity observed in mature OLs following TBI resulted in part from OL's direct response to the mechanical force. We also hypothesize that the Erk1/2 activation contributed to the myelin protein loss in the OLs.

To directly assess the affect of mechanical injury in OLs, we developed an *in vitro* OL injury system, in which OL cultures are established on deformable silicone membrane that can be uniaxially stretched to trigger mechanical injury on the OLs. The configuration of the injury system only allows OLs in the midline to be stretch injured while leaving cells in the distal region uninjured (Figure 6.2B). This allows direct comparison of the OL response to mechanical injury within the same culture.

OPCs were placed on silicone membrane and allowed to differentiate into mature OLs. The OLs were then stretch injured at 70%, $30sec^{-1}$. Thirty minutes later, the cultures were fixed and immunostained for phospho-Erk1/2 and Olig2. Immunoreactivity to phospho-Erk1/2 appeared in OLs within the midline while cells in the distal region were negative for the staining. Quantification showed 38.4% of the Olig2+ cells responded to the injury (Figure 6.2C). Treatment with U0126, an MEK inhibitor, abrogated the Erk1/2 activation. This result indicates that direct mechanical injury to OL activates Erk1/2.

6.4.3 Mechanical injury induces myelin protein loss in OLs in an Erk1/2-dependent manner

Next, we assess the effect of stretch injury on the differentiation state of OLs. Specifically, we monitored the effects of stretch injury on OL morphology, myelin protein expression, and cell death. Twenty-four hours after injury, cultures were immunostained for MBP (Figure 6.3A). Cell death was monitored by TUNEL assay. Stretch injury resulted in an aberrant accumulation of MBP or complete MBP loss within Olig2+ OLs. While 85.6% of the OL in distal region maintained MBP expression, there was a 29.6% decrease in the MBP+ OLs within the injury area. We also observed retraction of MBP+ membrane branches in the OLs following injury (Figure 6.3B). No cell death was observed, indicating that the OL response occurred in viable cells (Figure 6.3C).

In our previous study, we reported that ectopic Erk1/2 activation is sufficient to down-regulate myelin protein expression and degrade myelin in mature OLs. To determine whether the injury-induced Erk1/2 activation contributed to the MBP loss, we pre-treated the OL cultures with U0126 prior to the injury. Inhibition of Erk1/2 activation prevented the MBP loss in the OLs following injury (Figure 6.3D). Altogether, our data indicate that mechanical injury on mature OL initiates Erk1/2 signaling that contributes to the myelin protein loss.

6.4.4 Mechanical injury initiates intracellular Ca^{++} increase in OLs

Mechanotransduction in mammalian cells are often initiated by Ca^{++} influx into cells that subsequently activates downstream signaling proteins. To

determine whether the OL response to injury was accompanied by intracellular Ca^{++} increase, mature OLs were loaded with Fluo4-AM, a fluorescence-based Ca^{++} sensitive dye and the changes in the fluorescence intensity was monitored following stretch injury. The time-lapse images collected after stretch injury showed a rapid increase in intracellular Ca^{++} levels, which then returned to the base levels within 60 seconds (Figures 6.4A and B). Next, we asked whether the Ca^{++} increase was due to an influx of extracellular Ca^{++}. OLs were stretch-injured in Ca^{++} free media and the Ca^{++} changes were monitored as above. Surprisingly, intracellular Ca^{++} increase was detected in the OLs following injury in the absence of extracellular Ca^{++} source (Figure 6.4B). This result suggests that mechanical injury in OL initiates a signaling cascade that triggers Ca^{++} release from intracellular compartments.

6.4.5 Ca^{++} dependent Erk1/2 activation contributes to myelin protein loss in OL following mechanical injury

Removal of extracellular Ca^{++} did not affect Erk1/2 activation in OLs following stretch injury (Figure 6.4C). In astrocytes, Ca^{++} dependent-Erk1/2 activation has been reported following mechanical stimuli (Neary et al., 2003). To determine whether the injury-induced Erk1/2 activation in OL was initiated by the intracellular Ca^{++} increase, OLs were treated with BAPTA-AM, a cell permeable Ca^{++} chelator prior to the injury and Erk1/2 activation was monitored as above. In the presence of BAPTA-AM, stretch injury failed to induce Erk1/2 activation in OLs (Figure 6.4D).

Next, we determined whether intracellular Ca^{++} increase is sufficient to activate Erk1/2 in OLs. Mature OLs were treated with A23187, a membrane permeable Ca^{++} ionophore and Erk1/2 activation was monitored by Western blot analysis. A23187 treatment alone was sufficient to induce Erk1/2 activation in mature OLs (Figure 6.5A). A23187 treatment also induced MBP down-regulation in OL. The effects of A23187 on Erk1/2 activation and MBP were abrogated when co-treated with U0126, an MEK inhibitor (Figure 6.5B). Our data indicate that Ca^{++}-dependent Erk1/2 activation contributes to myelin loss in OL and the pathway may play a role in initiating myelin loss in OL following mechanical injury.

6.5 Discussion

Traumatic brain injury (TBI) is caused by sudden rotation of head resulting in a generation of inertial force to the head that can widely spread into the brain and cause a DAI. DAI does not only cause axonal damage, but it also causes myelin damage in the white matter tracts. Many studies have shown OL demyelination following TBI *in vivo*, however, these studies were limited in their analysis to determine a direct OL response to the injury due to the complexity of the brain. To overcome this limitation, we developed an *in vitro* OL injury model that allows us to examine a direct response of OLs to injury. Here, we identified Erk1/2 as an important transducer of the injury signal that triggers myelin loss in OLs. Furthermore, we showed that the injury-induced Erk1/2 activation is initiated by intracellular Ca^{++} increase in OLs. Blocking Erk1/2 activation or chelating intracellular Ca^{++} attenuates myelin loss in OL following injury. More importantly, we show that *in vivo* TBI activates Erk1/2 in white matter OL, indicating that the OL and myelin pathology following TBI may be associated with aberrant Erk1/2 activation in the OL.

During development of OLs, Erk1/2 functions as a positive regulator of myelin formation. Erk1/2 activity is required for OPC proliferation and survival: expression of dominant-negative Erk1/2 impairs OPC survival *in vitro* (Xiao et al., 2012). During myelin formation, deletion of Erk1/2 activity in OL attenuates myelin formation whereas constitutive activation of Erk1/2 results in hypermyelination (Fyffe-Maricich et al., 2013; Ishii et al., 2013). Accordingly, endogenous Erk1/2 activity in OLs remains high during active myelination, and

then drops to an undetectable level after the completion of myelin formation in the adult. Furthermore, in adult, keeping the kinase activity low in mature OL appears to be important for myelin maintenance since ectopic activation of Erk1/2 in adult OL results in myelin destabilization (Ishii et al., 2014, 2016). Therefore, under a pathological condition, such as in TBI, an extracellular signal that activates Erk1/2 in mature OL is likely to disrupt myelin stability, resulting in the myelin loss.

One of the consequences of TBI is excessive Ca^{++} elevation in cells of the brain. *In vitro*, stretch injury on cortical neurons results in increased intracellular Ca^{++} (Wolf et al., 2001; Shahlaie et al., 2010). The intracellular Ca^{++} increase is linked to injury-associated axonal abnormalities that lead to axon degeneration (Wolf et al., 2001). Injury-induced Ca^{++} increase has also been shown in astrocyte following stretch injury (Rzigalinski et al., 1998).

Our data indicate that stretch injury also induce a rapid increase in intracellular Ca^{++} in mature OL. However, the increase appears to occur from Ca^{++} release from intracellular Ca^{++} storage since removing extracellular Ca^{++} did not affect the Ca^{++} increase following injury. Previous studies have shown that Ca^{++} influx from the extracellular source is a main injury response in axons at the initial site of the injury. And, the increased Ca^{++} is responsible for activation of downstream signaling cascades that result in axonal degeneration (Wolf et al., 2001; Magou et al., 2015). However, a recent study has also shown that injury-induced initial Ca^{++} release from intracellular stores is important for induction of secondary influx of Ca^{++} from extracellular source (Staal et al., 2010).

The intracellular cellular source of Ca^{++} that contributes to the Ca^{++} increase in OL following stretch injury is yet to be elucidated. It has been shown that following mechanical injury, integrin-mediated PLC activation generates IP_3 from PIP_2 on the plasma membrane, which then binds to the PI_3 receptors on the ER to release Ca^{++}. The initial Ca^{++} increase can also activate PLC to further increase intracellular Ca^{++}. The newly produced DAG from the PLC activity has been shown to activate protein kinase C (PKC) and subsequently the downstream Erk1/2 signaling pathway (Dhillon et al., 1999). *In vivo*, TBI induces both PLS and PKC activation in the brain (Sun and Faden, 1994; Dhillon et al., 1999). It is not known whether the integrin-PLC-PKC pathway activation is associated with the Ca^{++} and Erk1/2 activity increase in OL following stretch injury. In our study, the mature OLs were maintained on laminin, a ligand for integrin, suggesting that the integrin mediated mechanotransduction may be involved in evoking the OL injury response. During the development, cells in the OL lineage express integrin that interacts with laminin in the ECM. The laminin-mediated integrin signaling is also important for OL survival and myelin membrane formation (Buttery and ffrench-Constant, 1999; Frost et al., 1999; Corley et al., 2001; Câmara et al., 2009). Moreover, the integrin signaling in OL has been shown to play a role in initiating OL injury response (Corley et al., 2001; Hemphill et al., 2015). Considering that integrin is the most widely used initiator of mechanotransduction signaling pathways (Iqbal and Zaidi, 2005). We propose an involvement of integrin signaling in initiating the Ca^{++}-dependent Erk1/2 signaling in OL in response to stretch injury.

Our data indicate that stretch injury results in myelin protein loss in mature OL without cell death. The injury response was blocked when the cells were pretreated with either Ca^{++} chelator or an Erk1/2 pathway inhibitor. It is unknown whether the myelin protein loss was due to a decrease in myelin protein synthesis or an increase in the protein degradation. Under pathologic conditions, such as MS and in TBI, an increase in proteinase activities has been reported, which is thought to contribute to axonal degeneration and myelin protein degradation (Saatman et al., 1996; Buki et al., 1999; McCracken et al., 1999; Shields et al., 1999; Stone et al., 2002).

Calpain, a Ca^{++}-activated neutral protease, has been shown to become active following TBI and the activity degrades MBP (Liu et al., 2006). In addition, Ca^{++}-dependent calpain activity in neurons has been shown to activate Erk1/2 that results in hyper-phosphorylated neurofilament (NF) (Veeranna et al., 2004).

In our previous study, we observed that ectopic Erk1/2 activation in mature and myelinating OL is sufficient to initiate myelin protein loss and myelin breakdown, respectively. In the present study, we show that Erk1/2 activation induced by mechanical injury plays a role in initiating myelin loss in mature OL. These data suggest the role of Erk1/2 in destabilizing the myelin program in mature or myelinating OLs. *In vivo*, following TBI, many factors associated with the injury are likely to induce Erk1/2 activation in the neighboring OLs. As shown in our study, direct mechanical force activates Erk1/2 in OLs. TBI induces neuronal hyperexcitability that increases glutamate release into the brain (Katayama et al., 1990; Zauner and Bullock, 1995). Functions of glutamate

receptors, especially that of the NMDA receptor has been implicated in myelin damage (Micu et al., 2005; Káradóttir et al., 2006). NMDA receptor activation has also been shown to induce Ca^{++} dependent Erk1/2 activation in OLs (Krapivinsky et al., 2003). Cytokines and growth factors that are known to accumulate in lesions following TBI are also capable of activating the Erk1/2 pathway in OLs (Fressinaud et al., 1993; Bansal and Pfeiffer, 1997; Canoll et al., 1999; Horiuchi et al., 2006). It is possible that Erk1/2 may function as a converging point for various injury-associated stimuli in OL that lead to myelin breakdown. In fact, we observed Erk1/2 activation in white matter OLs following TBI. A future *in vivo* study is needed to elucidate the significance of the Erk1/2 activation in OL and its contribution to the myelin and OL pathology in TBI.

6.6. Figures and Figure legends

Figure 6.1.

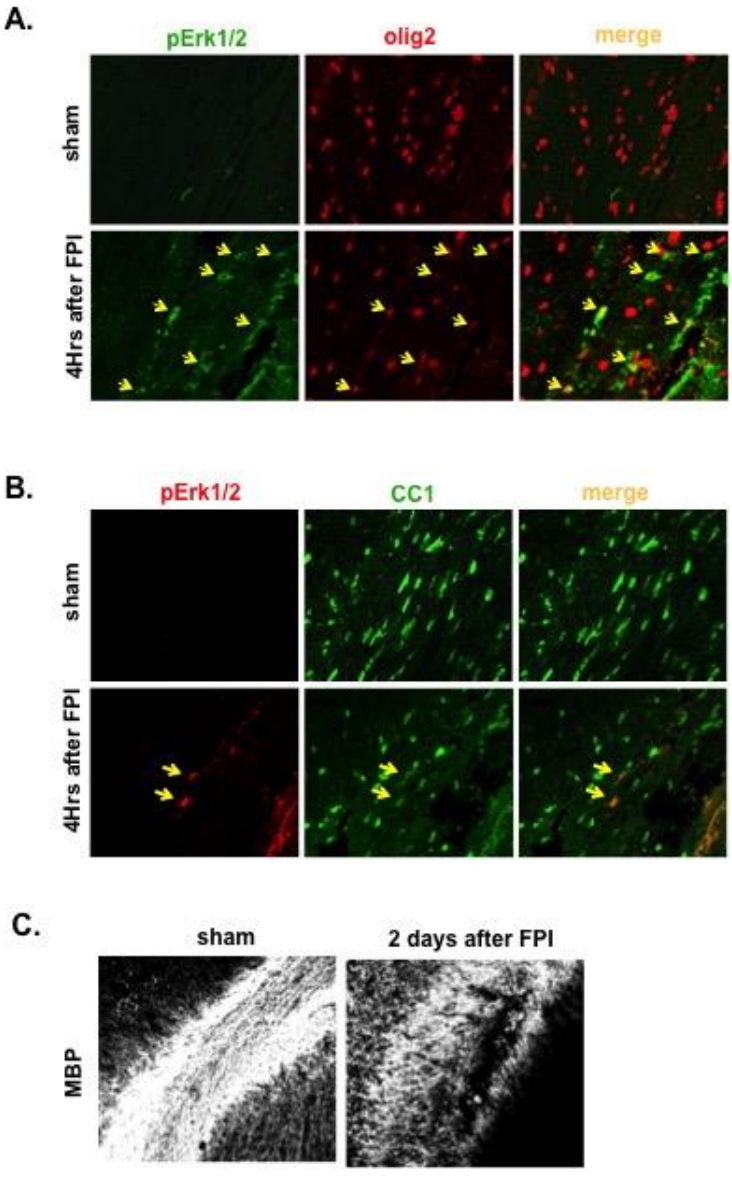

Figure 6.1. Traumatic brain injury induces Erk1/2 activation in white matter OLs.

(A-B) Control and TBI-brain sections were prepared from a rat brain collected 4 hours after FPI and stained for phospho-Erk1/2 with either olig2 or CC1. Phospho-Erk1/2 immunoreactivity was seen in OL lineage cells (Olig2+ cells) and mature OLs (CC1+ cells) within the external capsule (yellow arrows). (C) Loss of MBP expression in external capsule area of the brain was observed 2 days after FPI.

Figure 6.2.

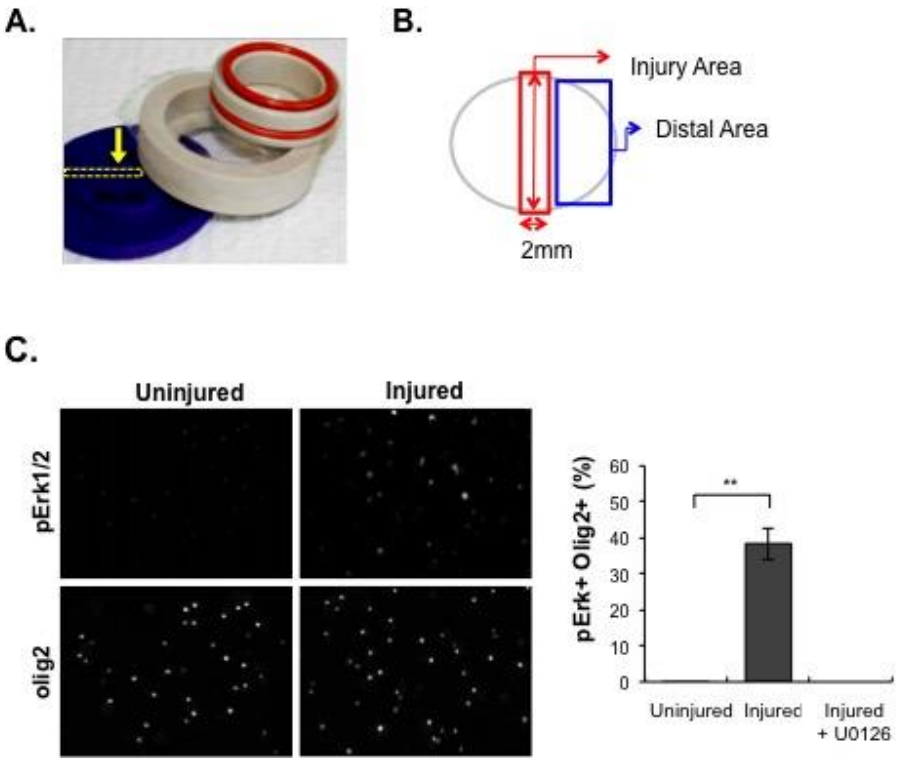
A.
B.
Injury Area
Distal Area
2mm
C.
Uninjured
Injured
pErk1/2
olig2
pErk+ Olig2+ (%)
60
50
40
30
20
10
0
**
Uninjured
Injured
Injured
+ U0126

Figure 6.2. *In vitro* stretch injury on differentiated OLs induces MBP down regulation without cell death.

(A) Images of the injury well components. Two O-rings (red rings in the image) are used to hold silicone membrane, on which cells are cultured. Deformation mask (arrow) that has a 2mm gap in the center where air pulse is applied is also seen in (B, red). (B) Schematic of the division of the area within an injury well. Injured area indicates the middle of an area, which is stretched by the air pulse (red). Distal area indicates the rest of the area, which is not stretched in the same injury well (blue). (C) Differentiated OLs were stretched at 70% strain, 30 sec^{-1}. Thirty minutes after injury, cells were fixed and immunostained for pErk1/2. Increased Erk1/2 activation was shown in individual OLs (left) and a percentage of phospho Erk1/2-positive cells was calculated by the number of phospho Erk1/2 and olig2 double-labeled cells over a number of total olig2 positive cells. The quantification shows that injury induces Erk1/2 activation in OLs (right). The means +/- SEM were determined from three independent experiments.

Figure 6.3.

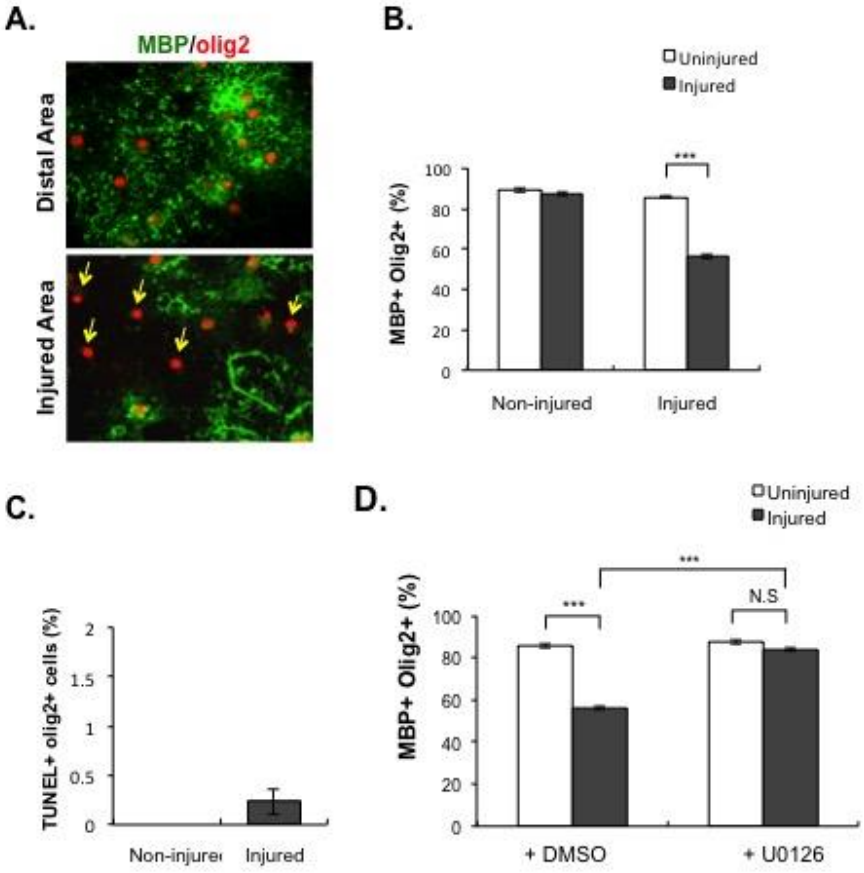
A.
MBP/olig2
Distal Area
Injured Area
B.
Uninjured
Injured
MBP+ Olig2+ (%)
100
80
60
40
20
0
***
Non-injured
Injured
C.
TUNEL+ olig2+ cells (%)
2
1.5
1
0.5
0
Non-injure
Injured
D.
Uninjured
Injured
MBP+ Olig2+ (%)
100
80
60
40
20
0
***
***
N.S
+ DMSO
+ U0126

Figure 6.3. Stretch injury-induced MBP loss is mediated by Erk1/2 activation in OLs. (A) OPCs are plated on the silicone membrane. Once OPCs are differentiated into OLs, a stretch injury was applied at 70% strain, 30 sec^{-1}. Twenty-four hours after injury, myelin protein expressing OLs were visualized by immunostaining for MBP and olig2. (B) Percentage of MBP+ among olig2+ cells was counted and compared to a non-injured control or uninjured (distal) area in the same culture (right). Decreased MBP expression in cells was observed following injury. *** $p<0.001$, The means +/- SEM were determined from three independent experiments. (C) OL apoptosis was not observed by the TUNEL assay of the OLs. The means +/- SEM were determined from two independent experiments. (D) Differentiated OLs were injured in the presence or absence of 10μM Erk1/2 inhibitor, U0126. While a drastic decrease in MBP expression is seen in OLs following stretch injury in absence of Erk1/2 inhibitor, a treatment with 10μM Erk1/2 inhibitor prevents the injury-induced MBP loss following stretch injury as shown in the quantification. *** $p<0.001$, The means +/- SEM were determined from three independent experiments.

Figure 6.4.

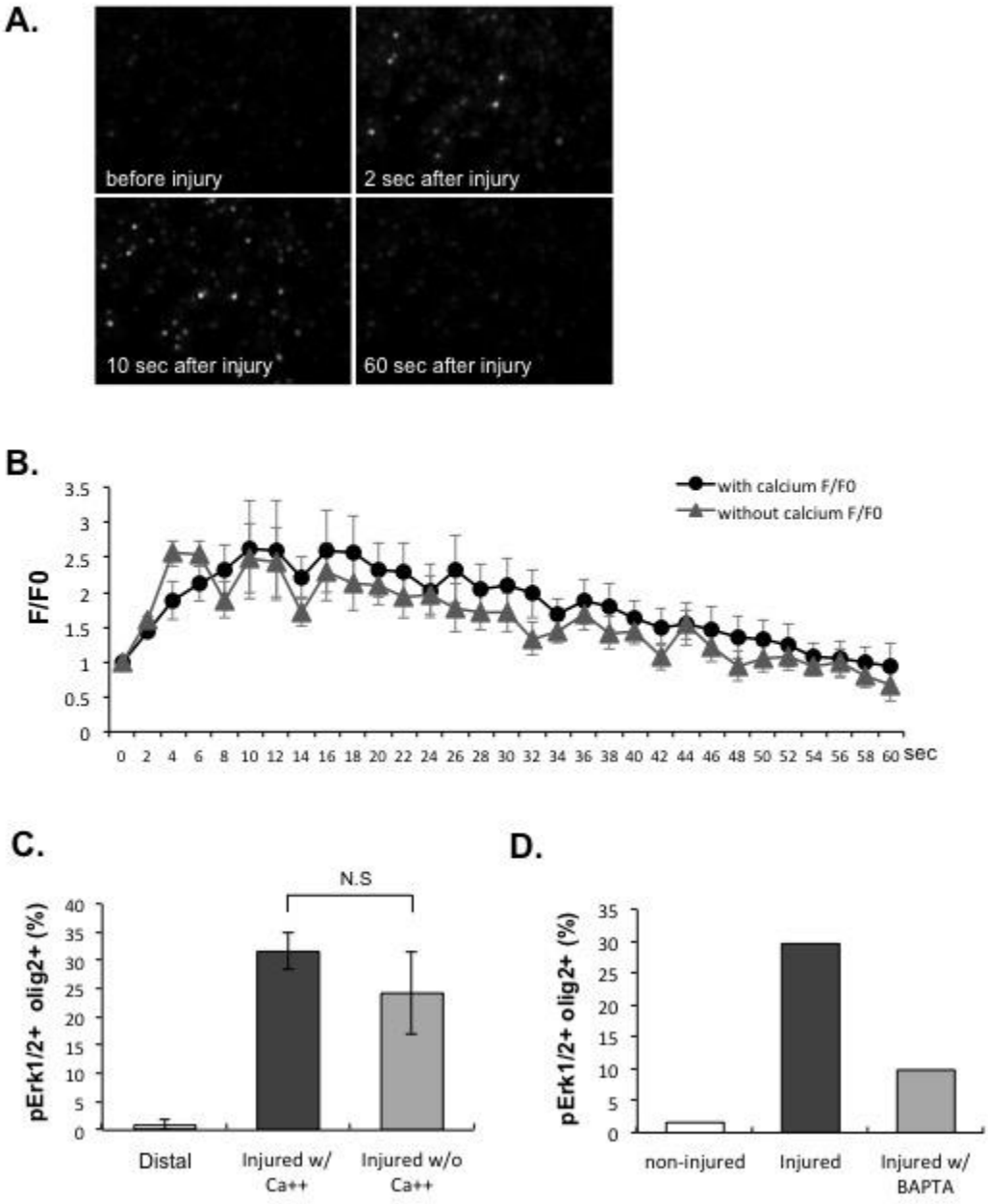
A.
before injury
2 sec after injury
10 sec after injury
60 sec after injury
B.
with calcium F/F0
without calcium F/F0
F/F0
sec
C.
N.S
pErk1/2+ olig2+ (%)
Distal
Injured w/ Ca++
Injured w/o Ca++
D.
pErk1/2+ olig2+ (%)
non-injured
Injured
Injured w/ BAPTA

Figure 6.4. Stretch injury induces intracellular Ca^{++} increase and extracellular Ca^{++} is not required for the Erk1/2 activation in OLs.

(A and B) Differentiated OLs were loaded with Fluo-4 then stretch-injured at 70% strain, 30 sec^{-1}. A transient increase in the intensity of Fluo-4 can be seen in individual OLs in the presence or in absence of extracellular Ca^{++}. The means +/- SEM were determined from two to three independent experiments.

(C) Differentiated OLs were stretch-injured at 70% strain, 30 sec^{-1} in presence or absence of extracellular Ca^{++}. Thirty minutes later, cells were fixed and immunostained for pErk1/2 and olig2. No significant differences were observed in Erk1/2 activation between both conditions. The means +/- SEM were determined from three independent experiments. (D) Twenty-five micromoles of BAPTA-AM, a cell permeable Ca^{++} chelator, was pre-treated and kept while cells were stretch-injured. Cells were fixed and immunostained for pErk1/2 and olig2. Chelating intracellular Ca^{++} reduced Erk1/2 activation following injury compared to the control.

Figure 6.5.

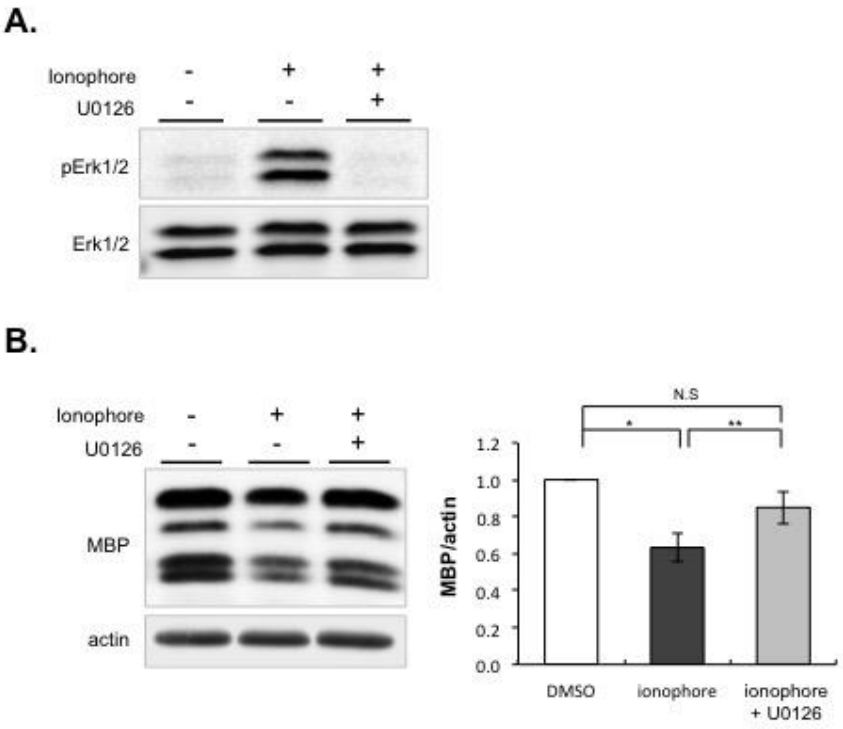
A.
Ionophore - + +
U0126 - - +
pErk1/2
Erk1/2
B.
Ionophore - + +
U0126 - - +
MBP
actin
N.S
*
**
MBP/actin
1.2
1.0
0.8
0.6
0.4
0.2
0.0
DMSO
ionophore
ionophore + U0126

Figure 6.5. Intracellular Ca^{++} increase is sufficient to activate Erk1/2 and induces MBP loss in differentiated OLs. (A) Differentiated OLs were treated with 10μM of Ca^{++} ionophore, A23187, for 30 minutes and cells were lysed. Immunoblots for pErk1/2 show that increasing intracellular Ca^{++} induces transient Erk1/2 activation. (B) Differentiated OLs were treated with 10μM of Ca^{++} ionophore, which was removed after 30 minutes. Cultures were kept in OL culture media for another 24 hours and cells were lysed. Immunoblots for MBP shows that Ca^{++} ionophore treatment induces MBP down-regulation. Treatment with 10μM of Erk1/2 inhibitor prevents the Ca^{++} ionophore-induced MBP loss as shown in the blots (left) and quantification (right). * $p<0.05$, ** $p<0.01$, The means +/- SEM were determined from three independent experiments.

7. Discussion and Future directions

7.1 Myelin dysfunctions in the nervous system

7.1.1 Abnormal myelin formation in CMT4B1

Myelin structure is important for rapid saltatory conduction. It also provides structural and metabolic support for axons. Under pathological conditions, defects in myelin structure impair the nerve signal transmission and survival of axons. Over time, this myelin damage will affect functions of the nervous system. Myelin dysfunctions can be caused from aberrant myelin formation during development or from a disruption of myelin homeostasis.

During myelination, acute intracellular signaling pathways regulate SC myelination, including SC differentiation and membrane expansion. These precisely controlled signaling pathways regulate gene expression machinery during myelination. These changes in intracellular signaling accompanied with membrane sorting, trafficking, and expansion are required for temporal and spatial control of myelin formation. Mutations in genes, misregulation of intracellular signaling, or mistrafficking of proteins and lipids that are associated with myelin formation were found in demyelinating diseases, including CMT.

Among the different types of CMT, CMT4 is caused by mutations in different genes that are associated with myelin formation or maintenance. For example, in CMT4B1, mutations in the MTMR2 gene have been shown to induce a myelin outfolding phenotype. MTMR2 gene expression has been shown in both neurons and SCs, however, it was shown that this myelin outfolding resulted from the effects of MTMR2 loss in SCs, not in motor neurons (Bolis et al., 2005).

MTMR2 is a PI-3 phosphatase that dephosphorylates $PI(3,5)P_2$ (Robinson and Dixon, 2006). It has been shown that mutations of MTMR2 gene results in accumulation of $PI(3,5)P_2$ levels in fibroblasts. In addition, the study showed that rebalance of $PI(3,5)P_2$ levels by inhibiting PIKfyve activity, which is a kinase that regulates generation of $PI(3,5)P_2$, rescues the myelin outfolding in MTMR2 KO SCs (Vaccari et al., 2011). The phospholipid, $PI(3,5)P_2$, is shown as a signaling lipid and heavily localizes in late endosomes and lysosomes that are important for endosomal membrane trafficking (Mayinger, 2012). This suggests that accumulation of this $PI(3,5)P_2$ levels in MTMR2 deficient SCs might induce abnormal intracellular trafficking that is involved in SC myelination. Endosomal trafficking is important for temporal and spatial distribution of newly synthesized myelin proteins and lipids during myelination. Defects in this trafficking process in MTMR2 deficient SCs may fail to transport myelin protein and lipids to myelin membranes evenly. A study showed that MTMR2 negatively regulates membrane formation and remodeling by interacting with discs large 1 (Dlg1), which is a scaffold protein that is involved in trafficking and membrane addition. In the absence of MTMR2 function in SCs, negative regulation of Dlg1 function by MTMR2 is reduced resulting in excessive membrane addition (Bolis et al., 2009). This suggests that myelin outfolding produced by local excessive myelin membrane growth may be due to this defective trafficking process in MTMR2 deficient SCs.

Nrg1-ErbB signaling is a crucial for SC myelination by activating AKT/ mTOR signaling pathways in SCs (Taveggia et al., 2005; Norrmén and Suter,

2013). Previously, over-activation of AKT signaling in both PTEN KO mice and constitutive AKT activation in SCs have shown hypermyelination and myelin outfolding in sciatic nerves (Goebbels et al., 2012; Domenech-Estevez et al., 2016). Our data showed that there were no significant differences in levels of AKT and Erk1/2, which are downstream of Nrg1-ErbB signaling pathway (Figure 4.2B). Also, a recent paper confirmed that there were no changes in AKT and Erk1/2 levels in sciatic nerves from MTMR2 KO mice. However, interestingly, the level of ErbB2 and ErbB3 receptors phosphorylation were increased in MTMR2 KO without affecting AKT and Erk1/2 activities (Bolino et al., 2016). They concluded that this may be due to the impaired regulation of ErbB receptor trafficking, resulting in a local increase of signaling during myelination. Furthermore, down-regulation of Nrg1 signaling by knocking it down or Niacin treatment, which is a drug known to activate TACE activity, rescued the myelin outfolding phenotype in MTMR2 KO (Bolino et al., 2016). This suggests that Nrg1 contributes to the pathology of demyelinating CMTs.

In MTMR2 KD SCs, increased mTORC1 activity was observed and this increased mTORC1 activity was reversed by inhibition of PIKfyve (Figure 4.6B). This suggests that misregulation of $PI(3,5)P_2$ levels resulting in mTORC1 activation in MTMR2 KD SCs may be involved in myelin outfolding in CMT4B1. Previous study has shown that rapamycin treatment, an inhibitor for mTORC1, reduced myelin outfolding in the PTEN KO mice (Goebbels et al., 2012). This suggests that phospholipids-associated mTORC1 signaling pathways may result in myelin defects, such as myelin outfolding.

In CMT4B1 patients, dysmyelination and hypomyelination also have been observed in addition to myelin outfolding (Bolino et al., 2004). Dysmyelination is usually caused by failures in SC differentiation. During SC differentiation, Krox-20 increases and regulates expression of myelin-associated genes. Our data showed increased mTORC1 activity in MTMR2 KD SCs in the early stage of myelination *in vitro* (Figure 4.3B). It was also associated with decreased Krox-20 expression. In a previous study, SC-specific deletion of mTOR showed an increase in Krox-20 expression (Sherman et al., 2012). This suggests the level of Krox-20 expression is related to mTORC1 signaling pathway. To support this, recently, mTORC1 signaling has been shown to regulate Krox-20 during the SC myelination. High mTORC1 activity following deletion of TSC1, suppressed expression of Krox-20 (Figlia et al., 2017). Taken together, these results suggest a possible mechanism that increased mTORC1 activity in MTMR2 KD in the early stage of myelination may be associated with the dysmyelination phenotype in CMT4B1 patients. In addition, mTORC1 activity was shown to be high before myelination and it decreases as SCs differentiate into myelinating SCs, resulting in releasing the Krox-20 suppression (Figlia et al., 2017). This indicates that acute regulation of mTORC1 signaling is required for both myelin formation and maintenance.

In our study, decreased Krox-20 expression in late stage of myelination *in vitro* in MTMR2 KD SCs did not affect myelin protein expression level (Figure 4.8B). An autophagy defect was identified in MTMR2 KD SCs by showing decreased ULK1 and TFEB activities (Figures 4.6C and D). A previous study has

shown that autophagy is important in SC myelination by showing that activation of autophagy through the use of an inhibitor of mTORC1 promotes SC myelination (Rangaraju et al., 2010). Therefore, it suggests that MTMR2 loss induces dysmyelination by inhibiting Krox-20 expression in the early stages of myelination. However, over time during the myelination, MTMR2 loss also induces an inhibition of autophagy, which may result in abnormal trafficking of myelin protein and lipids.

Taken together, dysregulation of $PI(3,5)P_2$ during myelination may be associated with an imbalance of anabolic and catabolic metabolisms of myelin proteins and lipids in SCs, resulting in excessive myelin protein/ or membrane production that may associate with outfolding in CMT4B1.

7.1.2 Demyelination in TBI

Myelin dysfunctions can also be induced by demyelination. Axonal degeneration and demyelination are common features of TBI patients that are accompanied with OL death, resulting in demyelination following moderate to severe injury. However, a recent study showed that intact axons can undergo demyelination after mild TBI without OL death (Mierzwa et al., 2015). This suggests that TBI initiates a response in OLs leading to demyelination without affecting the axons associated with myelinating OLs. There are many factors that can induce injury response in OLs, including growth factors, cytokines, and neurotransmitters (Katayama et al., 1990; Fressinaud et al., 1993; Bansal et al., 2003; Hutchinson et al., 2007; Magou et al., 2015). These factors possibly affect

myelin stability in the OLs. For example, previous studies showed overload of NMDA, FGF-2, or IFN-γ ablated myelin (Fressinaud et al., 1993; Corbin et al., 1996; Bansal et al., 2003; Micu et al., 2005).

Another possiblity that causes demyelination would be direct impact of the mechanical injury. Many studies have investigated direct effects of the mechanical injury in neurons or astrocytes, showing increased intracellular calcium and changes in signaling pathways in cells following the injury. In addition, injury-induced Erk1/2 also has been shown in different cell types. For example, Erk1/2 activation was observed in neurons and astrocytes in TBI-brains (Mori et al., 2002). In addition, Erk1/2 activation was observed in SCs following the PNS injury and inhibition of Erk1/2 activation was sufficient to inhibit myelin breakdown (Guertin et al., 2005). However, how mature OLs in adult brains repond to the mechanical injury is not known. In addition, it is also not known whether mechanical injury signals trigger changes in intracellular signaling in OLs associated with myelin breakdown.

Here, we showed that mechanical injury induces calcium-dependent Erk1/2 activation, resulting in myelin loss. This result suggests that activation of Erk1/2 in mature OLs may play a negative role in OL myelin. To support this, a recent paper has shown that ectopic activation of Erk1/2 in adult OLs induces myelin breakdown (Ishii et al., 2016). Furthermore, our previous study showed that expression of constitutively active Erk1/2 in mature OLs is sufficient to induce myelin protein loss (unpublished data).

These are interesting results since previously Erk1/2 signaling pathway has been shown to be a positive regulator for myelination in OLs by regulating OPC proliferation and differentiation into mature OLs (Ishii et al., 2013, 2014). This suggests that Erk1/2 pathway has a dual role in OL myelination. Erk1/2 is not only important for myelin formation, but also for the myelin maintenance and homeostasis.

These different roles in Erk1/2 pathway in OPCs and OLs may be regulated by different signaling mechanisms or by interacting with other cells in the brain. Further molecular mechanisms of how Erk1/2 pathways shows dual functions in different stages of same lineage cells will be interesting to investigate. Especially, understanding acute regulation of the Erk1/2 pathway may give us insights into protecting myelin from the insults or into developing a strategy for improving remyelination or myelin repair.

7.2 Future directions

In the demyelinating disease, damage or loss of myelin leads to impaired nerve conduction and neurological dysfunction in the nervous system. In the disease conditions, multiple factors have been shown to induce myelin abnormalities and/ or myelin loss, such as genetic/ metabolic defects, cytokines, growth factors, or injury to the myelin. Among many types of demyelinating diseases, this study focused on identifying the unknown signaling pathways of myelinating cells, specifically within CMT4B1 in the PNS and TBI in the CNS.

Acute regulation of intracellular signaling pathways in myelinating cells is required for maintaining the myelin homeostasis. However, the molecular mechanisms that control myelin homeostasis are not well understood. Therefore, elucidating the molecular mechanisms that are involved in the process of myelin homeostasis will provide insights to understand the progression of demyelinating disease. Our study points out the signaling pathways that are associated with the demyelinating conditions of CMT4B1 and TBI.

7.2.1. MTMR2 knockdown increases mTORC1 activity in SCs

In the first section of the study, we studied the function of MTMR2 in SCs. Mutations in the MTMR2 gene have been shown to cause CMT4B1, a demyelinating disease in the PNS. Since MTMR2 functions as a phosphoinositide 3- phosphatase that regulates the level of $PI(3,5)P_2$ localized in endosomal/ or lysosomal membranes, it was thought to impair endo-lysosomal signaling pathways when MTMR2 functions are disrupted. Here, we showed that a loss of MTMR2 function induced an abnormal increase of mTORC1 activity. This increased mTORC1 activity was associated with an increased phosphorylation of ULK1 and down-regulated TFEB activity, indicating the defects in autophagy formation and lysosomal biogenesis, respectively (Figure 7.1).

Although we found a new signaling mechanism that is associated with MTMR2 functions in SC, further experiments should be performed to answer following questions.

7.2.1.1. Is down-regulated TFEB activity in MTMR2 KD SCs associated with myelin defect?

Our data showed that MTMR2 loss induces an aberrant increase of mTORC1 activity, resulting in defects, which are increased phosphorylation of ULK1 and decreased TFEB functions. TFEB is a transcription factor that regulates genes, which control lysosomal biogenesis and functions. TFEB activity is regulated by mTORC1. Our data showed a decrease of TFEB activity in the absence of the function of MTMR2 in SCs by using the CLEAR assay. The decreased TFEB activity in MTMR2 KD SCs was associated with defects in autophagy induction. Although functions of TFEB in regulating autophagy to lysosomal biogenesis were actively studied, a role of TFEB in SC myelination is not well known.

Although we found that MTMR2 regulates PI(3,5)P_2-mediated mTORC1 signaling pathways, we could not observe myelin outfolding defects in MTMR2 KD-DRG co-cultures possibly due to the remaining 20-30% of functional MTMR2 proteins in our KD cells. The future studies addressing whether decreased TFEB activity in MTMR2 deficient SCs is associated with myelin defects can be tested. To support this, our preliminary data showed the myelin was inhibited when TFEB was overexpressed in SC using lenti-viral transduction of CA-TFEB (data not shown). This may give us a clue that TFEB may have an important role in myelin formation and defects in TFEB functions may be associated with myelin abnormality *in vitro*.

7.2.1.2 Is there another signaling pathway that increases PI(3,5)P2-associated mTORC1 activity in MTMR2 KD SCs?

Elevated mTORC1 activity in MTMR2 KD SCs was likely due to an increased recruitment of mTORC1 to the lysosomal membrane. However, another possible mechanism that can induce $PI(3,5)_2$-associated mTORC1 activation is through the Ca^{++} channel on lysosomal membrane. It has been shown that $PI(3,5)P_2$ on lysosomal membrane activates Ca^{++} channel, TRPML, leading to the activation of mTORC1 in fibroblasts (Dong et al., 2010).

Further experiments to test whether $PI(3,5)P_2$-dependent TRPML opening contributes to an aberrant increase of mTORC1 activity in MTMR2 KD SCs can be performed. Currently, we observed an increased mTORC1 activity after treating SC TRPML agonist to SCs, which mimics the effect of MTMR2 KD (data not shown). Supporting this, our preliminary result showed that BAPTA treatment, Ca^{++} chelator, reversed the increased mTORC1 activity in MTMR2 KD SCs transiently, suggesting that an increased mTORC1 activity in MTMR2 deficient cells may also be due to an increased $PI(3,5)P_2$-mediated TRPML opening. Further experiments to answer how abnormal increased mTORC1 activity affects SC myelination will need to be conducted.

Recently, a study has shown that late endosomes/lysosomes contains MPZ, an abundant myelin protein, in SCs. In this study, the author that lysosomal exocytosis contributes to SC remyelination following a sciatic nerve injury by showing an reduced remyelination in Rab27a mutants, which have defects in the trafficking of lysosomes to the plasma membrane (Chen et al., 2012) In addition,

proteolipid protein (PLP), was shown to be localized in late endosomes/ lysosomes of OLs. This stored PLP was transported to the plasma membrane by exocytosis (Trajkovic et al., 2006). Since Ca^{++} signaling has been suggested to be important for lysosomal exocytosis (Reddy et al., 2001), the possibility that increased intracellular Ca^{++} may induce excessive lysosome exocytosis, which may result in excessive myelin expansion, will need to be considered in MTMR2 deficient cells.

7.2.2. Mechanical injury activates Ca^{++}-dependent Erk1/2, resulting in myelin loss in mature OLs

In the third section of the study, we studied the molecular mechanism in OLs that is caused by TBI. Previously, it was limited to see the OL cell autonomous injury response following TBI due to the complexity of the brain *in vivo*. By grafting the OL monooculture methods onto a stretch injury system, we could conduct the experiments to monitor the direct injury responses to mature OLs. Here, we showed that mechanical injury induces Erk1/2 activation mediated by intracellular Ca^{++} increase, resulting in myelin protein loss.

Although our results showed the Ca^{++}-dependent Erk1/2 activation following stretch injury induces loss of myelin protein as described in Figure 7.2, several following questions should be addressed by performing further experiments.

7.2.2.1 What is the source of injury-induced increased Ca^{++}?

Increased intracellular Ca^{++} levels in cells were observed following TBI that can induce several downstream signaling pathways (Shahlaie et al., 2010; Weber, 2012). Our data has identified that the stretch injury induces a transient increase of intracellular Ca^{++} level associated with Erk1/2 activation (Figure 6.4). This Ca^{++} increase was due to the efflux of Ca^{++} from the intracellular organelles. There are several organelles that Ca^{++} is stored within the cell, such as the ER, lysosome, or mitochondria. For example, Ca^{++} release from the ER has been shown to contribute to the intracellular Ca^{++} increase in neurons (Lu et al., 2006). IP3 receptors and ryanodine receptors mediate release of intracellular Ca^{++} from ER. To determine the involvement of the intracellular source, pharmacological inhibitors to IP3 or ryanodine receptors, 2-ABP or ryanodine respectively, can be used to identify the source of the increased Ca^{++} in OL following the injury.

7.2.2.2 Do viable OLs contribute to remyelination after mechanical injury?

Following injury, an important challenge for recovery will be to regain or promote remyelination. Remyelination of demyelinated axons process is important for improving functional impairment following the injury. Previous studies have shown that OPCs are mainly responsible for the remyelination. However, it is not well understood whether the damaged OLs could regenerate and contribute to remyelination. A study has reported loss of myelin in TBI-brains is due to the death of OLs (Flygt et al., 2013). However, our data showed that while OLs lose MBP expression following injury, this loss of MBP loss was not

accompanied with cell death. Previously, studies have indicated OL plasticity following myelin damage by showing the re-entry of OLs into cell cycles in OLs following FGF-2 treatment (Fressinaud et al., 1995; Grinspan et al., 1996). This suggests that OLs that have survived from an injury may contribute to remyelination. Although maintenance or protection of the axon-myelin unit following TBI is important, understanding the possibility of whether damaged OLs can contribute to remyelination will also need to be further explored.

Figure 7.1.

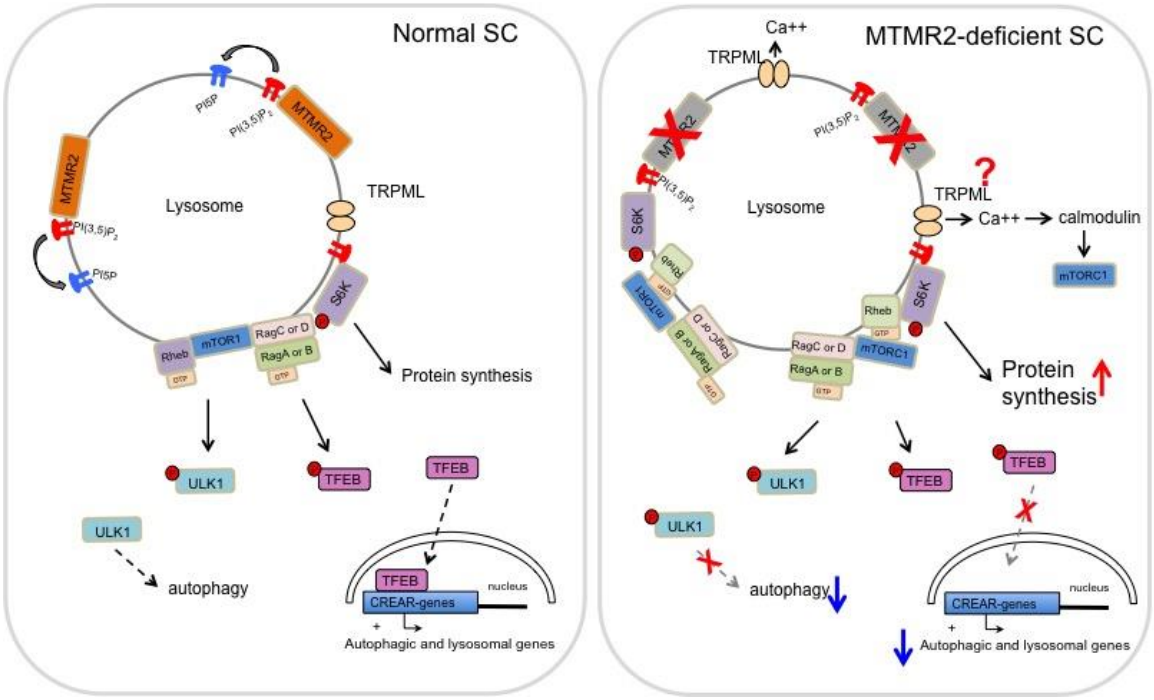
Normal SC
PI5P
PI(3,5)P2
MTMR2
MTMR2
PI(3,5)P2
PI5P
Lysosome
TRPML
S6K
Rheb
mTOR1
RagC or D
RagA or B
GTP
GTP
Protein synthesis
ULK1
TFEB
TFEB
ULK1
autophagy
TFEB
CREAR-genes
nucleus
Autophagic and lysosomal genes
MTMR2-deficient SC
Ca++
TRPML
PI(3,5)P2
MTMR2
MTMR2
PI(3,5)P2
Lysosome
TRPML
?
Ca++
calmodulin
mTORC1
S6K
Rheb
mTOR1
RagA or B
RagC or D
GTP
Rheb
GTP
S6K
RagC or D
mTORC1
RagA or B
GTP
Protein synthesis
ULK1
TFEB
TFEB
ULK1
autophagy
CREAR-genes
nucleus
Autophagic and lysosomal genes

Figure 7.1. Proposed model for the role of MTMR2 in SCs. In a normal SC, mTORC1 is a kinase that controls cellular metabolic balances in responses to extracellular and intracellular stimuli to the cell by regulating anabolic and catabolic processes such as protein synthesis, lipid synthesis, lysosome biogenesis, and autophagy. In the absence of MTMR2 functions, the level of $PI(3,5)P_2$ on the lysosomal membrane increases, resulting in activating mTORC1 signaling pathway. Increased mTORC1 activity induces S6K activation, which controls protein synthesis and inhibits of ULK1 and TFEB activities, which inhibits autophagy and lysosome biogenesis. This could result in an imbalance between the catabolic and anabolic regulation of myelin proteins, resulting in disruption of myelin homeostasis in SCs.

Figure 7.2.

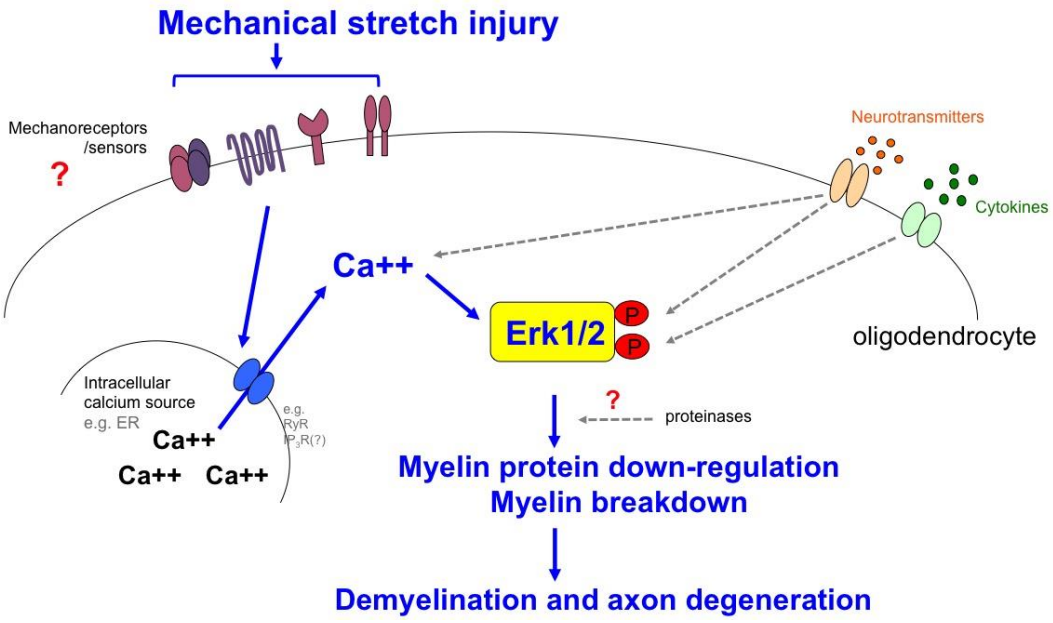
Mechanical stretch injury
Mechanoreceptors
/sensors
?
Neurotransmitters
Cytokines
Ca++
Erk1/2
P
P
oligodendrocyte
Intracellular
calcium source
e.g. ER
Ca++
Ca++ Ca++
e.g.
RyR
IP3R(?)
?
proteinases
Myelin protein down-regulation
Myelin breakdown
Demyelination and axon degeneration

Figure 7.2. Schematic of TBI-induced mechanical injury signaling pathways in OL. The mechanical stretch injury induces efflux of calcium from the intracellular organelles, such as ER, mitochondria, or lysosomes. Increased intracellular calcium is sufficient to activate Erk1/2 in OLs, and increased Erk1/2 induces myelin loss.

8. References

Ali S, Driscoll HE, Newton VL, Gardiner NJ (2014) Matrix metalloproteinase-2 is downregulated in sciatic nerve by streptozotocin induced diabetes and/or treatment with minocycline: Implications for nerve regeneration. Exp Neurol 261:654–665.

Amour A, Slocombe PM, Webster A, Butler M, Knight CG, Smith BJ, Stephens PE, Shelley C, Hutton M, Knäuper V, Docherty AJ p, Murphy G (1998) TNF-α converting enzyme (TACE) is inhibited by TIMP-3. FEBS Lett 435:39–44.

Apte SS, Olsen BR, Murphy G (1995) The gene structure of tissue inhibitor of metalloproteinases (TIMP)-3 and its inhibitory activities define the distinct TIMP gene family. J Biol Chem 270:14313–14318.

Arroyo EJ, Scherer SS (2000) On the molecular architecture of myelinated fibers. Histochem Cell Biol 113:1–18.

Arthur-Farraj PJ, Latouche M, Wilton DK, Quintes S, Chabrol E, Banerjee A, Woodhoo A, Jenkins B, Rahman M, Turmaine M, Wicher GK, Mitter R, Greensmith L, Behrens A, Raivich G, Mirsky R, Jessen KR (2012) c-Jun Reprograms Schwann Cells of Injured Nerves to Generate a Repair Cell Essential for Regeneration. Neuron 75:633–647.

Bansal R, Magge S, Winkler S (2003) Specific Inhibitor of FGF receptor signaling-FGF2 mediated effects on proliferation-differentiation and MAPK activation are inhibited by PD173074 in oligodendrocyte lineage cells. J Neurosci Res 74:486–493.

Bansal R, Pfeiffer SE (1997) FGF-2 converts mature oligodendrocytes to a novel phenotype. J Neurosci Res 50:215–228.

Bar-Peled L, Sabatini DM (2012) SnapShot: MTORC1 signaling at the lysosomal surface. Cell 151:1390–1390.e1.

Baumann N, Pham-dinh D (2001) Biology of Oligodendrocyte and Myelin in the Mammalian Central Nervous System. Physiol Rev 81:871–927.

Bergles DE, Richardson WD (2015) Oligodendrocyte Development and Plasticity. Cold Spring Harb Perspect Biol 8:a020453.

Betz C, Hall MN (2013) Where is mTOR and what is it doing there? J Cell Biol

203:563–574.

Bolino A, Bolis A, Previtali SC, Dina G, Bussini S, Dati G, Amadio S, Del Carro U, Mruk DD, Feltri ML, Cheng CY, Quattrini A, Wrabetz L (2004) Disruption of Mtmr2 CMT4B1-like neuropathy with myelin outfolding and impaired spermatogenesis. J Cell Biol 167:711–721.

Bolino A, Muglia M, Conforti FL, LeGuern E, Salih MM, Georgiou D-M, Christodoulou K, Hausmanowa-Petusewicz I, Mandich P, Schenone A, Gambardella A, Bono F, Quattrone A, Devoto M, Monaco AP (2000) Charcot-Marie-Tooth type 4B is caused by mutations in the gene encoding myotubularin-related protein-2. Nat Genet 25:17–19.

Bolino A, Piguet F, Alberizzi V, Pellegatta M, Rivellini C, Guerrero-Valero M, Noseda R, Brombin C, Nonis A, D 'adamo P, Taveggia C, Previtali SC (2016) Niacin-mediated Tace activation ameliorates CMT neuropathies with focal hypermyelination. EMBO Mol Med 8:1438–1454.

Bolis A, Coviello S, Bussini S, Dina G, Pardini C, Previtali SC, Malaguti M, Morana P, Del Carro U, Feltri ML, Quattrini A, Wrabetz L, Bolino A (2005) Loss of Mtmr2 phosphatase in Schwann cells but not in motor neurons causes Charcot-Marie-Tooth type 4B1 neuropathy with myelin outfoldings. J Neurosci 25:8567–8577.

Bolis A, Coviello S, Visigalli I, Taveggia C, Bachi A, Chishti AH, Hanada T, Quattrini A, Previtali SC, Biffi A, Bolino A (2009) Dlg1, Sec8, and Mtmr2 regulate membrane homeostasis in Schwann cell myelination. J Neurosci 29:8858–8870.

Bourboulia D, Stetler-Stevenson WG (2010) Matrix metalloproteinases (MMPs) and tissue inhibitors of metalloproteinases (TIMPs): Positive and negative regulators in tumor cell adhesion. Semin Cancer Biol 20:161–168.

Bramlett HM, Dietrich WD (2002) Quantitative structural changes in white and gray matter 1 year following traumatic brain injury in rats. Acta Neuropathol 103:607–614.

Bridges D, Ma J-T, Park S, Inoki K, Weisman LS, Saltiel AR (2012) Phosphatidylinositol 3,5-bisphosphate plays a role in the activation and

subcellular localization of mechanistic target of rapamycin 1. Mol Biol Cell 23:2955–2962.

Buki A, Siman R, Trojanowski JQ, Povlishock JT (1999) The role of calpain-mediated spectrin proteolysis in traumatically induced axonal injury. J Neuropathol Exp Neurol 58:365–375.

Buttery PC, ffrench-Constant C (1999) Laminin-2/Integrin Interactions Enhance Myelin Membrane Formation by Oligodendrocytes. Mol Cell Neurosci 14:199–212.

Câmara J, Wang Z, Nunes-Fonseca C, Friedman HC, Grove M, Sherman DL, Komiyama NH, Grant SG, Brophy PJ, Peterson A, Ffrench-Constant C (2009) Integrin-mediated axoglial interactions initiate myelination in the central nervous system. J Cell Biol 185:699–712.

Canoll PD, Kraemer R, Teng KK, Marchionni MA, Salzer JL (1999) GGF/Neuregulin Induces a Phenotypic Reversion of Oligodendrocytes. Mol Cell Neurosci 13:79–94.

Capruso DX, Levin HS (1992) Cognitive impairment following closed head injury. Neurol Clin 10:879–893.

Chen G, Zhang Z, Wei Z, Cheng Q, Li X, Li W, Duan S, Gu X (2012) Lysosomal exocytosis in Schwann cells contributes to axon remyelination. Glia 60:295–305.

Chew L-J, Coley W, Cheng Y, Gallo V (2010) Mechanisms of regulation of oligodendrocyte development by p38 mitogen-activated protein kinase. J Neurosci 30:11011–11027.

Chung S-H, Biswas S, Selvaraj V, Liu X-B, Sohn J, Jiang P, Chen C, Chmilewsky F, Marzban H, Horiuchi M, Pleasure DE, Deng W (2015) The p38[alpha] mitogen-activated protein kinase is a key regulator of myelination and remyelination in the CNS. Cell Death Dis 6:e1748.

Corbin JG, Kelly D, Rath EM, Baerwald KD, Suzuki K, Popko B (1996) Targeted CNS expression of interferon-gamma in transgenic mice leads to hypomyelination, reactive gliosis, and abnormal cerebellar development. Mol Cell Neurosci 7:354–370.

Corley SM, Ladiwala U, Besson A, Yong VW (2001) Astrocytes attenuate oligodendrocyte death *in vitro* through an alpha6 integrin-laminin-dependent mechanism. Glia 36:281–294.

Dhillon HS, Carman HM, Prasad RM (1999) Regional Activities of Phospholipase C after Experimental Brain Injury in the Rat. Neurochem Res 24:751–755.

Domenech-Estevez E, Baloui H, Meng X, Zhang Y, Deinhardt K, Dupree JL, Einheber S, Chrast R, Salzer JL (2016) Akt Regulates Axon Wrapping and Myelin Sheath Thickness in the PNS. J Neurosci 36:4506–4521.

Dong X, Shen D, Wang X, Dawson T, Li X, Zhang Q, Cheng X, Zhang Y, Weisman LS, Delling M, Xu H (2010) PI(3,5)P2 Mucolipin Ca2+ Controls Membrane Traffic by Direct Activation of Release Channels in the Endolysosome. Nature 1:1–21.

Dubourg O, Azzedine H, Verny C, Durosier G, Birouk N, Gouider R, Salih M, Bouhouche A, Thiam A, Grid D, Mayer M, Ruberg M, Tazir M, Brice A, Leguern E (2006) Autosomal-Recessive Forms of Demyelinating Charcot-Marie-Tooth Disease. Neuromolecular Med 8:75-86.

Duex JE, Nau JJ, Kauffman EJ, Weisman LS (2006) Phosphoinositide 5-phosphatase Fig4p is required for both acute rise and subsequent fall in stress-induced phosphatidylinositol 3,5-bisphosphate levels. Eukaryot Cell 5:723–731.

Eldridge CF, Bunge MB, Bunge RP (1989) Differentiation of axon-related Schwann cells *in vitro*: II. Control of myelin formation by basal lamina. J Neurosci 9:625–638.

Eskelinen E-L, Saftig P (2009) Autophagy: a lysosomal degradation pathway with a central role in health and disease. Biochim Biophys Acta 1793:664–673 Available at: http://dx.doi.org/10.1016/j.bbamcr.2008.07.014.

Falls DL (2003) Neuregulins: Functions, forms, and signaling strategies. EGF Recept Fam Biol Mech Role Cancer 284:15–31.

Fanarraga ML, Griffiths IR, Zhao M, Duncan ID (1998) Oligodendrocytes are not inherently programmed to myelinate a specific size of axon. J Comp Neurol 399:94–100.

Fernandez-Valle C, Fregien N, Wood PM, Bunge MB (1993) Expression of the protein zero myelin gene in axon-related Schwann cells is linked to basal lamina formation. Development 119:867–880.

Fernandez-valle C, Gwynn L, Wood PM, Carbonetto S, Bunge MB (1994) Anti-beta 1 lntegrin Antibody Inhibits Schwann Cell Myelination. J ofNeurobiology 25:1027–1226.

Figlia G, Norrme C, Pereira JA, Suter U (2017) Dual function of the PI3K-Akt-mTORC1 axis in myelination of the peripheral nervous system. Elife 40:1–27.

Fleck D, van Bebber F, Colombo A, Galante C, Schwenk BM, Rabe L, Hampel H, Novak B, Kremmer E, Tahirovic S, Edbauer D, Lichtenthaler SF, Schmid B, Willem M, Haass C (2013) Dual cleavage of neuregulin 1 type III by BACE1 and ADAM17 liberates its EGF-like domain and allows paracrine signaling. J Neurosci 33:7856–7869.

Flygt J, Djupsjö a, Lenne F, Marklund N (2013) Myelin loss and oligodendrocyte pathology in white matter tracts following traumatic brain injury in the rat. Eur J Neurosci 38:2153–2165.

Fontana X, Hristova M, Da Costa C, Patodia S, Thei L, Makwana M, Spencer-Dene B, Latouche M, Mirsky R, Jessen KR, Klein R, Raivich G, Behrens A (2012) C-Jun in Schwann cells promotes axonal regeneration and motoneuron survival via paracrine signaling. J Cell Biol 198:127–141.

Fortun J, Dunn W a, Joy S, Li J, Notterpek L (2003) Emerging role for autophagy in the removal of aggresomes in Schwann cells. J Neurosci 23:10672–10680.

Fragoso G, Haines JD, Roberston J, Pedraza L, Mushynski WE, Almazan G (2007) p38 Mitogen-Activated Protein Kinase Is Required for Central Nervous System Myelination. Glia 55:1416–1425.

Fragoso G, Robertson J, Athlan E, Tam E, Almazan G, Mushynski WE (2003) Inhibition of p38 mitogen-activated protein kinase interferes with cell shape changes and gene expression associated with Schwann cell myelination. Exp Neurol 183:34–46.

Fredrick TJ, Min J, Altieri SC, Mitchell NE, Wood TL (2007) Synergistic Induction of Cyclin D1 in Oligodendrocyte Progenitor Cells by IGF-I and FGF-2 Requires Differential Stimulation of Multiple Signaling Pathways. Am J Trop Med Hyg 55:1011–1022.

Fressinaud C, Laeng P, Labourdette G, Durand J, Vallat J-M (1993) The proliferation of mature oligodendrocytes *in vitro* is stimulated by basic fibroblast growth factor and inhibited by oligodendrocyte-type 2 astrocyte precursors. Dev Biol 158:317–329.

Fressinaud C, Vallat JM, Labourdette G (1995) Basic fibroblast growth factor down-regulates myelin basic protein gene expression and alters myelin compaction of mature oligodendrocytes *in vitro*. J Neurosci Res 40:285–293.

Frost EE, Buttery PC, Milner R, Ffrench-Constant C (1999) Integrins mediate a neuronal survival signal for oligodendrocytes. Curr Biol 9:1251–1254.

Fyffe-Maricich SL, Schott A, Karl M, Krasno J, Miller RH (2013) Signaling through ERK1/2 controls myelin thickness during myelin repair in the adult central nervous system. J Neurosci 33:18402–18408.

Garratt AN, Voiculescu O, Topilko P, Charnay P, Birchmeier C (2000) A dual role of erbB2 in myelination and in expansion of the Schwann cell precursor pool. J Cell Biol 148:1035–1046.

Gautier HOB, Evans KA, Volbracht K, James R, Sitnikov S, Lundgaard I, James F, Lao-Peregrin C, Reynolds R, Franklin RJM, Káradóttir RT (2015) Neuronal activity regulates remyelination via glutamate signalling to oligodendrocyte progenitors. Nat Commun 6:8518.

Gebauer F, Hentze MW (2004) Molecular mechanisms of translational control. NatRevMolCell Biol 5:827–835.

Goebbels S, Oltrogge JH, Wolfer S, Wieser GL, Nientiedt T, Pieper A, Ruhwedel T, Groszer M, Sereda MW, Nave KA (2012) Genetic disruption of Pten in a novel mouse model of tomaculous neuropathy. EMBO Mol Med 4:486–499.

Goldstein FC, Levin HS (2001) Cognitive outcome after mild and moderate traumatic brain injury in older adults. J Clin Exp Neuropsychol 23:739–753.

Grinspan J, Reeves M, Coulaloglou M, Nathanson D, Pleasure D (1996) Re-

entry into the cell cycle is required for bFGF-induced oligodendroglial dedifferentiation and survival. J Neurosci Res 46:456–464.

Guertin AD, Zhang DP, Mak KS, Alberta JA, Kim HA (2005) Microanatomy of Axon / Glial Signaling during Wallerian Degeneration. Culture 25:3478–3487.

Harrisingh MC, Perez-Nadales E, Parkinson DB, Malcolm DS, Mudge AW, Lloyd AC (2004) The Ras/Raf/ERK signalling pathway drives Schwann cell dedifferentiation. EMBO J 23:3061–3071.

Hemphill MA, Dauth S, Yu CJ, Dabiri BE, Parker KK (2015) Traumatic brain injury and the neuronal microenvironment: A potential role for neuropathological mechanotransduction. Neuron 85:1177–1192.

Hines JH, Ravanelli AM, Schwindt R, Scott EK, Appel B (2015) Neuronal activity biases axon selection for myelination *in vivo*. Nat Neurosci 18:683–689.

Hirrlinger J, Nave K (2014) Adapting Brain Metabolism to Myelination and Long-Range Signal Transduction. Glia 62:1749–1761.

Ho W-H, Armanini MP, Nuijens A, Philips HS, Osheroff PL (1995) Sensory and Motor Neuron-derived Factor. J Biol Chem 270:14523–14532.

Horiuchi M, Itoh A, Pleasure D, Itoh T (2006) MEK-ERK signaling is involved in interferon-γ-induced death of oligodendroglial progenitor cells. J Biol Chem 281:20095–20106.

Hutchinson PJ, O'Connell MT, Rothwell NJ, Hopkins SJ, Nortje J, Carpenter KLH, Timofeev I, Al-Rawi PG, Menon DK, Pickard JD (2007) Inflammation in human brain injury: intracerebral concentrations of IL-1alpha, IL-1beta, and their endogenous inhibitor IL-1ra. J Neurotrauma 24:1545–1557.

Iqbal J, Zaidi M (2005) Molecular regulation of mechanotransduction. Biochem Biophys Res Commun 328:751–755.

Isfort MC, Roggenbuck J, Arnold WD (2015) The genetics of Charcot – Marie – Tooth disease : current trends and future implications for diagnosis and management. Appl Clin Genet 8:235–243.

Ishii A, Furusho M, Bansal R (2013) Sustained Activation of ERK1/2 MAPK in Oligodendrocytes and Schwann Cells Enhances Myelin Growth and

Stimulates Oligodendrocyte Progenitor Expansion. J Neurosci 33:175–186.

Ishii A, Furusho M, Dupree JL, Bansal R (2014) Role of ERK1/2 MAPK Signaling in the Maintenance of Myelin and Axonal Integrity in the Adult CNS. J Neurosci 34:16031–16045.

Ishii A, Furusho M, Dupree JL, Bansal R (2016) Strength of Erk1/2 MAPK activation determines its effect on myelin and axonal integrity in the adult CNS. J Neurosci 36:6471–6487.

Ishii A, Fyffe-Maricich SL, Furusho M, Miller RH, Bansal R (2012) ERK1/ERK2 MAPK signaling is required to increase myelin thickness independent of oligodendrocyte differentiation and initiation of myelination. J Neurosci 32:8855–8864.

Jang SY, Shin YK, Park SY, Park JY, Rha S-H, Kim JK, Lee HJ, Park HT (2015) Autophagy Is Involved in the Reduction of Myelinating Schwann Cell Cytoplasm during Myelin Maturation of the Peripheral Nerve. PLoS One 10:e0116624 Available at: http://dx.plos.org/10.1371/journal.pone.0116624.

Jellinger KA (2004) Head injury and dementia. Curr Opin Neurol 17:719–723.

Jin N, Mao K, Jin Y, Tevzadze G, Kauffman EJ, Park S, Bridges D, Loewith R, Saltiel AR, Klionsky DJ, Weisman LS (2014) Roles for PI(3,5)P2 in nutrient sensing through TORC1. Mol Biol Cell 25:1171–1185.

Johns TG, Bernard CCA (1999) The structure and function of myelin oligodendrocyte glycoprotein. J Neurochem 72:1–9.

Jolivalt CG, Fineman M, Deacon CF, Carr RD, Calcutt NA (2011) GLP-1 signals via ERK in peripheral nerve and prevents nerve dysfunction in diabetic mice. Diabetes, Obes Metab 13:990–1000.

Káradóttir R, Cavelier P, Bergersen LH, Attwell D (2006) NMDA receptors are expressed in oligodendrocytes and activated in ischaemia. Nature 438:1162–1166.

Katayama Y, Becker D, Tamura T, Hovda DA (1990) Massive increases in extracellular potassium and the indiscriminate release of glutamate following concussive brain injury. J Neurosurg 73:889–900.

Krapivinsky G, Krapivinsky L, Manasian Y, Ivanov A, Tyzio R, Pellegrino C, Ben-

Ari Y, Clapham DE, Medina I (2003) The NMDA receptor is coupled to the ERK pathway by a direct interaction between NR2B and RasGRF1. Neuron 40:775–784.

La Fleur M, Underwood JL, Rappolee D a, Werb Z (1996) Basement membrane and repair of injury to peripheral nerve: defining a potential role for macrophages, matrix metalloproteinases, and tissue inhibitor of metalloproteinases-1. J Exp Med 184:2311–2326.

La Marca R, Cerri F, Horiuchi K, Bachi A, Feltri ML, Wrabetz L, Blobel CP, Quattrini A, Salzer JL, Taveggia C (2011) TACE (ADAM17) inhibits Schwann cell myelination. Nat Neurosci 14:857–865.

Laplante M, Sabatini DM (2013) mTOR signaling in growth control and disease. Cell 149:274–293.

Lee MH, Knäuper V, Becherer JD, Murphy G (2001) Full-length and N-TIMP-3 display equal inhibitory activities toward TNF-alpha convertase. Biochem Biophys Res Commun 280:945–950.

Levin HS, Hanten G (2005) Executive functions after traumatic brain injury in children. Pediatr Neurol 33:79–93.

Li X, Rydzewski N, Hider A, Zhang X, Yang J, Wang W, Gao Q, Cheng X, Xu H (2016) A molecular mechanism to regulate lysosome motility for lysosome positioning and tubulation. Nat Cell Biol 18:404–417.

Lippai M, Low P (2014) The role of the selective adaptor p62 and ubiquitin-like proteins in autophagy. Biomed Res Int 2014.

Liu MC, Akle V, Zheng W, Kitlen J, O'Steen B, Larner SF, Dave JR, Tortella FC, Hayes RL, Wang KKW (2006) Extensive degradation of myelin basic protein isoforms by calpain following traumatic brain injury. J Neurochem 98:700–712.

Lotocki G, Vaccari J de R, Alonso O, Molano JS, Nixon R, Safavi P, Dietrich WD, Bramlett HM (2011) Oligodendrocyte vulnerability following traumatic brain injury in rats. Neurosci Lett 499:143–148.

Lu S-G, Zhang X, Gold MS (2006) Intracellular calcium regulation among subpopulations of rat dorsal root ganglion neurons. J Physiol 577:169–190.

Ludwin SK (1995) Pathology of the myelin sheath (Waxman SG, Kocsis JD, Stys PK., eds), pp. 412-437. Oxford university press, Inc.

Luo X, Prior M, He W, Hu X, Tang X, Shen W, Yadav S, Kiryu-Seo S, Miller R, Trapp BD, Yan R (2011) Cleavage of neuregulin-1 by BACE1 or ADAM10 protein produces differential effects on myelination. J Biol Chem 286:23967–23974.

Magou GC, Guo Y, Choudhury M, Chen L, Hususan N, Masotti S, Pfister BJ (2011) Engineering a High Throughput Axon Injury System. J Neurotrauma 28:2203–2218.

Magou GC, Pfister BJ, Berlin JR (2015) Effect of acute stretch injury on action potential and network activity of rat neocortical neurons in culture. Brain Res 1624:525–535.

Masaki T, Matsumura K, Hirata A, Yamada H, Hase A, Arai K, Shimizu T, Yorifuji H, Motoyoshi K, Kamakura K (2002) Expression of dystroglycan and the laminin-alpha 2 chain in the rat peripheral nerve during development. Exp Neurol 174:109–117.

Maurel P, Salzer JL (2000) Axonal regulation of Schwann cell proliferation and survival and the initial events of myelination requires PI 3-kinase activity. J Neurosci 20:4635–4645.

Maxwell WL, Domleo A, McColl G, Jafari SS, Graham DI (2003) Post-acute alterations in the axonal cytoskeleton after traumatic axonal injury. J Neurotrauma 20:151–168.

Maxwell WL, Kosanlavit R, McCreath BJ, Reid O, Graham DI (1999) Freeze-fracture and cytochemical evidence for structural and functional alteration in the axolemma and myelin sheath of adult guinea pig optic nerve fibers after stretch injury. J Neurotrauma 16:273–284.

Mayinger P (2012) Phosphoinositides and vesicular membrane traffic. Biochim Biophys Acta - Mol Cell Biol Lipids 1821:1104–1113.

McAllister TW (2008) Neurobehavioral sequelae of traumatic brain injury: evaluation and management. World psychiatry 7:3–10.

McAllister TW (2011) Neurobiological consequences of traumatic brain injury.

Dialogues Clin Neurosci 13:287–300.

Mccartney AJ, Zhang Y, Weisman LS (2014) Phosphatidylinositol 3,5-bisphosphate: low abundance, high significance. Bioessays 36:52–64.

McCracken E, Hunter AJ, Patel S, Graham DI, Dewar D (1999) Calpain activation and cytoskeletal protein breakdown in the corpus callosum of head-injured patients. J Neurotrauma 16:749–761.

McKee KK, Yang D-H, Patel R, Chen Z-L, Strickland S, Takagi J, Sekiguchi K, Yurchenco PD (2012) Schwann cell myelination requires integration of laminin activities. J Cell Sci 125:4609–4619.

McMorris F a, McKinnon RD (1996) Regulation of oligodendrocyte development and CNS myelination by growth factors: prospects for therapy of demyelinating disease. Brain Pathol 6:313–329.

Medina DL, Di Paola S, Peluso I, Armani A, De Stefani D, Venditti R, Montefusco S, Scotto-Rosato A, Prezioso C, Forrester A, Settembre C, Wang W, Gao Q, Xu H, Sandri M, Rizzuto R, De Matteis MA, Ballabio A (2015) Lysosomal calcium signalling regulates autophagy through calcineurin and TFEB. Nat Cell Biol 17:288–299.

Melendez-Vasquez C V. (2004) Rho Kinase Regulates Schwann Cell Myelination and Formation of Associated Axonal Domains. J Neurosci 24:3953–3963.

Mendoza M, Er E., Blenis J (2011) The Ras-ERK and PI3K-mTOR Pathways: Cross-talk and Compensation. Trends Biochem Sci 36:320–328.

Menon S, Dibble CC, Talbott G, Hoxhaj G, Valvezan AJ, Takahashi H, Cantley LC, Manning BD (2014) Spatial control of the TSC complex integrates insulin and nutrient regulation of mTORC1 at the lysosome. Cell 156:771–785.

Meyer D, Yamaai T, Garratt A, Riethmacher-Sonnenberg E, Kane D, Theill LE, Birchmeier C (1997) Isoform-specific expression and function of neuregulin. Development 124:3575–3586.

Michailov G V, Sereda MW, Brinkmann BG, Fischer TM, Haug B, Birchmeier C, Role L, Lai C, Schwab MH, Nave K-A (2004) Axonal neuregulin-1 regulates myelin sheath thickness. Science 304:700–703.

Micu I, Jiang Q, Coderre E, Ridsdale A, Zhang L, Woulfe J, Yin X, Trapp BD,

McRory JE, Rehak R, Zamponi GW, Wang W, Stys PK (2005) NMDA receptors mediate calcium accumulation in myelin during chemical ischaemia. Nature 439:1–5.

Micu I, Plemel JR, Lachance C, Proft J, Jansen AJ, Cummins K, van Minnen J, Stys PK (2016) The molecular physiology of the axo-myelinic synapse. Exp Neurol 276:41–50.

Mierzwa AJ, Marion CM, Sullivan GM, Mcdaniel DP, Armstrong RC (2015) Components of Myelin Damage and Repair in the Progression of White Matter Pathology After Mild Traumatic Brain Injury. 74:218–232.

Mironova YA, Lenk GM, Lin JP, Lee SJ, Twiss JL, Vaccari I, Bolino A, Havton LA, Min SH, Abrams CS, Shrager P, Meisler MH, Giger RJ (2016) PI(3,5)P2 biosynthesis regulates oligodendrocyte differentiation by intrinsic and extrinsic mechanisms. Elife 5:1–29.

Mizushima N, Yoshimori T (2007) How to interpret LC3 immunoblotting. Autophagy 3:542–545.

Morgan L, Jessen KR, Mirsky R (1991) The effects of cAMP on differentiation of cultured schwann cells: Progression from an early phenotype (04+) to a myelin phenotype (P○+, GFAP-, N-CAM-, NGF-receptor-) depends on growth inhibition. J Cell Biol 112:457–467.

Napoli I, Noon LA, Ribeiro S, Kerai AP, Parrinello S, Rosenberg LH, Collins MJ, Harrisingh MC, White IJ, Woodhoo A, Lloyd AC (2012) A Central Role for the ERK-Signaling Pathway in Controlling Schwann Cell Plasticity and Peripheral Nerve Regeneration *In Vivo*. Neuron 73:729–742.

Nave K-A (2010) Myelination and support of axonal integrity by glia. Nature 468:244–252.

Nave K-A, Salzer JL (2006) Axonal regulation of myelination by neuregulin 1. Curr Opin Neurobiol 16:492–500.

Nave K-A, Sereda MW, Ehrenreich H (2007) Mechanisms of disease: inherited demyelinating neuropathies--from basic to clinical research. Nat Clin Pract Neurol 3:453–464.

Nave K, Ehrenreich H (2014) Myelination and Oligodendrocyte Functions in

Psychiatric Diseases. Neurosci Psychiatry 71:582–584.

Neary JT, Kang Y, Willoughby KA, Ellis EF (2003) Activation of Extracellular Signal-Regulated Kinase by Stretch-Induced Injury in Astrocytes Involves Extracellular ATP and P2 Purinergic Receptors. 23:2348–2356.

Newbern J, Birchmeier C (2010) Nrg1/ErbB signaling networks in Schwann cell development and myelination. Semin Cell Dev Biol 21:922–928.

Newbern JM, Li X, Shoemaker SE, Zhou J, Zhong J, Wu Y, Bonder D, Hollenback S, Coppola G, Geschwind DH, Landreth GE, Snider WD (2011) Specific Functions for ERK/MAPK Signaling during PNS Development. Neuron 69:91–105.

Ng A a., Logan AM, Schmidt EJ, Robinson FL (2013) The CMT4B disease-causing phosphatases Mtmr2 and Mtmr13 localize to the Schwann cell cytoplasm and endomembrane compartments, where they depend upon each other to achieve wild-type levels of protein expression. Hum Mol Genet 22:1493–1506.

Ng HK, Mahaliyana RD, Poon WS (1994) The pathological spectrum of diffuse axonal injury in blunt head trauma ; assessment with axon and myelin stains. Clin Neurol Neurosurg. 96(1): 24-31.

Nnah IC, Khayati K, Dobrowolski R, Access O (2015) Cellular metabolism and lysosomal mTOR signaling. Cell Death Ther 1:11–22.

Norrmén C, Figlia G, Lebrun-Julien F, Pereira JA, Trötzmüller M, Köfeler HC, Rantanen V, Wessig C, van Deijk ALF, Smit AB, Verheijen MHG, Rüegg MA, Hall MN, Suter U (2014) mTORC1 controls PNS myelination along the mTORC1-RXRγ-SREBP-lipid biosynthesis axis in Schwann cells. Cell Rep 9:646–660.

Norrmén C, Suter U (2013) Akt/mTOR signalling in myelination. Biochem Soc Trans 41:944–950.

Notterpek L, Shooter EM, Snipes GJ (1997) Upregulation of the endosomal-lysosomal pathway in the trembler-J neuropathy. J Neurosci 17:4190–4200.

Ogata T, Iijima S, Hoshikawa S, Miura T, Yamamoto S, Oda H, Nakamura K, Tanaka S (2004) Opposing extracellular signal-regulated kinase and Akt

pathways control Schwann cell myelination. J Neurosci 24:6724–6732.

Otani N, Nawashiro H, Fukui S, Nomura N, Shima K (2002) Temporal and spatial profile of phosphorylated mitogen-activated protein kinase pathways after lateral fluid percussion injury in the cortex of the rat brain. J Neurotrauma 19:1587–1596.

Pareyson D, Marchesi C (2009) Diagnosis , natural history , and management of Charcot – Marie – Tooth disease. Lancet Neurol 8:654–667.

Parkinson DB, Bhaskaran A, Arthur-Farraj P, Noon LA, Woodhoo A, Lloyd AC, Feltri ML, Wrabetz L, Behrens A, Mirsky R, Jessen KR (2008) c-Jun is a negative regulator of myelination. J Cell Biol 181:625–637.

Pereira J a, Lebrun-Julien F, Suter U (2012) Molecular mechanisms regulating myelination in the peripheral nervous system. Trends Neurosci 35:123–134.

Pfister BJ, Weihs TP, Betenbaugh M, Bao G (2003) An *in vitro* uniaxial stretch model for axonal injury. Ann Biomed Eng 31:589–598.

Preitschopf A, Li K, Schörghofer D, Kinslechner K, Schütz B, Pham HTT, Rosner M, Joo GJ, Röhrl C, Weichhart T, Stangl H, Lubec G, Hengstschläger M, Mikula M (2014) MTORC1 is essential for early steps during schwann cell differentiation of amniotic fluid stem cells and regulates lipogenic gene expression. PLoS One 9:1–9.

Previtali SC, Quattrini A, Bolino A (2007) Charcot-Marie-Tooth type 4B demyelinating neuropathy: deciphering the role of MTMR phosphatases. Expert Rev Mol Med 9:1–16.

Puertollano R (2014) mTOR and lysosome regulation. F1000Prime Rep 8:1–7.

Raghupathi R, Muir JK, Fulp CT, Pittman RN, McIntosh TK (2003) Acute activation of mitogen-activated protein kinases following traumatic brain injury in the rat: Implications for posttraumatic cell death. Exp Neurol 183:438–448.

Rangaraju S, Verrier JD, Madorsky I, Nicks J, Dunn W a, Notterpek L (2010) Rapamycin activates autophagy and improves myelination in explant cultures from neuropathic mice. J Neurosci 30:11388–11397.

Rapti M, Atkinson SJ, Lee M-H, Trim A, Moss M, Murphy G (2008) The isolated

N-terminal domains of TIMP-1 and TIMP-3 are insufficient for ADAM10 inhibition. Biochem J 411:433–439.

Reddy A, Caler E V., Andrews NW (2001) Plasma membrane repair is mediated by Ca2+-regulated exocytosis of lysosomes. Cell 106:157–169.

Reeves TM, Phillips LL, Povlishock JT (2005) Myelinated and unmyelinated axons of the corpus callosum differ in vulnerability and functional recovery following traumatic brain injury. Exp Neurol 196:126–137.

Robinson FL, Dixon JE (2006) Myotubularin phosphatases: policing 3-phosphoinositides. Trends Cell Biol 16:403–412.

Rowitch DH, Kriegstein AR (2010) Developmental genetics of vertebrate glial-cell specification. Nature 468:214–222.

Ryan M, Ibrahim M, Parmar HA (2014) Secondary Demyelination Disorders and Destruction of White Matter. Radiol Clin North Am 52:337–354.

Rzigalinski BA, Weber JT, Willoughby KA, Ellis EF (1998) Intracellular free calcium dynamics in stretch-injured astrocytes. J Neurochem 70:2377–85.

Saatman KE, Bozyczko-Coyne D, Marcy V, Siman R, Mcintosh TK (1996) Prolonged calpain-mediated spectrin breakdown occurs regionally follwoing expeirmental brain injury in the rat. J Neuropathol Exp Neurol 55:850–860.

Saher G, Quintes S, Möbius W, Wehr MC, Krämer-Albers E-M, Brügger B, Nave K-A (2009) Cholesterol Regulates the Endoplasmic Reticulum Exit of the Major Membrane Protein P0 Required for Peripheral Myelin Compaction. J Neurosci 29:6094–6104.

Salzer JL (2008) Switching myelination on and off. J Cell Biol 181:575–577.

Scherer SS, Arroyo EJ (2005) Schwann Cells.

Schmitt S, Cantuti Castelvetri L, Simons M (2015) Metabolism and functions of lipids in myelin. Biochim Biophys Acta - Mol Cell Biol Lipids 1851:999–1005.

Schreiner B, Ingold-Heppner B, Pehl D, Locatelli G, Berrit-Sch??nthaler H, Becher B (2015) Deletion of Jun proteins in adult oligodendrocytes does not perturb cell survival, or myelin maintenance *in vivo*. PLoS One 10:1–11.

Shahlaie K, Lyeth BG, Gurkoff GG, Muizelaar JP, Berman RF (2010) Neuroprotective effects of selective N-type VGCC blockade on stretch-injury-

induced calcium dynamics in cortical neurons. J Neurotrauma 27:175–187.

Shaw K, MacKinnon MA, Raghupathi R, Saatman KE, McLntosh TK, Graham DI (2001) TUNEL-positive staining in white and grey matter after fatal head injury in man. Clin Neuropathol 20:106–112.

Sherman DL, Krols M, Wu L MN, Grove M, Nave KA., Gangloff YG, Brophy PJ (2012) Arrest of Myelination and Reduced Axon Growth When Schwann Cells Lack mTOR. J Neurosci 32:1817–1825.

Shields DC, Schaecher KE, Saido TC, Banik NL (1999) A putative mechanism of demyelination in multiple sclerosis by a proteolytic enzyme, calpain. Proc Natl Acad Sci U S A 96:11486–11491.

Spitzer S, Volbracht K, Lundgaard I, Karaddottir RT (2016) Glutamate signalling: A multifaceted modulator of oligodendrocyte lineage cells in health and disease. Neuropharmacology 110:574–585.

Staal JA, Dickson TC, Gasperini R, Liu Y, Foa L, Vickers JC (2010) Initial calcium release from intracellular stores followed by calcium dysregulation is linked to secondary axotomy following transient axonal stretch injury. J Neurochem 112:1147–1155.

Stone JR, Okonkwo DO, Singleton RH, Mutlu LK, Helm G a, Povlishock JT (2002) Caspase-3-mediated cleavage of amyloid precursor protein and formation of amyloid Beta peptide in traumatic axonal injury. J Neurotrauma 19:601–614.

Sun F-Y, Faden AI (1994) N-methyl-D-aspartate receptors mediate post-traumatic increases of protein kinase C in rat brain. Brain Res 661:63–69.

Sun W, Fu Y, Shi Y, Cheng J-X, Cao P, Shi R (2012) Paranodal Myelin Damage after Acute Stretch in Guinea Pig Spinal Cord. J Neurotrauma 29:611–619.

Syed N, Reddy K, Yang DP, Taveggia C, Salzer JL, Maurel P, Kim HA (2010) Soluble neuregulin-1 has bifunctional, concentration-dependent effects on Schwann cell myelination. J Neurosci 30:6122–6131.

Tapinos N, Ohnishi M, Rambukkana A (2006) ErbB2 receptor tyrosine kinase signaling mediates early demyelination induced by leprosy bacilli. Nat Med 12:961–966.

Taveggia C, Zanazzi G, Petrylak A, Yano H, Rosenbluth J, Einheber S, Xu X, Esper RM, Loeb JA, Shrager P, Chao M V., Falls DL, Role L, Salzer JL (2005) Neuregulin-1 type III determines the ensheathment fate of axons. Neuron 47:681–694.

Topilko P, Schneider-Maunoury S, Levi G, Baron-Van Evercooren a, Chennoufi a B, Seitanidou T, Babinet C, Charnay P (1994) Krox-20 controls myelination in the peripheral nervous system. Nature 371:796–799.

Trajkovic K, Dhaunchak AS, Goncalves JT, Wenzel D, Schneider A, Bunt G, Nave KA, Simons M (2006) Neuron to glia signaling triggers myelin membrane exocytosis from endosomal storage sites. J Cell Biol 172:937–948.

Tran HT, Sanchez L, Brody DL (2012) Inhibition of JNK by a peptide inhibitor reduces traumatic brain injury-induced tauopathy in transgenic mice. J Neuropathol Exp Neurol 71:116–129.

Trapp BD, Andrews SB, Cootauco C, Quarles R (1989) The myelin-associated glycoprotein is enriched in multivesicular bodies and periaxonal membranes of actively myelinating oligodendrocytes. J Cell Biol 109:2417–2426.

Urbanski MM, Kingsbury L, Moussouros D, Kassim I, Mehjabeen S, Paknejad N, Melendez-Vasquez C V. (2016) Myelinating glia differentiation is regulated by extracellular matrix elasticity. Sci Rep 6:33751.

Vaccari I, Dina G, Tronchère H, Kaufman E, Chicanne G, Cerri F, Wrabetz L, Payrastre B, Quattrini A, Weisman LS, Meisler MH, Bolino A (2011) Genetic interaction between MTMR2 and FIG4 phospholipid phosphatases involved in Charcot-Marie-Tooth neuropathies. PLoS Genet 7:e1002319.

Veeranna, Kaji T, Boland B, Odrljin T, Mohan P, Basavarajappa BS, Peterhoff C, Cataldo A, Rudnicki A, Amin N, Li BS, Pant HC, Hungund BL, Arancio O, Nixon RA (2004) Calpain mediates calcium-induced activation of the erk1,2 MAPK pathway and cytoskeletal phosphorylation in neurons: relevance to Alzheimer's disease. Am J Pathol 165:795–805.

Verheijen MHG, Camargo N, Verdier V, Nadra K, de Preux Charles A-S, Médard J-J, Luoma A, Crowther M, Inouye H, Shimano H, Chen S, Brouwers JF,

Helms JB, Feltri ML, Wrabetz L, Kirschner D, Chrast R, Smit AB (2009) SCAP is required for timely and proper myelin membrane synthesis. Proc Natl Acad Sci U S A 106:21383–21388.

Wahl SE, McLane LE, Bercury KK, Macklin WB, Wood TL (2014) Mammalian Target of Rapamycin Promotes Oligodendrocyte Differentiation, Initiation and Extent of CNS Myelination. J Neurosci 34:4453–4465.

Wang W, Gao Q, Yang M, Zhang X, Yu L, Lawas M, Li X, Bryant-Genevier M, Southall NT, Marugan J, Ferrer M, Xu H (2015) Up-regulation of lysosomal TRPML1 channels is essential for lysosomal adaptation to nutrient starvation. Proc Natl Acad Sci:201419669.

Weber JT (2012) Altered calcium signaling following traumatic brain injury. Front Pharmacol 3:60.

Willem M, Garratt AN, Novak B, Citron M, Kaufmann S, Rittger A, DeStrooper B, Saftig P, Birchmeier C, Haass C (2006) Control of peripheral nerve myelination by the beta-secretase BACE1. Science 314:664–666.

Wolf J a, Stys PK, Lusardi T, Meaney D, Smith DH (2001) Traumatic axonal injury induces calcium influx modulated by tetrodotoxin-sensitive sodium channels. J Neurosci 21:1923–1930.

Xiao J, Ferner AH, Wong AW, Denham M, Kilpatrick TJ, Murray SS (2012) Extracellular signal-regulated kinase 1/2 signaling promotes oligodendrocyte myelination *in vitro*. J Neurochem 122:1167–1180.

Yang DP, Kim J, Syed N, Tung Y, Bhaskaran A, Mindos T, Mirsky R, Jessen KR, Maurel P, Parkinson DB, Kim H (2012) p38 MAPK activation promotes denervated Schwann cell phenotype and functions as a negative regulator of Schwann cell differentiation and myelination. J Neurosci 32:7158–7168.

Zauner A, Bullock R (1995) The role of excitatory amino acids in severe brain trauma: opportunities for therapy: a review. J Neurotrauma 12:547–554.

Zhang J-X, Feng Y-F, Qi Q, Shen L, Wang R, Zhou J-S, Lü H-Z, Hu J-G (2014) JNK is necessary for oligodendrocyte precursor cell proliferation induced by the conditioned medium from B104 neuroblastoma cells. J Mol Neurosci 52:269–276.

Zou J, Hu B, Arpag S, Yan Q, Hamilton a., Zeng Y-S, Vanoye CG, Li J (2015) Reactivation of Lysosomal Ca2+ Efflux Rescues Abnormal Lysosomal Storage in FIG4-Deficient Cells. J Neurosci 35:6801–6812.